



Structural Magnetostrictive Alloys:

*From Flexible Sensors to Energy Harvesters and
Magnetically Controlled Auxetics*

Prof. Alison Flatau & MANY OTHERS!!!

***Magnetostrictive Materials Group
Department of Aerospace Engineering
University of Maryland, College Park***

Primary Research Sponsors: ONR, NSF, DARPA, DOT, State of Maryland

CEMAG - Gijón Spain - 11/30/2018



IEEE Magnetics Society

- **IEEE Magnetics Society Home Page: www.ieeemagnetics.org**
 - 3000+ full members
 - 300 student members
- **The Society**
 - Conference organization (INTERMAG, MMM, TMRC, etc.)
 - Student support for conferences
 - Large conference discounts for members
 - Graduate Student Summer Schools (June 3-8, 2018 Quito, Ecuador)
 - Local chapter activities
 - Distinguished lecturers
- **Journals (Free Electronic Access for Members)**
 - IEEE Transactions on Magnetics
 - IEEE Magnetics Letters
- **Online Application for IEEE Membership: www.ieee.org/join**
 - 360,000+ members
 - IEEE student membership - IEEE full membership

Outline



Intro to Magnetostriction

Actuators: the “direct” effect

Sensors: the “inverse” (or Villari) effect

Structural Magnetostrictive Alloys

Magnetostrictive, magnetic & mechanical properties

Thin, highly textured rolled sheet

Introduction to auxetic behavior

Applications that use Galfenol and/or Alfenol

Bending sensor applications

Implantable wireless bone fixity sensor (Tech Univ. Dresden)

Nanowire sensors (Univ. Minn. & UMD)

Applications for auxeticity?

Micro-motors (Kanazawa University, Japan)

Energy Harvesting (Kanazawa Univ, UMD & Techno Sciences, Inc., Oscilla Power)

Summary

What is Magnetostriction?



“A change in dimensions exhibited by ferromagnetic materials when subjected to a magnetic field.” (*Random House Dictionary*)

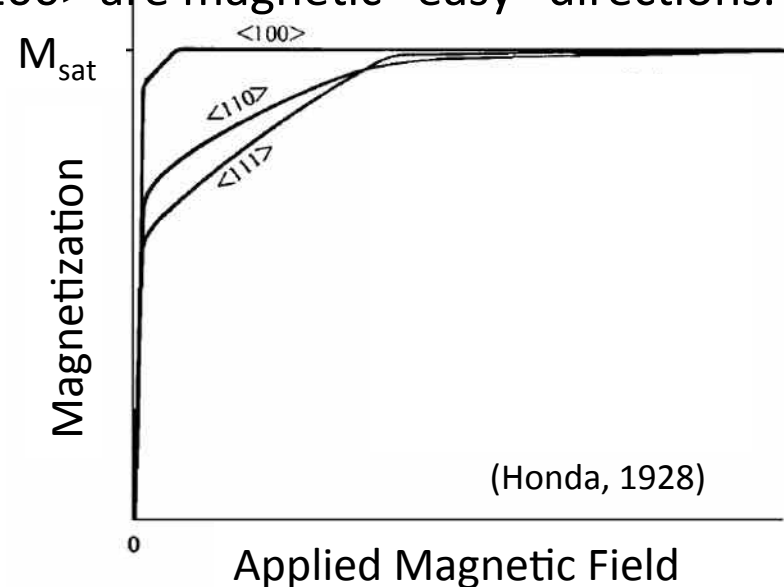
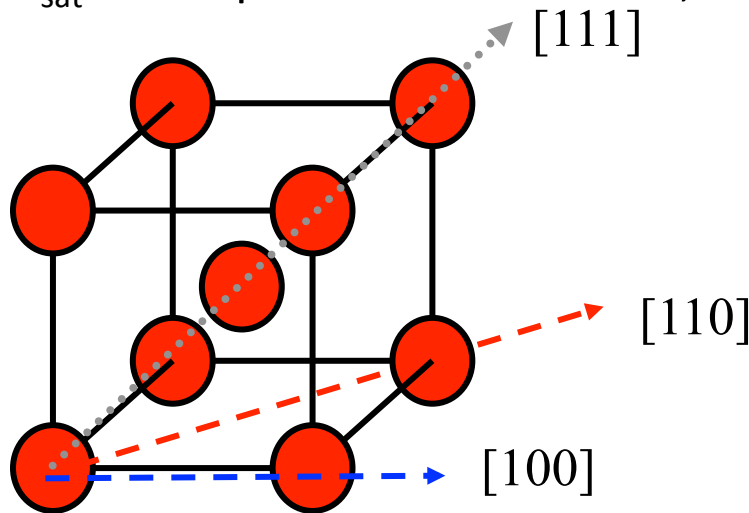
- 1st documented by James Joule in 1842. – Attribute of iron, nickel, and other ferromagnetic metals
- Effect will not “de-pole”
- Above Curie temperature ($\sim 750^{\circ}\text{C}$ for Fe-Ga alloys) domain ordering vanishes, but order returns when cooled below Curie temperature.



What Produces Magnetostriction?

Magnetostriction arises from magnetic-field induced changes in crystal structure

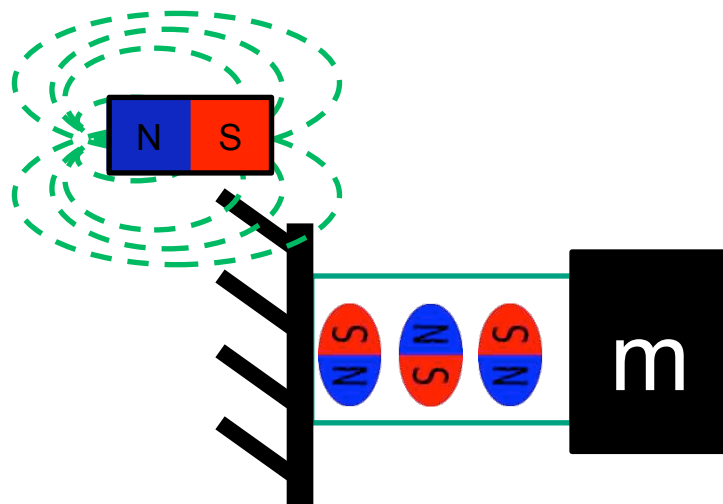
- Reorientation of electron spins to align fields with an externally applied magnetic field changes inter-atomic spacing while maintaining conservation of volume.
- Simple body centered cubic structure of Fe has maximum magnetostriction (λ_{sat}) along the $\langle 100 \rangle$ directions. ($\lambda_{\text{sat}} \langle 100 \rangle > \lambda_{\text{sat}} \langle 110 \rangle > \lambda_{\text{sat}} \langle 111 \rangle$)
- M_{sat} is independent of direction, but $\langle 100 \rangle$ are magnetic “easy” directions.



Typical uses for Magnetostriction?

ACTUATION

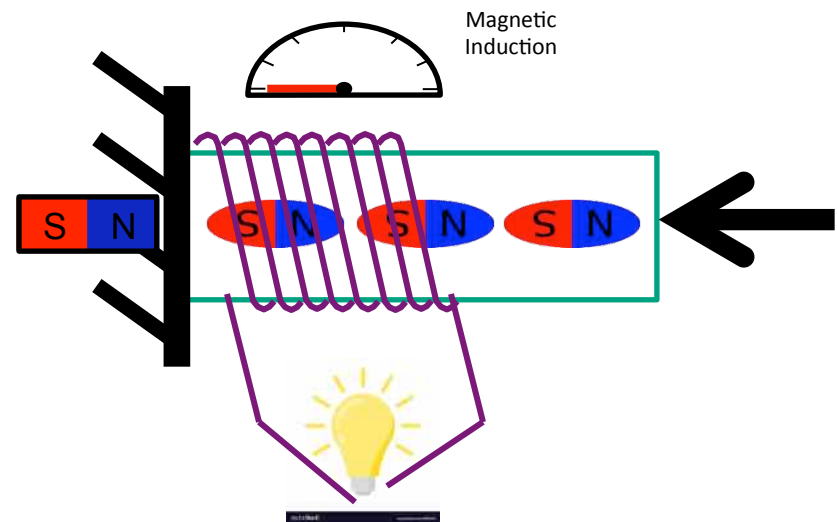
- Moving a mass
- Producing a force



SENSING & ENERGY

HARVESTING

- Detecting motion or strain
- Detecting a force or moment
- Voltage in a surrounding coil proportional to dB/dt



Magnetostriction often modeled using
1-D Linear constitutive equations

Actuation along [100] axis modeled by the
“direct effect” (Joule magnetostriction):

$$\varepsilon = \sigma / E_y^H + d_{33}H + \alpha\Delta T$$

Sensing along [100] axis modeled by the
“inverse effect” (Villari effect):

$$B = d_{33}^*\sigma + \mu^\sigma H + P\Delta T$$

where $H=nl$

Magnetostriction often modeled using
1-D Linear constitutive equations

Actuation along [100] axis modeled by the
“direct effect” (Joule magnetostriction):

$$\varepsilon = \sigma / E_y^H + d_{33}H + \alpha\Delta T$$

Sensing along [100] axis modeled by the
“inverse effect” (Villari effect):

$$B = d_{33}^*\sigma + \mu^\sigma H + P\Delta T$$

where $H=nl$

Magnetostriction often modeled using
1-D Linear constitutive equations

Actuation along [100] axis modeled by the
“direct effect” (Joule magnetostriction):

$$\varepsilon = \sigma / E_y^H + d_{33}H + \alpha\Delta T$$

Sensing along [100] axis modeled by the
“inverse effect” (Villari effect):

$$B = d_{33}^*\sigma + \mu^\sigma H + P\Delta T$$

The 33 subscript indicates the effect and response
are in the same directions

Magnetostriction often modeled using
1-D Linear constitutive equations

Actuation along [100] axis modeled by the
“direct effect” (Joule magnetostriction):

$$\varepsilon = \sigma / E_y^H + d_{33}H + \alpha\Delta T$$

Sensing along [100] axis modeled by the
“inverse effect” (Villari effect):

$$B = d_{33}^*\sigma + \mu^\sigma H + P\Delta T$$

where $H=nl$

Magnetostriction often modeled using
1-D Linear constitutive equations

Actuation along [100] axis modeled by the
“direct effect” (Joule magnetostriction):

$$\varepsilon = \sigma / E_y^H + d_{33} H + \alpha \Delta T$$

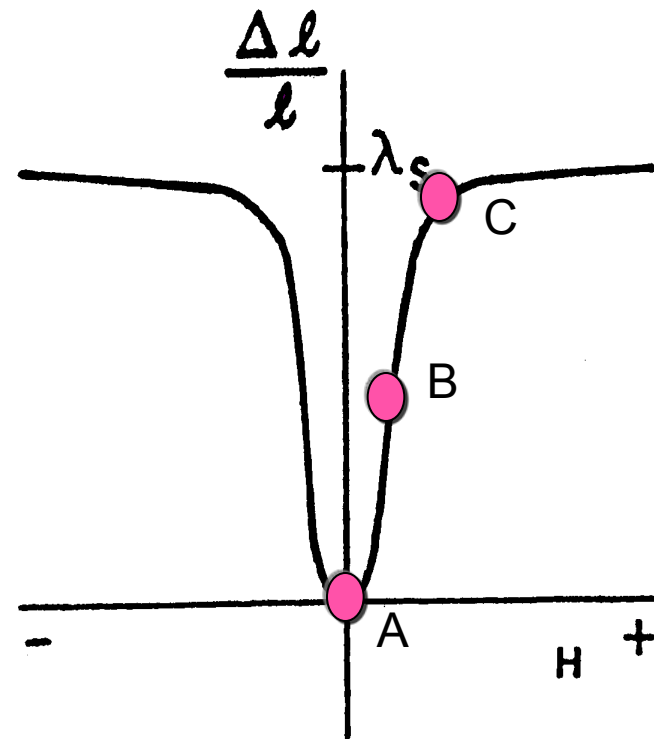
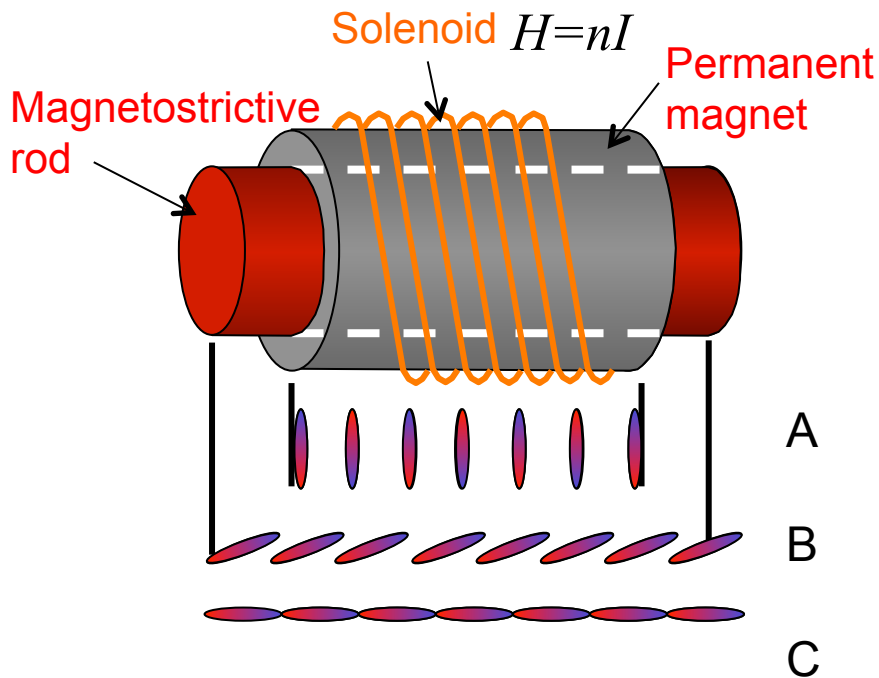
Sensing along [100] axis modeled by the
“inverse effect” (Villari effect):

$$B = d_{33}^* \sigma + \mu^\sigma H + P \Delta T$$

Magneto-mechanical coupling terms where $H = \mu_0^{-1} B$

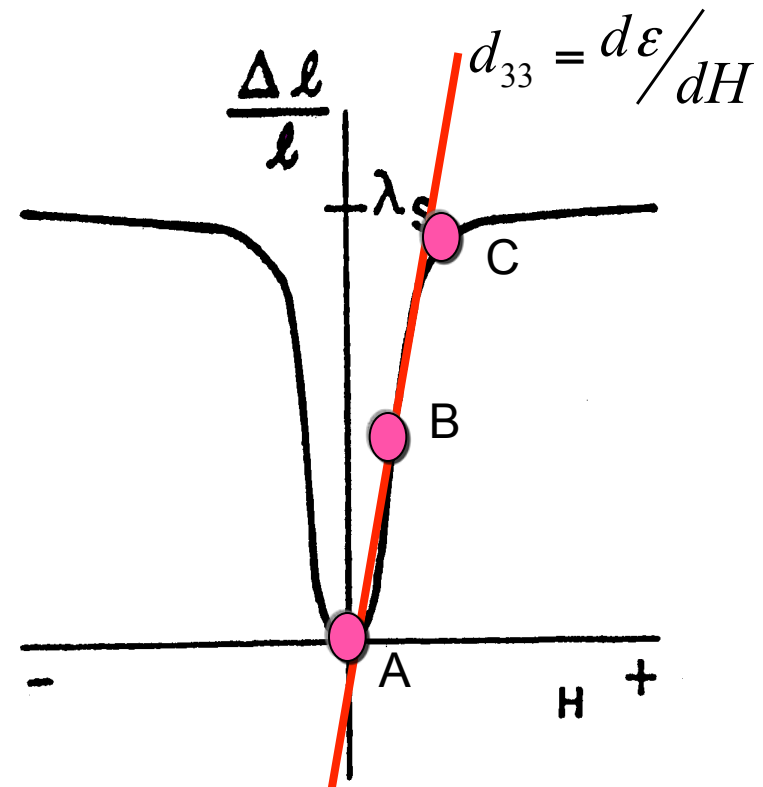
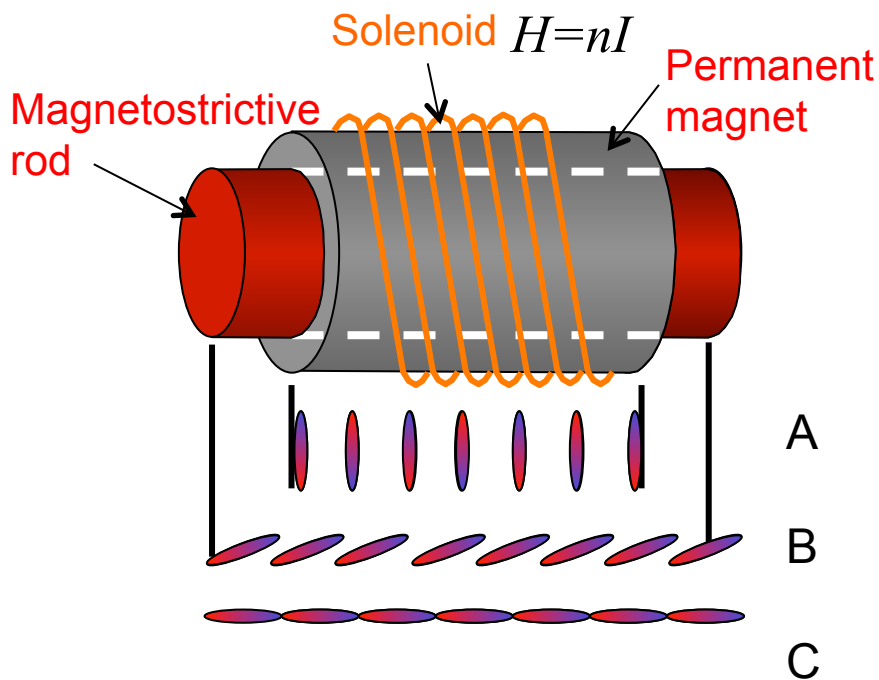
The Direct Effect (Joule magnetostriction):
The change in the dimensions of a ferromagnetic body
caused by a change in its state of magnetization.

$$\Delta H \rightarrow \Delta \lambda$$



The Direct Effect (Joule magnetostriction):
 The change in the dimensions of a ferromagnetic body caused by a change in its state of magnetization.

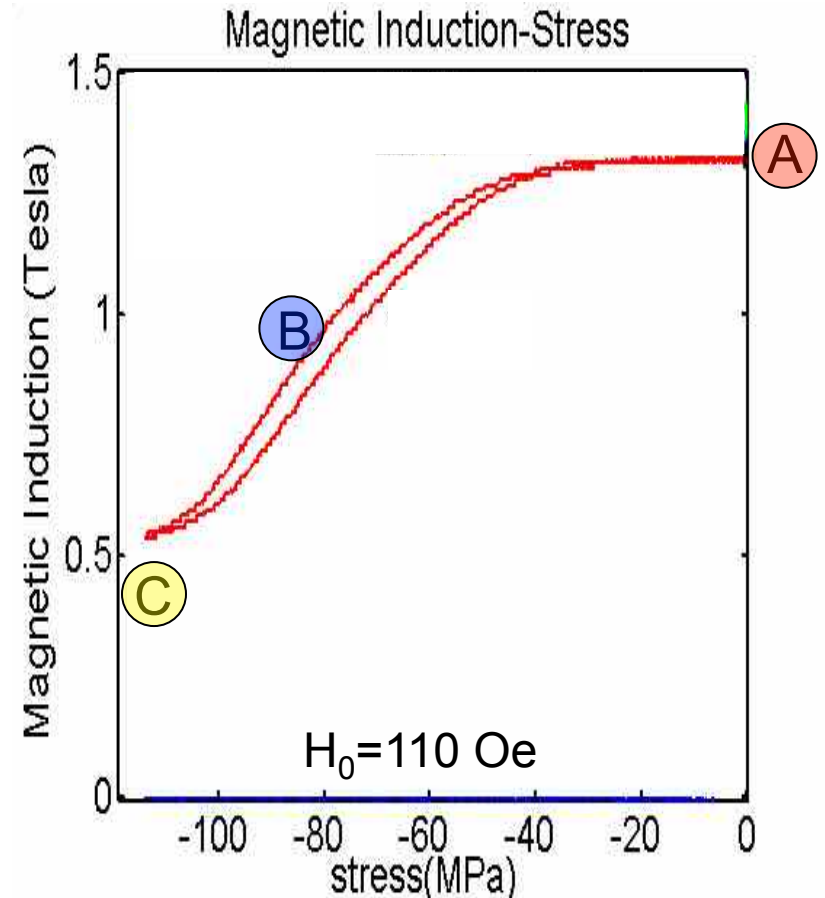
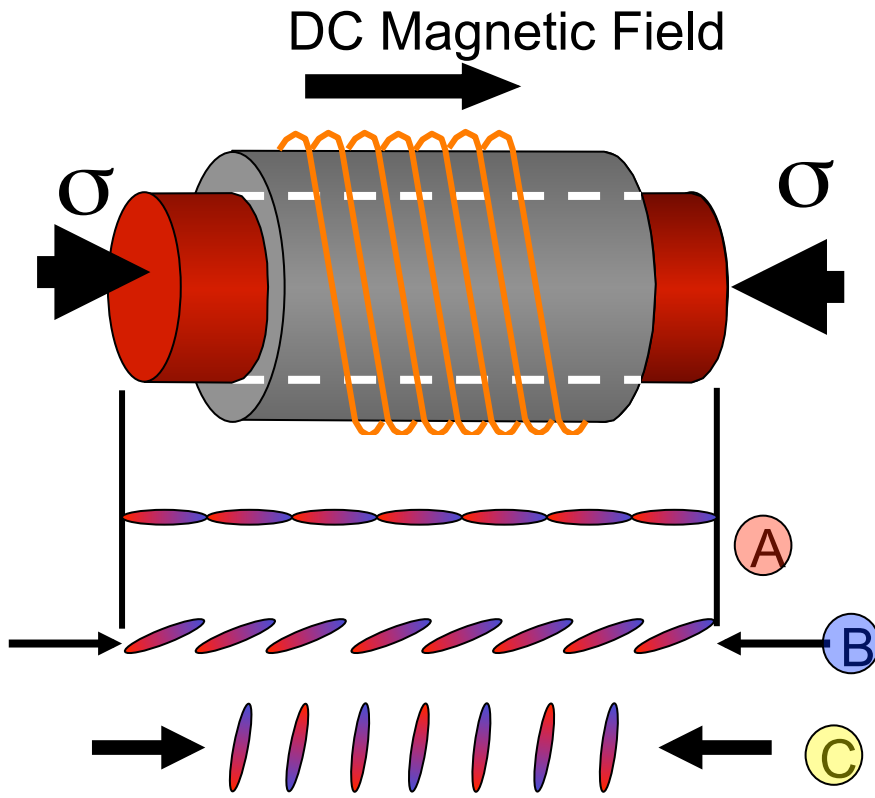
$$\Delta H \rightarrow \Delta \lambda$$



The Inverse Effect (Villari effect):

A change in magnetic state caused by a change in stress.

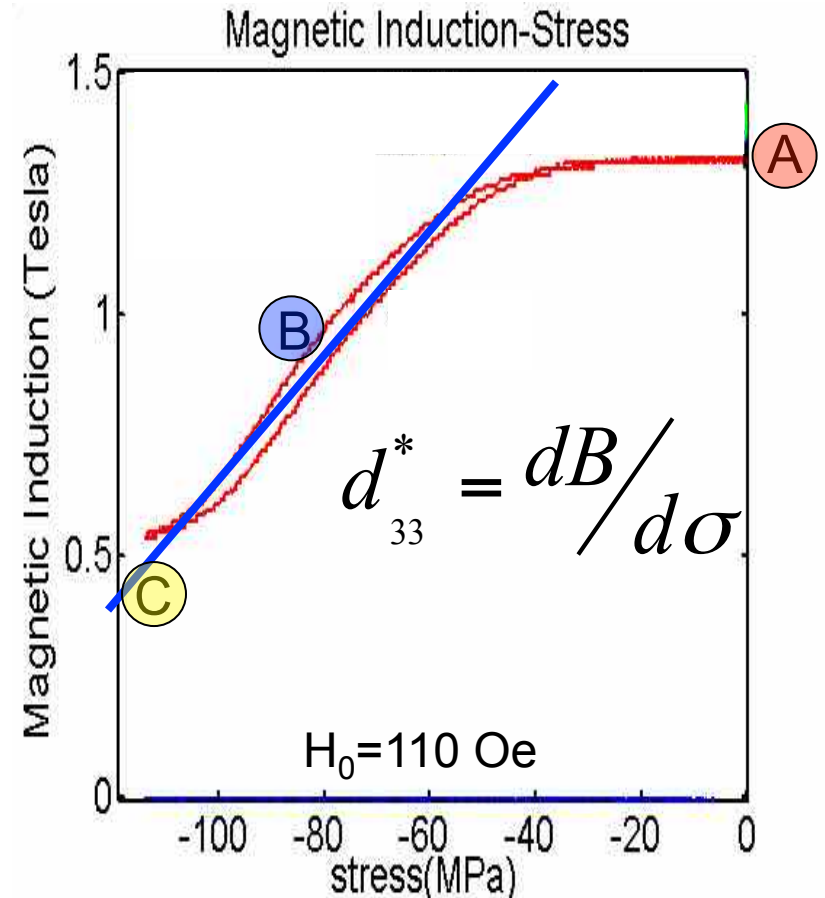
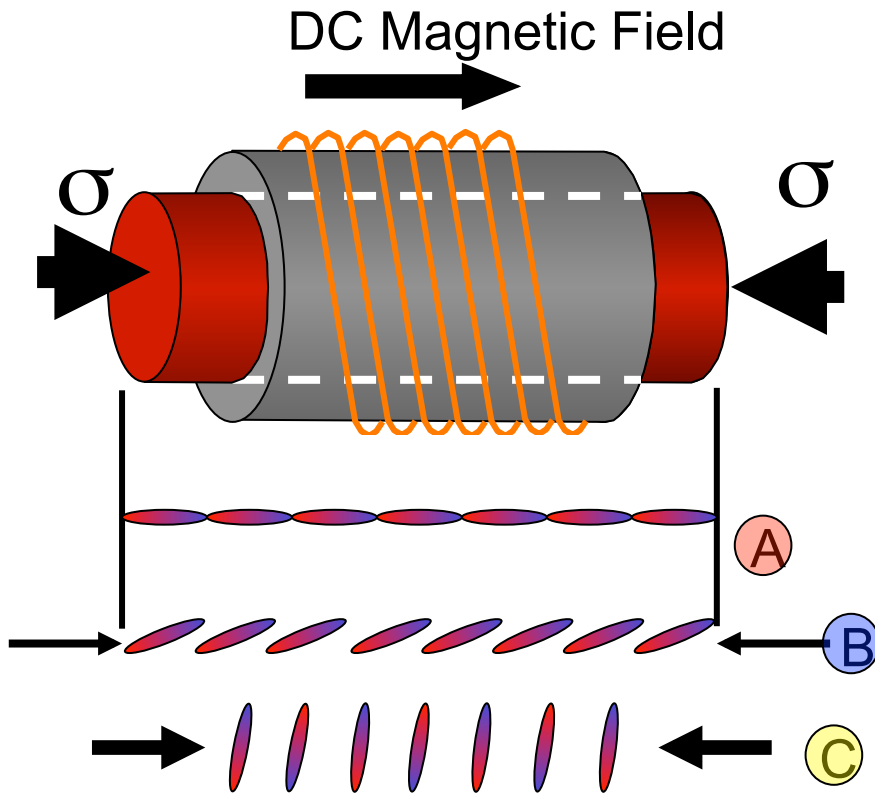
$$\Delta\sigma \longrightarrow \Delta B$$



The Inverse Effect (Villari effect):

A change in magnetic state caused by a change in stress.

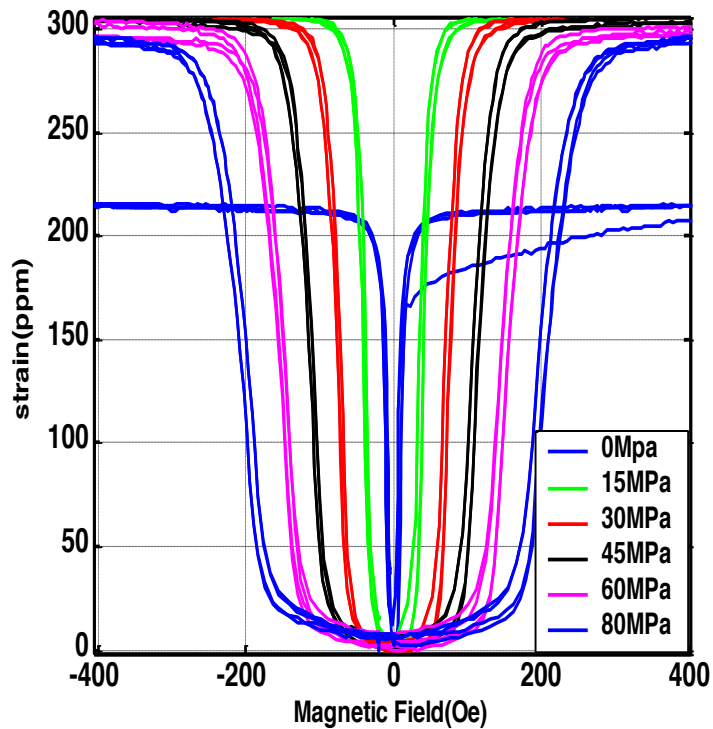
$$\Delta\sigma \longrightarrow \Delta B$$



19% Ga single crystal Galfenol

The Direct Effect:

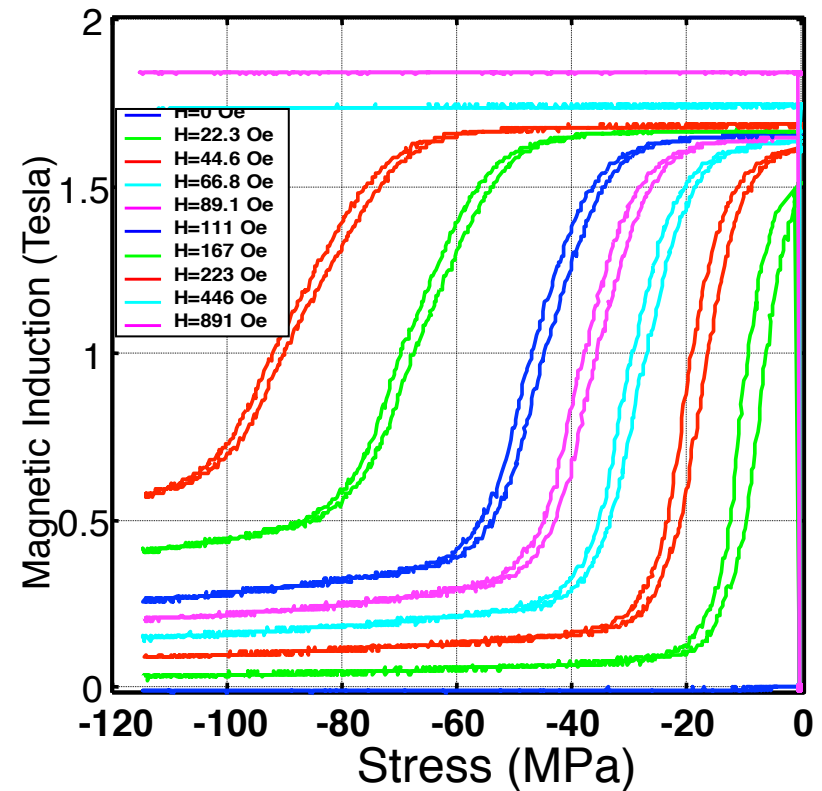
The change in the dimensions of a ferromagnetic body caused by a change in its state of magnetization.



$$\Delta H \Rightarrow \Delta \lambda$$

The Inverse Effect:

A change in magnetic state caused by a change in stress.

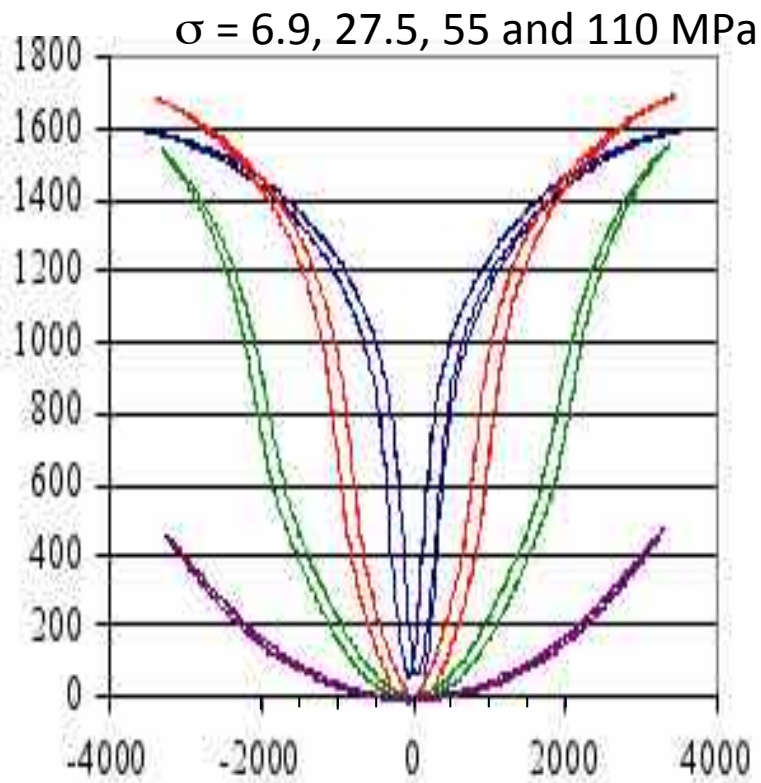


$$\Delta \sigma \Rightarrow \Delta B$$

Production grade Terfenol-D

The Direct Effect:

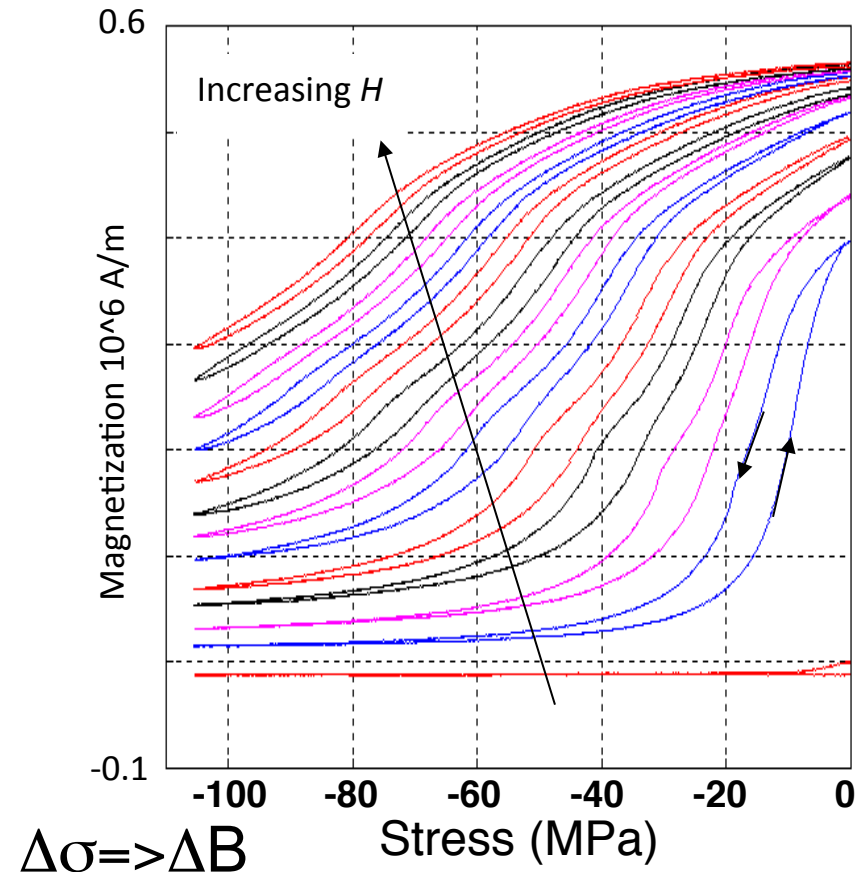
The change in the dimensions of a ferromagnetic body caused by a change in its state of magnetization.



$$\Delta H \Rightarrow \Delta \lambda$$

The Inverse Effect:

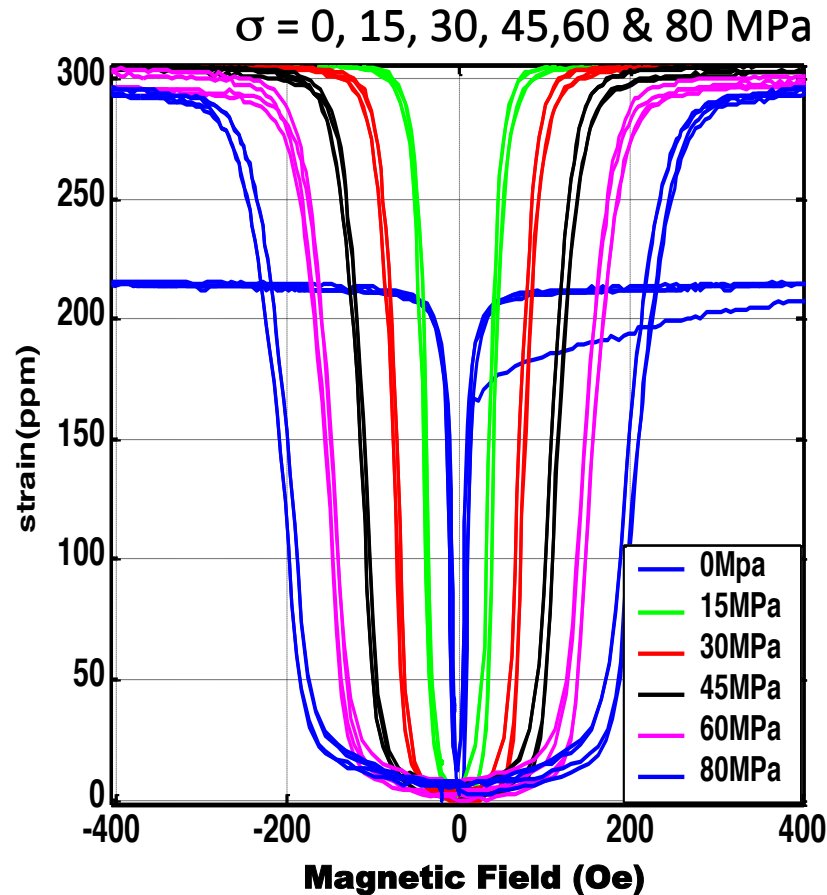
A change in magnetic state caused by a change in stress.



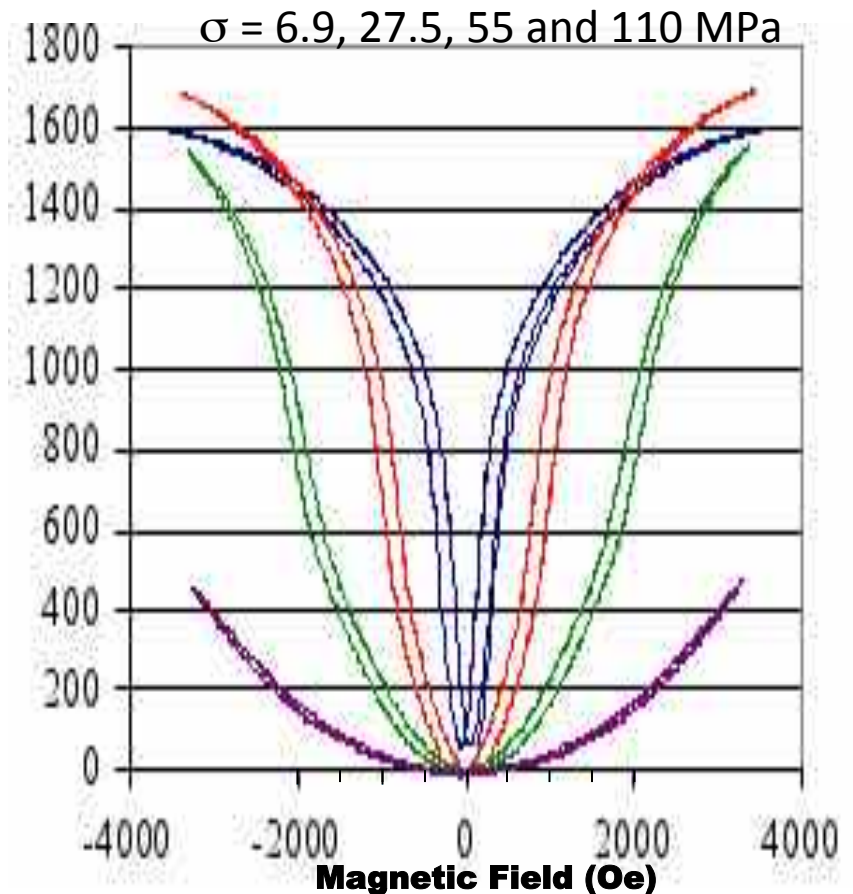
$$\Delta \sigma \Rightarrow \Delta B$$

Comparison of direct effect in Galfenol (left) and Terfenol-D (right)

19% Ga single crystal Galfenol



Production grade Terfenol-D

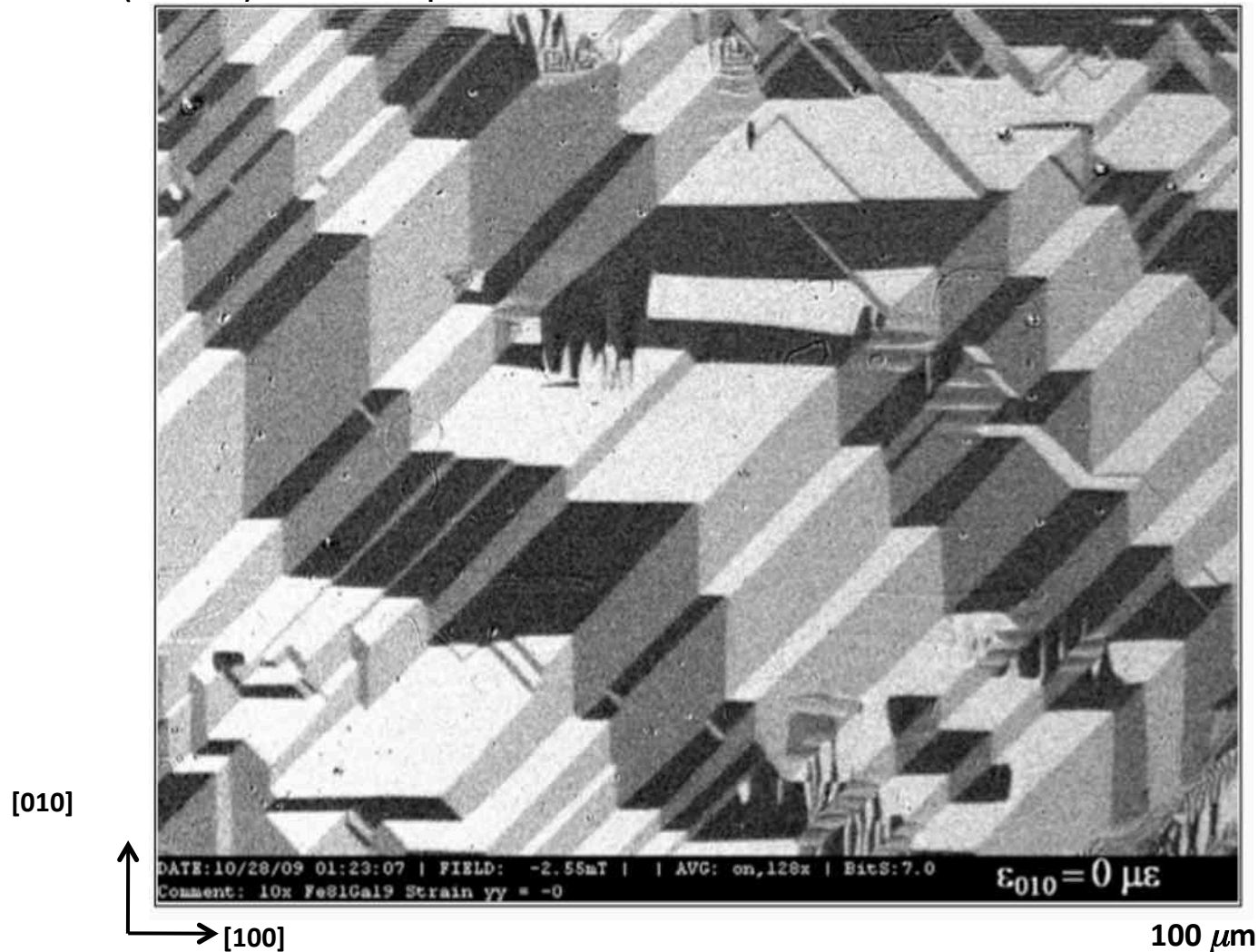
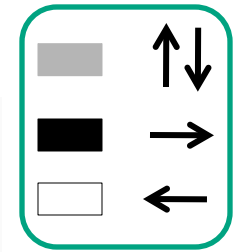


Galfenol data from Dr. J. "Atul" Atulasimha's dissertation (2006)

Terfenol-D data from ETREMA Products, Inc. product sheet

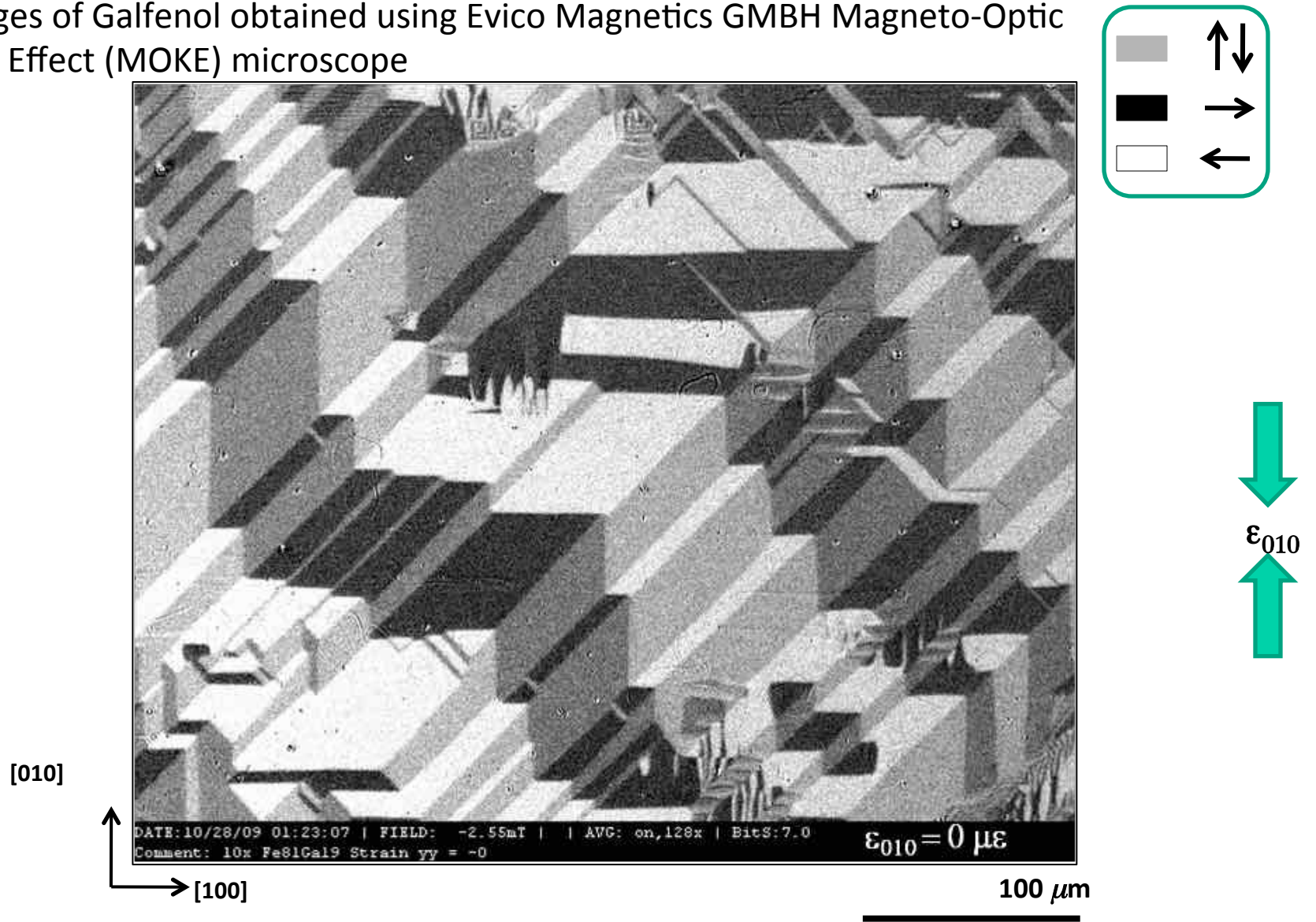
MOKE images of quenched $\text{Fe}_{81}\text{Ga}_{19}$ under compressive stress/strain (0-1500 microstrain)

Images of Galfenol obtained using Evico Magnetics GMBH Magneto-Optic Kerr Effect (MOKE) microscope



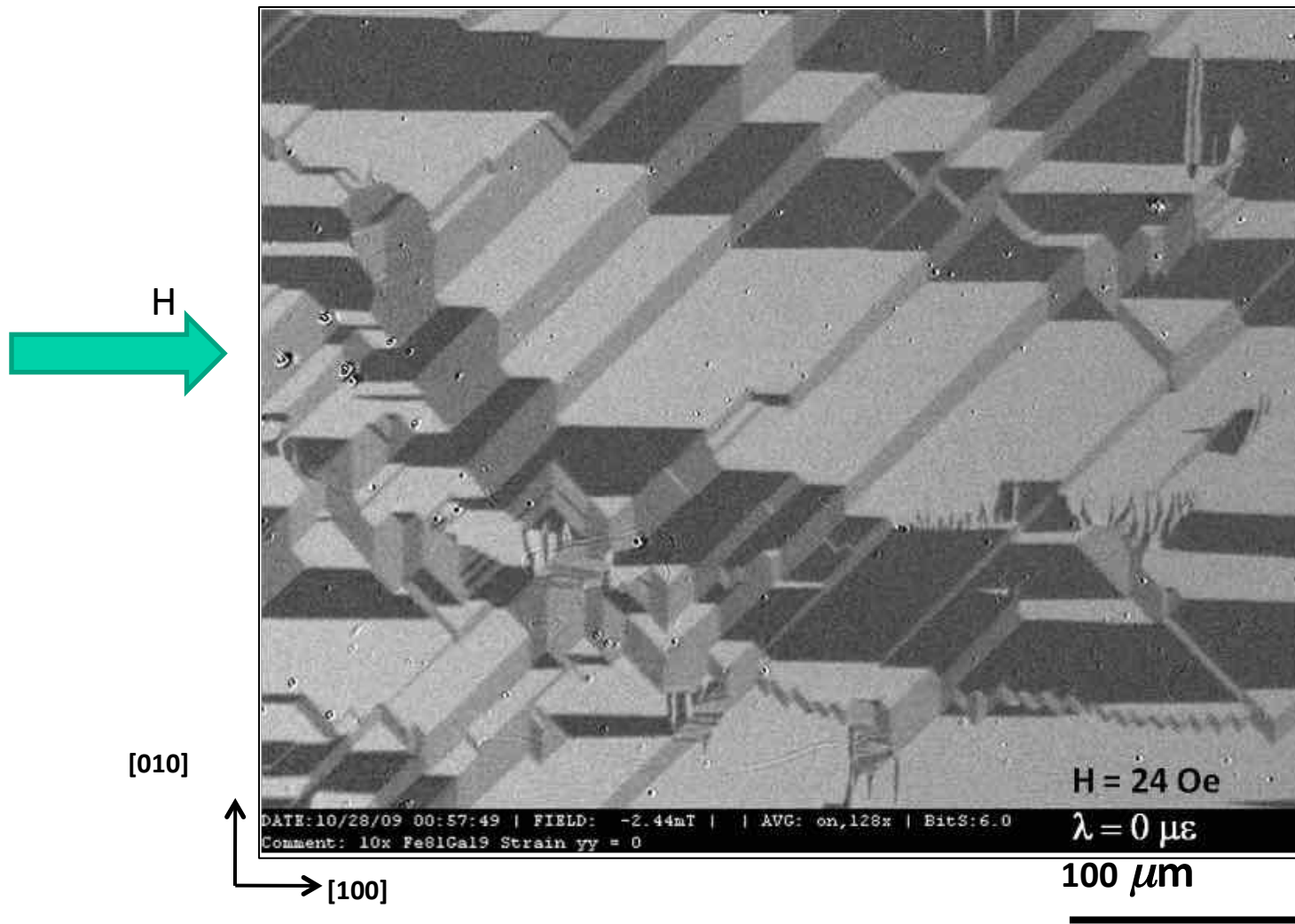
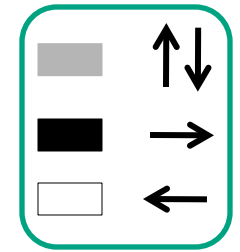
MOKE images of quenched $\text{Fe}_{81}\text{Ga}_{19}$ under compressive stress/strain (0-1500 microstrain)

Images of Galfenol obtained using Evico Magnetics GMBH Magneto-Optic Kerr Effect (MOKE) microscope



MOKE images of quenched $\text{Fe}_{81}\text{Ga}_{19}$ under magnetic field (0-200+ Oe)

Images of Galfenol obtained using Evico Magnetics GMBH Magneto-Optic Kerr Effect (MOKE) microscope



Outline

Intro to Magnetostriction

Actuators: the “direct” effect

Sensors: the “inverse” (or Villari) effect

Structural Magnetostrictive Alloys

Magnetostrictive, magnetic & mechanical properties

Thin, highly textured rolled sheet

Introduction to auxetic behavior

Applications that use Galfenol

Bending sensor applications

Implantable wireless bone fixity sensor (Tech Univ. Dresden)

Nanowire sensors (Univ. Minn. & UMD)

Applications for auxeticity?

Micro-motors (Kanazawa University, Japan)

Energy Harvesting (Kanazawa Univ, UMD & Techno Sciences, Inc., Oscilla Power)

Summary

Common Magnetostrictive Materials

STRUCTURAL Magnetostrictive Alloys

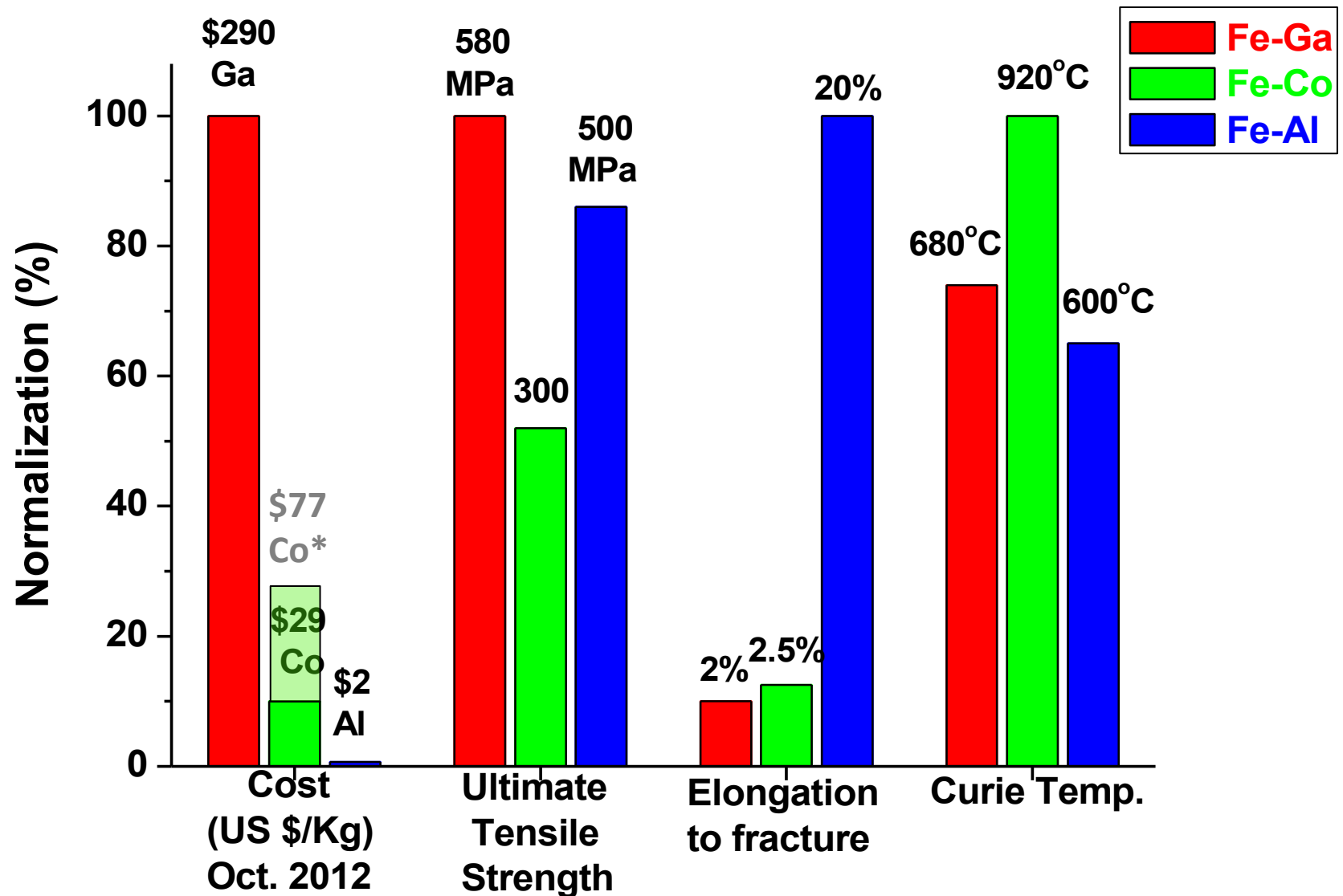
	Terfenol-D	Iron	Nickel	$\text{Fe}_{1-x}\text{Co}_x$	$\text{Fe}_{1-x}\text{Al}_x$	$\text{Fe}_{1-x}\text{Ga}_x$
$3/2 \lambda_s$ (μstrain)	1600-2400	-24	-66	140-220	185	~400
Modulus (GPa)	25-35	200	207	270	65	65
Relative Permeability	2-10	5000	100-600	~3000	100	70-100
Saturation Magnetization	1.0 T	1.6-2.2 T	~0.6 T	~2T	1.4 T	1.6 T
Ultimate Tensile Strength (MPa)	28 (& very brittle)	400	500	300-870	500-800	500-600
Hysteresis in λ -H and B-H curves	Moderate	Low	Low	Very Low	Very Low	Very Low

High magnetostriction
Poor magnetic & mechanical properties

Low magnetostriction
Good mechanical properties

Good magnetostriction
Good magnetic and mechanical properties

Comparison of binary **Fe-Ga** ($\lambda=400 \mu\epsilon$), **Fe-Co** ($\lambda=150\mu\epsilon$) and **Fe-Al** ($\lambda=175\mu\epsilon$)



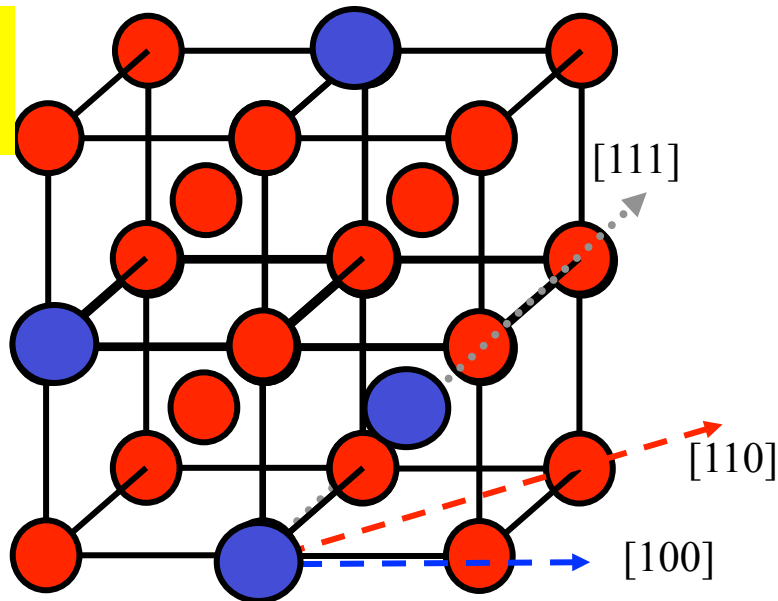
Galfenol - $\text{Fe}_{1-x}\text{Ga}_x$
($0.13 < x < 0.35$)

Gallium + Iron (Fe) +
Naval Ordnance
Laboratory

Alfenol - $\text{Fe}_{1-x}\text{Al}_x$
($0.13 < x < 0.35$)

Aluminium + Iron (Fe) +
Naval Ordnance
Laboratory

X% Fe replaced with
Ga (or Al)
Start with BCC
Iron Lattice



● Iron atoms

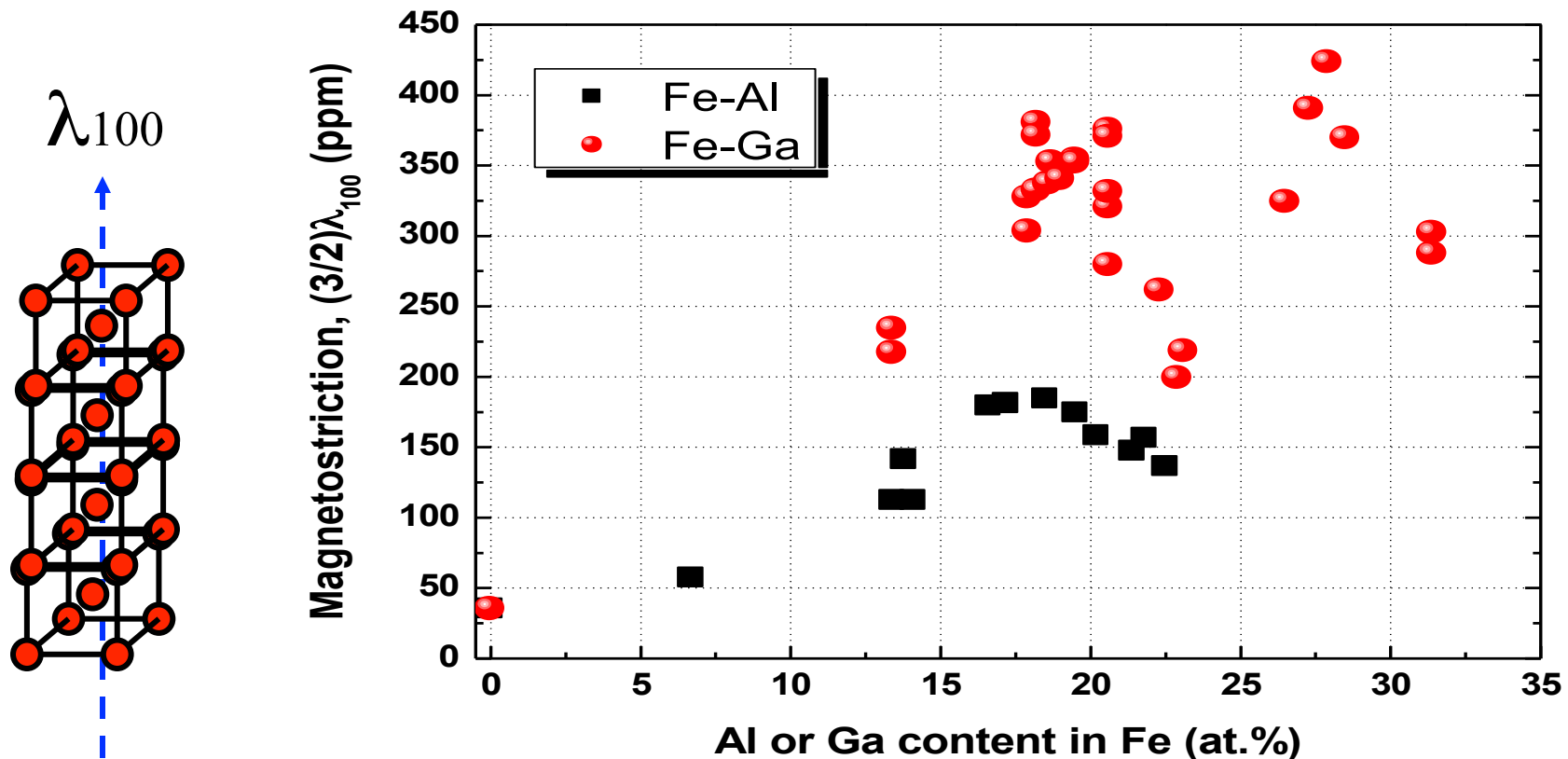
● Gallium (or Aluminum) atoms

Galfenol - $\text{Fe}_{1-x}\text{Ga}_x$
($0.13 < x < 0.35$)

Gallium + Iron (Fe) +
Naval Ordnance

Alfenol - $\text{Fe}_{1-x}\text{Al}_x$
($0.13 < x < 0.35$)

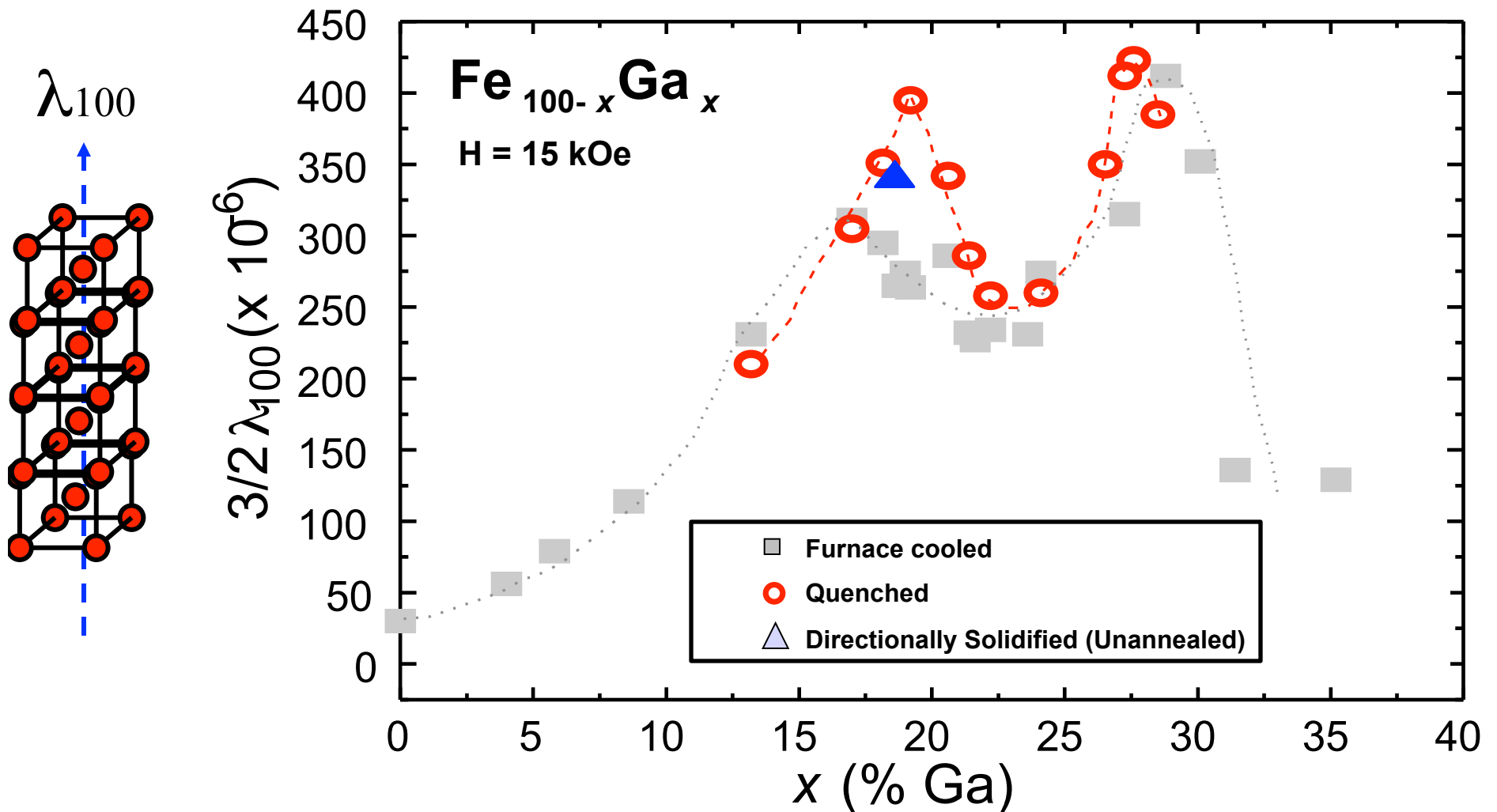
Aluminum + Iron (Fe) +
Naval Ordnance



Plotting single crystal data at 15 kOe from [Restorff et al. JAP 111, 023905 (2012)]

Magnetostriction of Galfenol

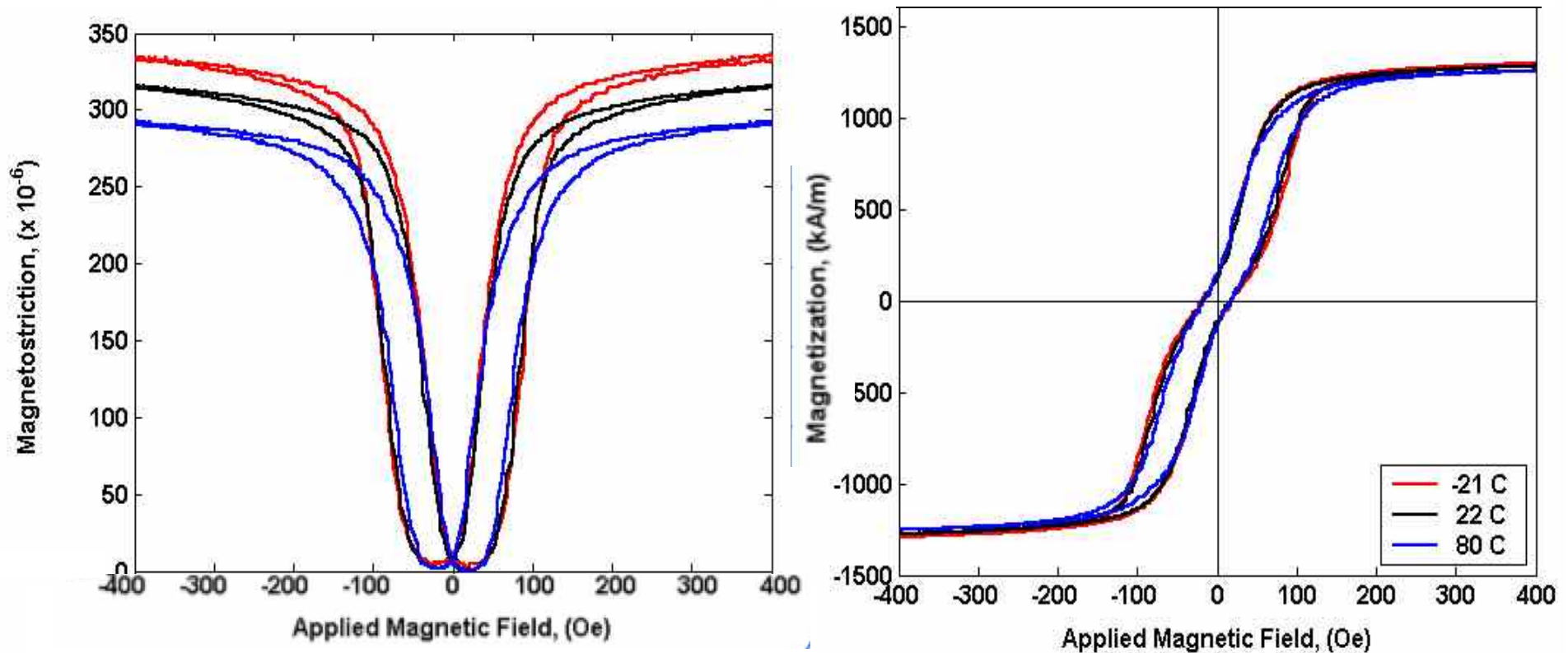
- Sensitive to composition and to heat treatment [Clark et al. 2003]



Temperature Dependencies of $\lambda(H)$ & $M(H)$ in 19% Ga Fe-Ga Single Crystal

$\text{Fe}_{81}\text{Ga}_{19}$ Single crystal @ 45.3 MPa. -22°C (red) to +80°C (blue)

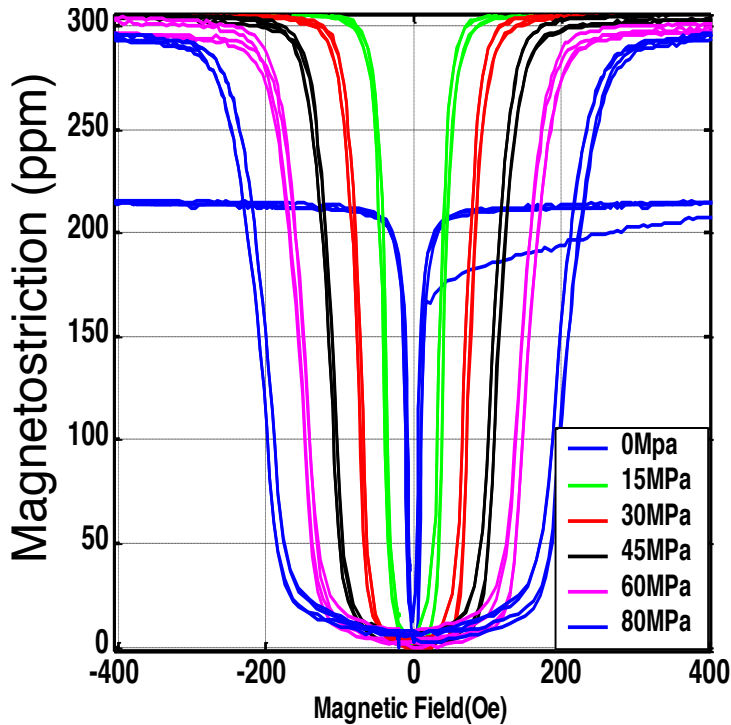
Note: hysteresis is induced by transducer bushing – is not in FeGa rod



The Direct Effect: The change in the dimensions of a ferromagnetic body caused by a change in its state of magnetization.

Single Crystal FeGa

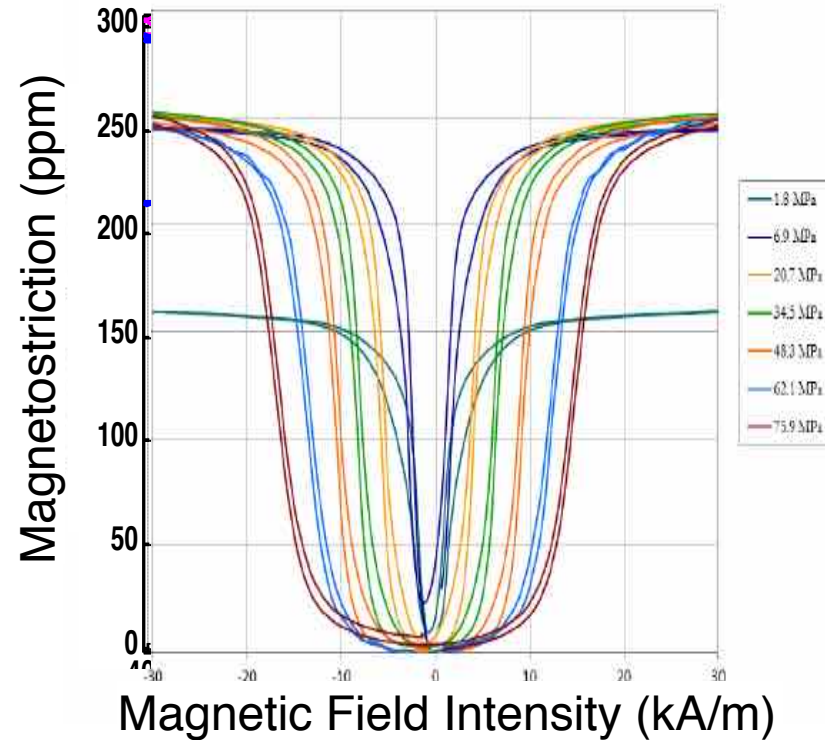
\$\$\$\$\$



Magnetic Field Intensity (Oe)

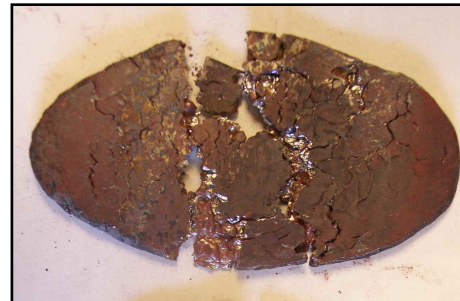
Polycrystalline FeGa

\$\$

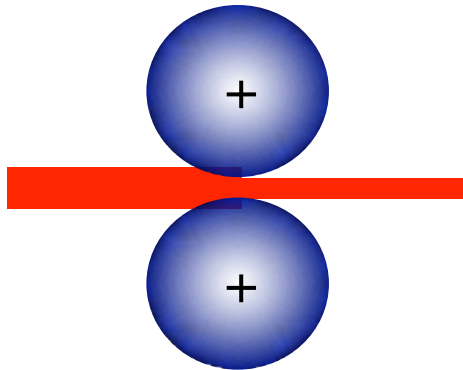


Magnetic Field Intensity (kA/m)

Rolling Steps to Lower Fabrication Costs

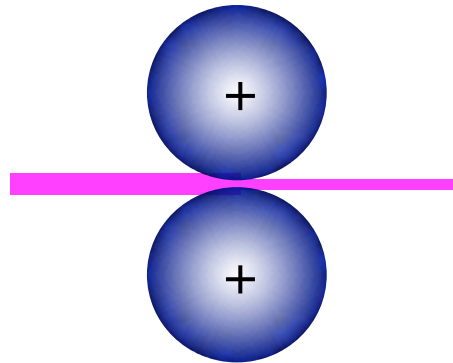


• Binary alloy experienced intergranular fracture

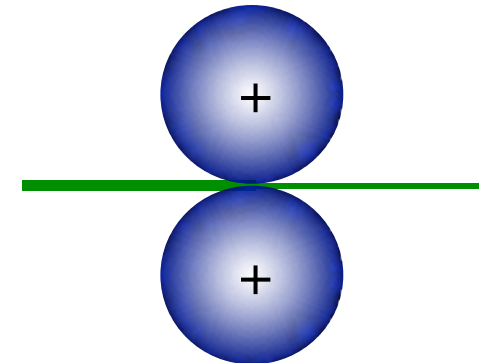


Hot Rolling

- Arc-melted buttons
- Roller set in 0.0031 inch
- 1000/800°C for 10 min. every 2 passes
- Seal in 321 Stainless



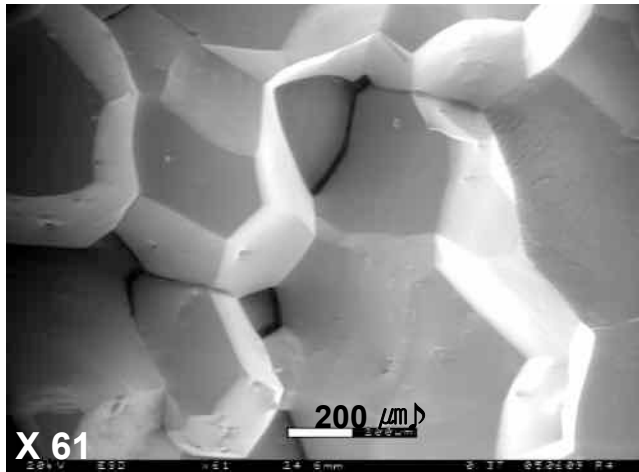
Warm Rolling



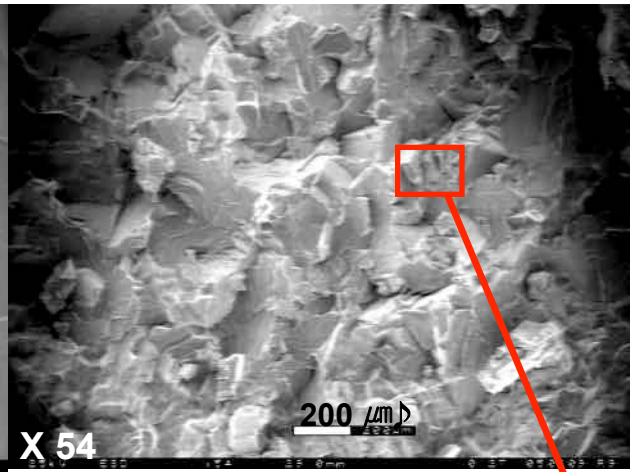
Cold Rolling

Intergranular Fracture Mode Changed to Intragranular with trace Additions of B or NbC

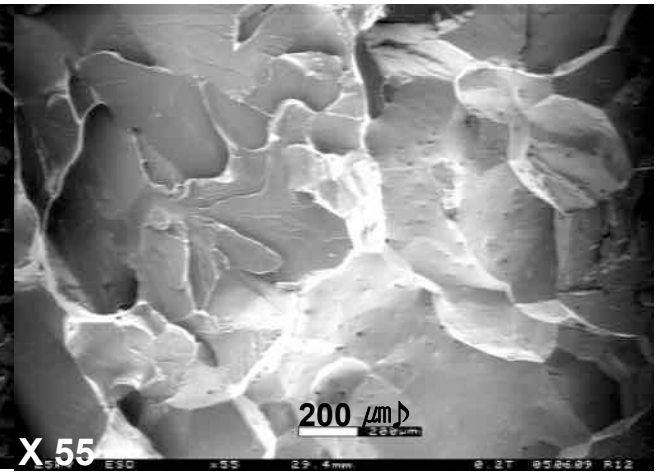
Fe-18.7% Ga



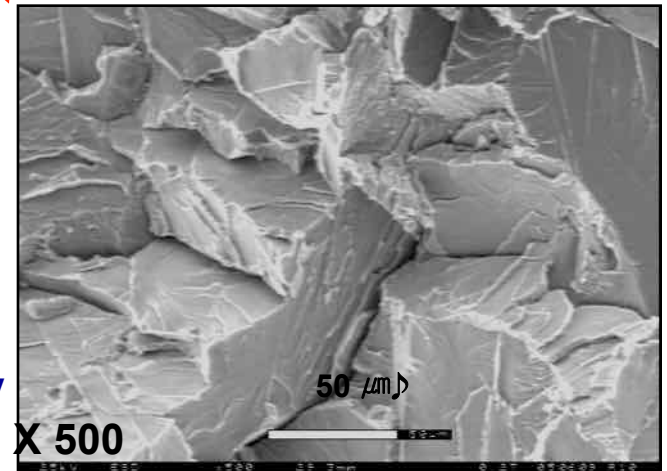
Addition of 0.5% B



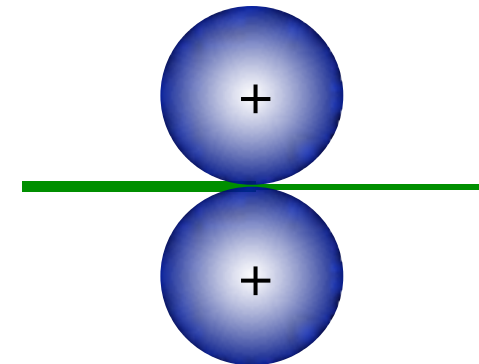
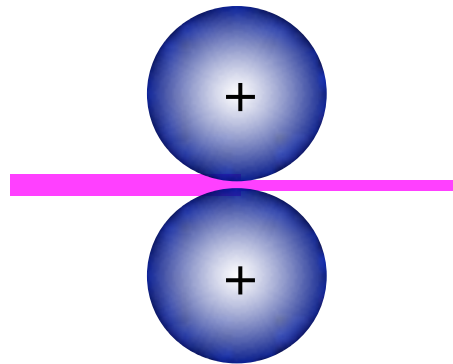
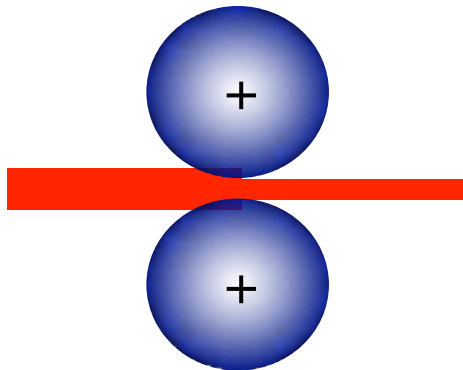
Addition of 1.0% B



- Fracture surface of the B-free Galfenol clearly appeared to a typical **intergranular mode** by crack propagation along grain boundaries.
- Fracture surface of the B-added Galfenol was changed to a **transgranular mode** by crack propagation through the grains and the grain size was also small (grain refinement).
- **Boron has a great effect on improvement of ductility due to suppressing grain boundaries fracture.**



Rolling Steps



Hot Rolling

- Arc-melted buttons
- Roller set in 0.0031 inch
- 1000/800°C for 10 min. every 2 passes
- Seal in 321 Stainless

Warm Rolling

- Roller set in 0.002 inch
- 600/400°C for 10 min. every 1 pass
- Intermediate annealing @ 800°C for 2 hrs in Ar

Cold Rolling

- Roller set in 0.0005 inch
- Subsequent annealing @ 1000 ~ 1200°C under flowing argon, sulfur atmosphere

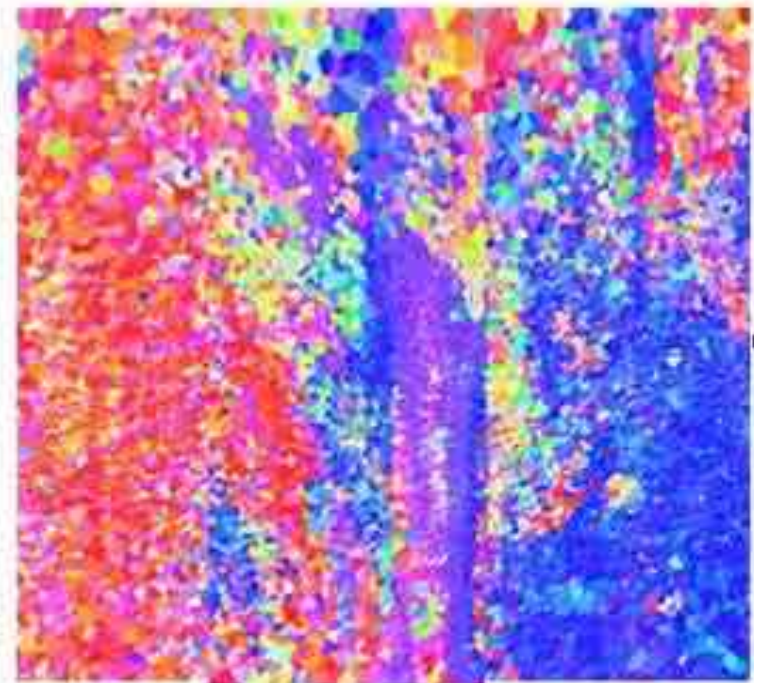
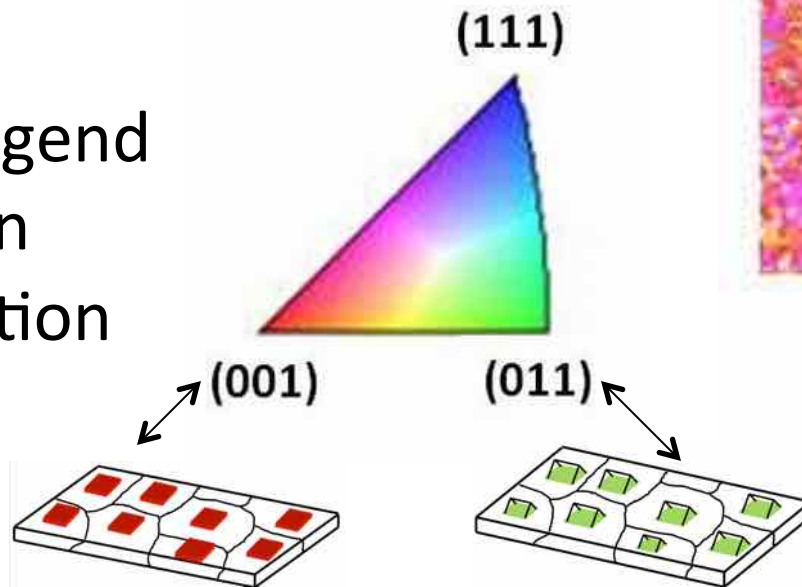
As-rolled sheet: $\lambda_{\text{sat}} \sim 60$ ppm

Goss or Cube texture $\sim 7X$ more magnetostrictive

Electron BackScatter Diffraction (EBSD) images show as-rolled grains are tilted at random orientations

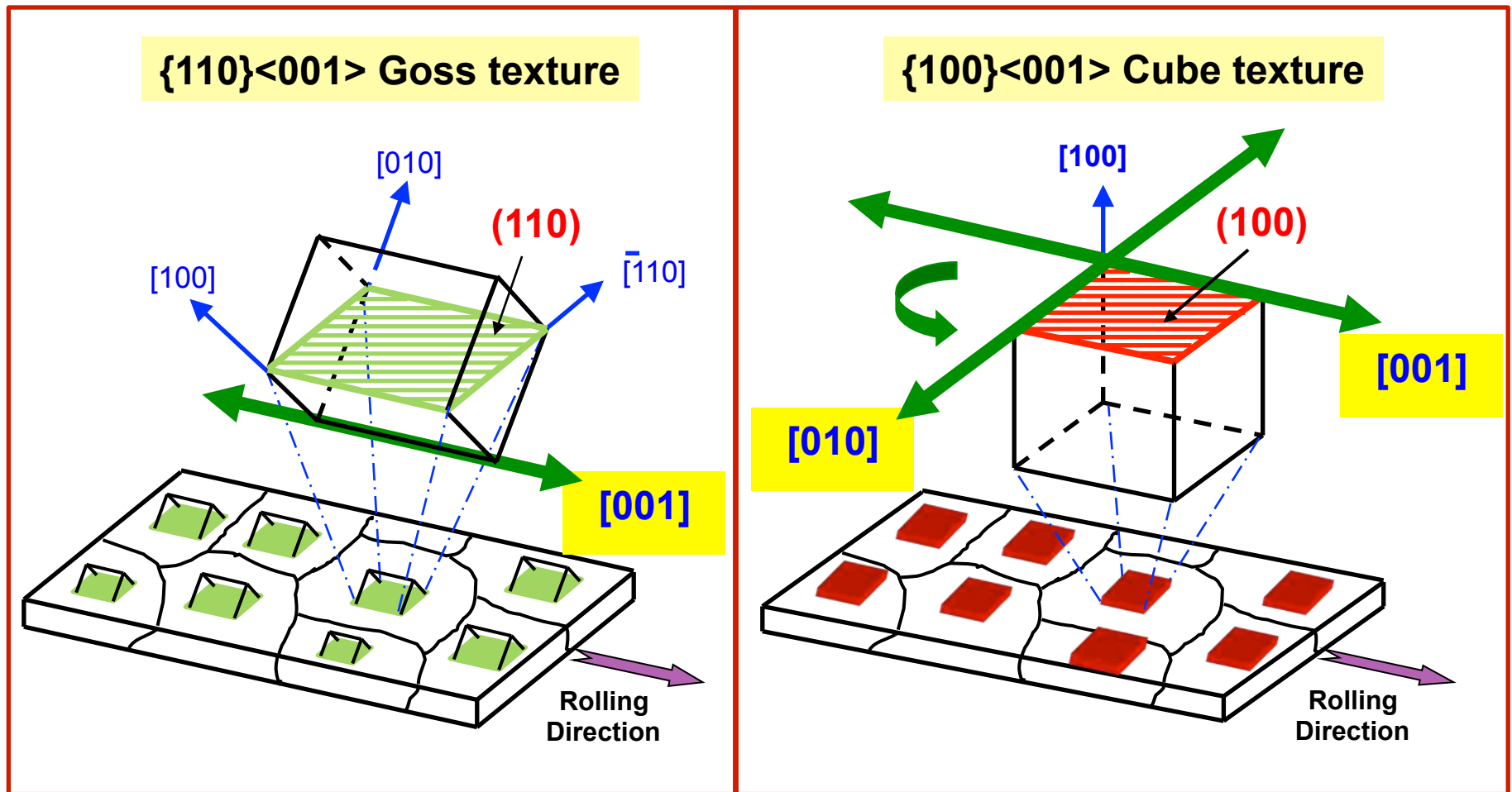
$\lambda_{\text{sat}} \sim 60$ ppm

EBSD legend for grain orientation



As-rolled
(γ -fiber & rotated cube textures)

Once rolling achieved, need to develop a preferred texture in rolled sheet



Texturing of Polycrystalline Galfenol

Inexpensive production of rolled sheet Galfenol (Alfenol) relies on the abnormal grain growth of surface textures

Goss texture {110}

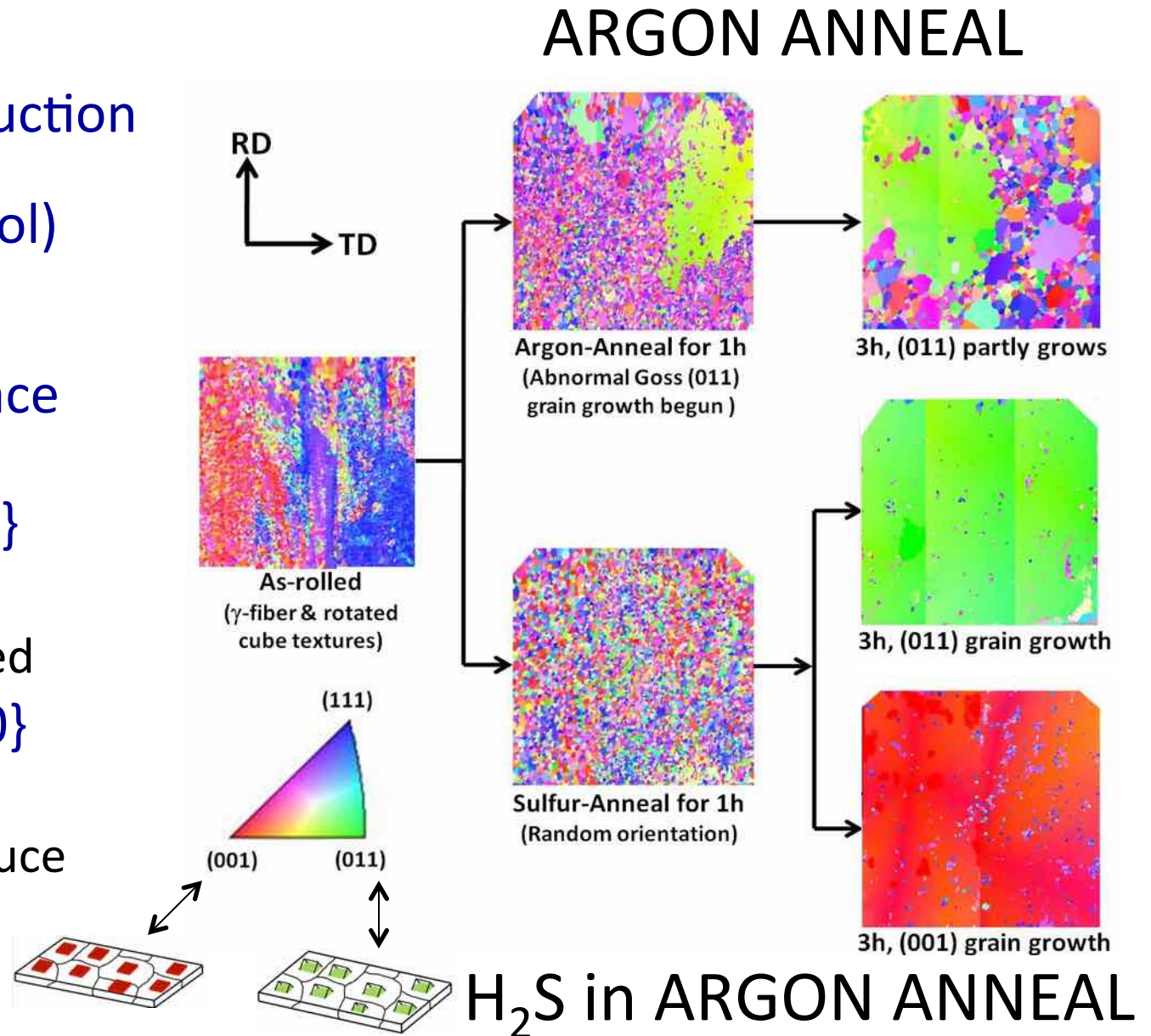
$\lambda_{100} \sim 200$ ppm

Easily reproduced

Cube texture {100}

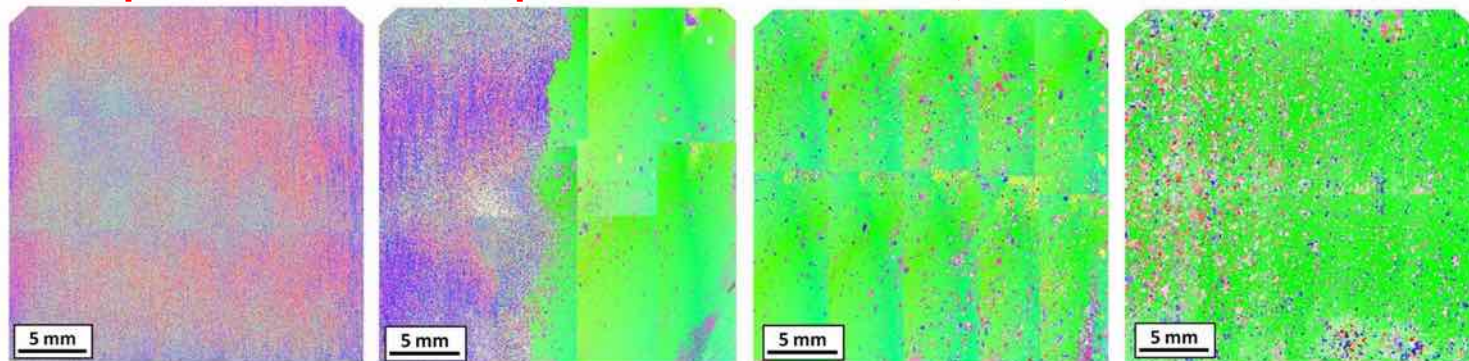
$\lambda_{100} \sim 350$ ppm

Difficult to produce



Texturing of Rolled Sheet Alfenol

- **NbC-added 20%Alfenol rolled sheets annealed under a sulfur atmosphere.**
- **Single (011) grain is abnormally grown, with $\lambda = \sim 177$ ppm.**
- **Large single (011) grains were fully grown in the samples, covering 80-99% of sample surface for sample thicknesses of 0.2, 0.35, and 0.5 mm.**

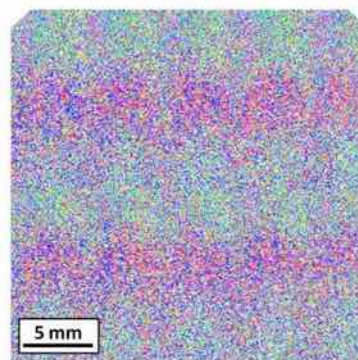
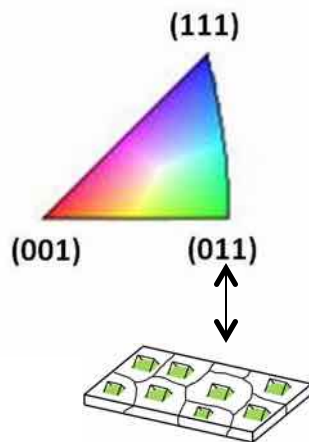


(a) 0.75%NbC, 1150°C

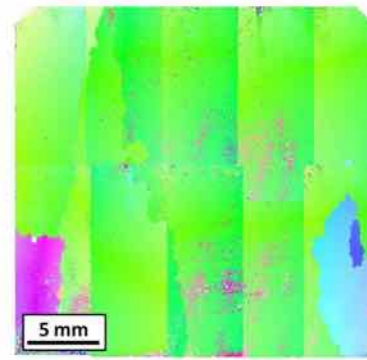
(b) 0.75%NbC, 1200°C

(c) 0.75%NbC, 1250°C

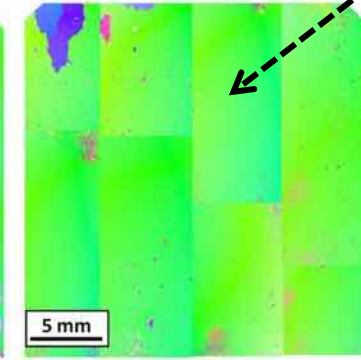
(d) 0.75%NbC, 1300°C



(e) 1.0%NbC, 1200°C



(f) 1.0%NbC, 1250°C



(g) 1.0%NbC, 1300°C

(011) Grain with $\langle 100 \rangle$ orientation

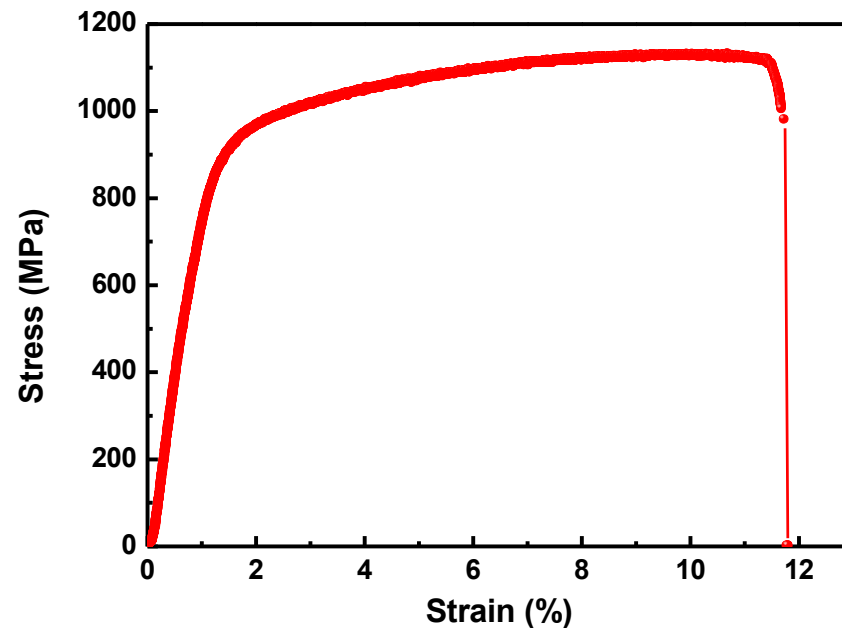
*JAP 115, 17A913 (2014)

Seeking additional insights lead to an unexpected result



(3) Tensile Test

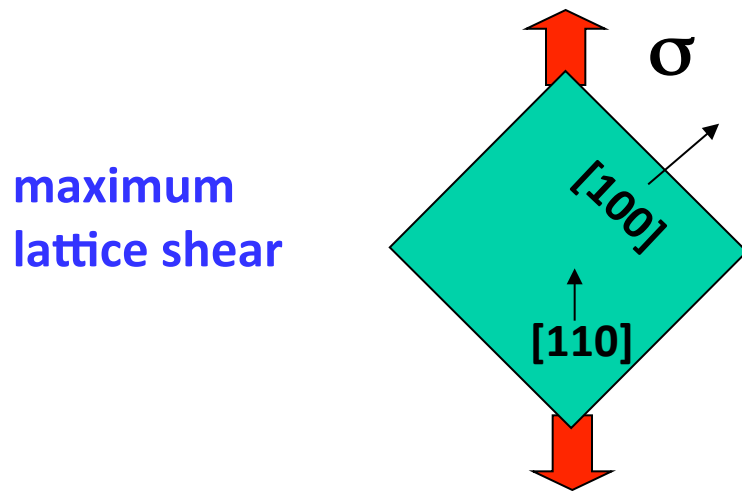
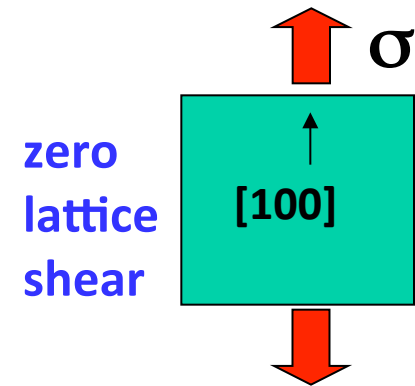
- 1) Test specimen thickness: 0.1, 0.2, 0.35, 0.5 mm
- 2) The test specimens were prepared according to ASTM A370-12a (Standard Test Methods and Definitions for Mechanical Testing).
- 3) Machine: MTS 858 Mini Bionix 25kN servo-hydraulic load frame at a rate of 0.0025 mm/s. The strain was monitored with a gauge length of 25 mm.



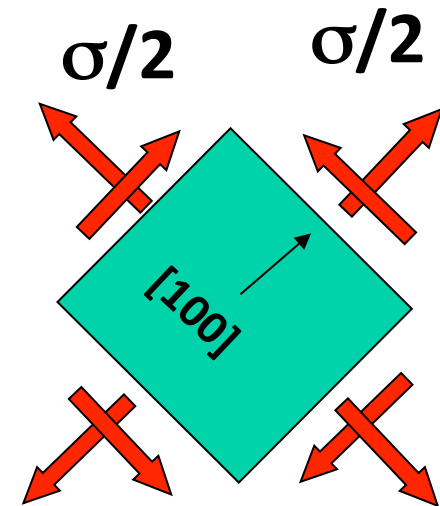
Tensile Loading to Study Slip Planes

Two Test Configurations: [100] & [110] Single Crystal Samples

- Emphasize mechanical anisotropy
- High symmetry crystal orientations
- Use axial loading (tension)



≡



Single Crystal Galfenol Samples

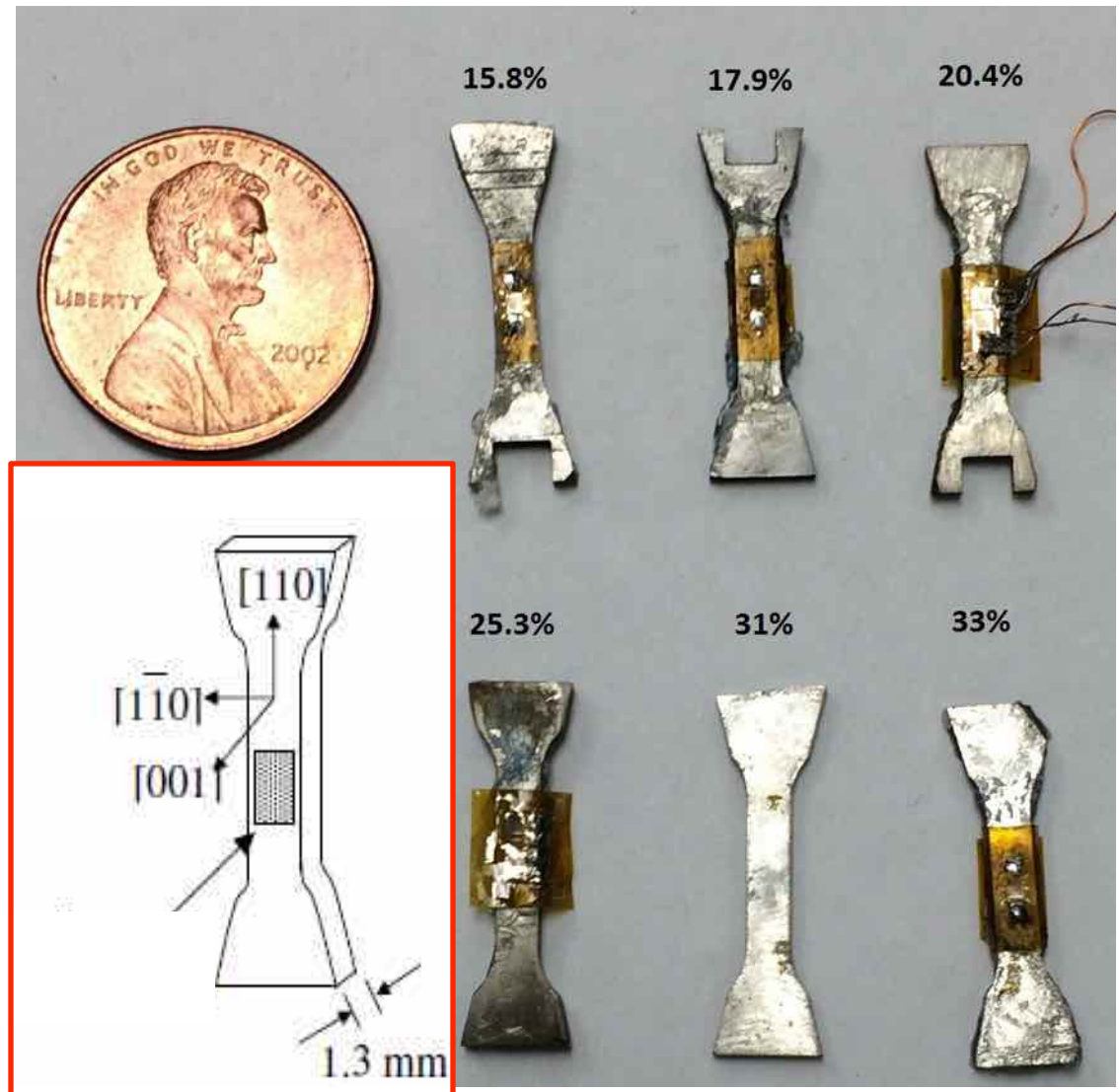
Single crystal $\text{Fe}_{100-x}\text{Ga}_x$
 $x = 15.8, 17.9, 20.4, 25.3, 31.0$ &
 33.0

Composition verification:
Laue X-ray back reflection

Dogbones Cut:
EDM along (100) face in
[100] & **[110]** directions

Strain measurement:
Bi-directional **strain gage**
rosettes **[100]** & **[110]**

RUS samples (notches) cut
from dogbones after testing



Monotonic Tension Tests

Setup & Procedure:

Longitudinal and transverse strain gages

Room temperature

MTS machine pull - constant rate mode @ $0.5 \mu\text{m/s}$

Elastic regime $\sim 3 \mu\epsilon/\text{s}$

Plastic regime $\sim 18 \mu\epsilon/\text{s}$

Pulled specimens
 $\sim 2\%$ strain

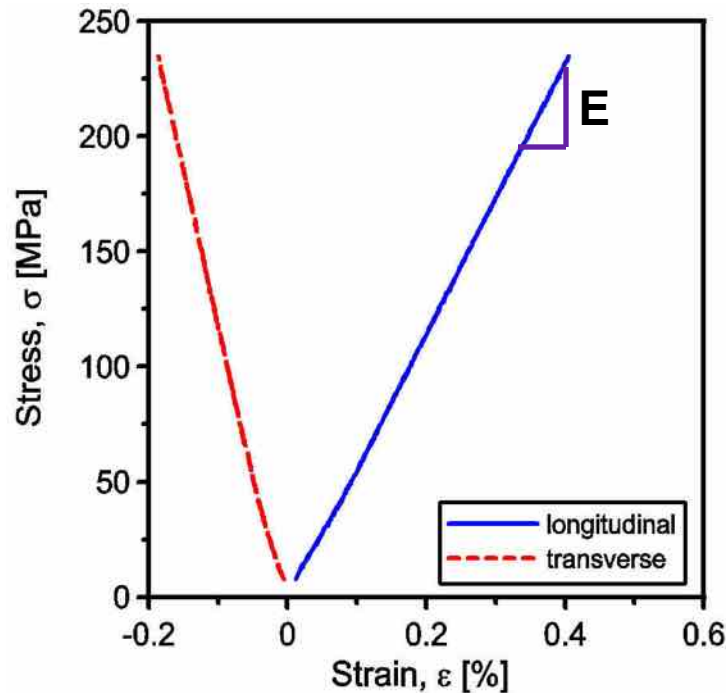
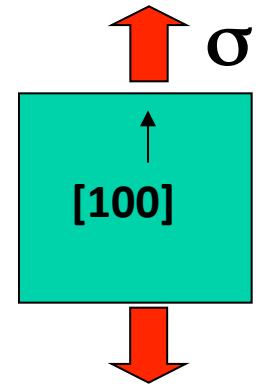
Testing under magnetic fields also conducted

from Dr. R. Kellogg's Dissertation

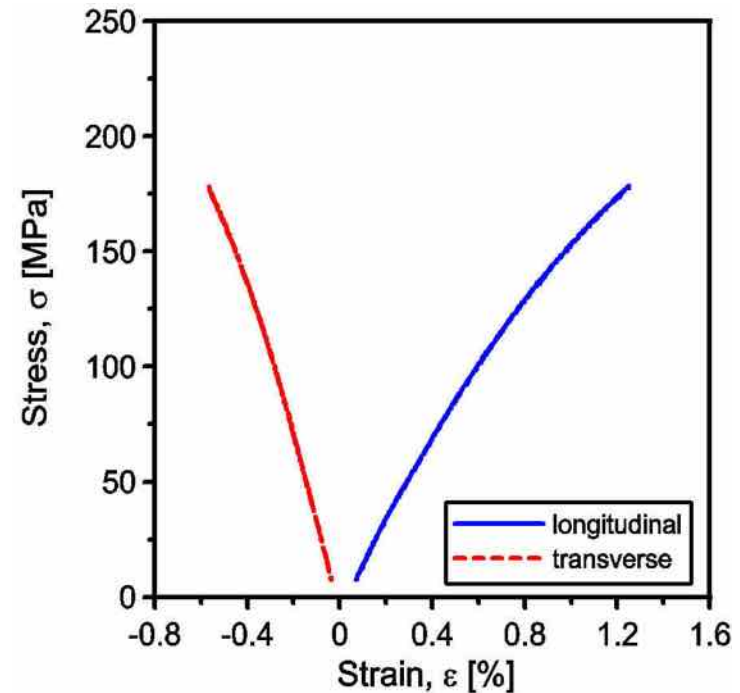


[100] Tension Test Experimental Results

- Load applied along [100] direction, measure strain responses in the longitudinal & transverse directions
- Ratio of stress & strain give elastic modulus, E
- Negative ratio of longitudinal and transverse strains gives the Poisson ratio, ν , (ν)



• 18.6% Ga



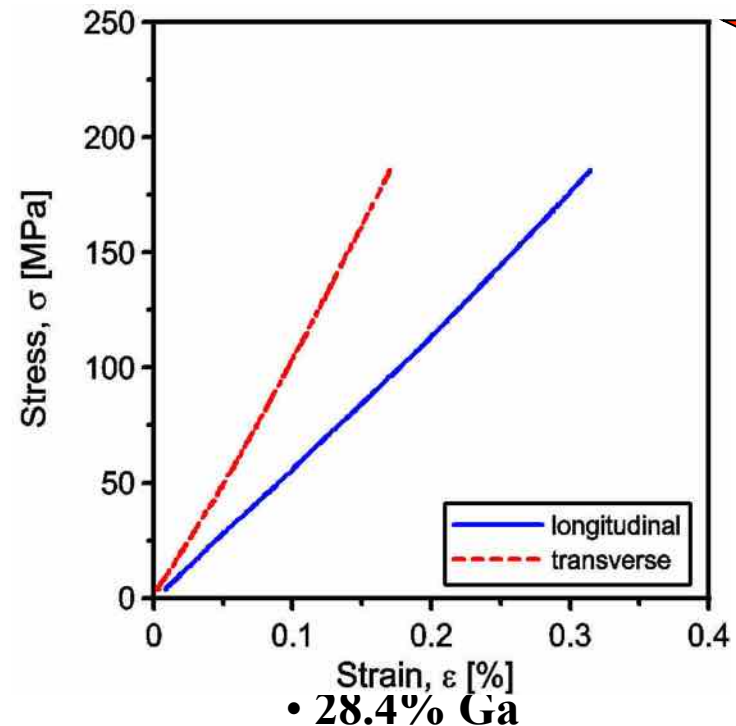
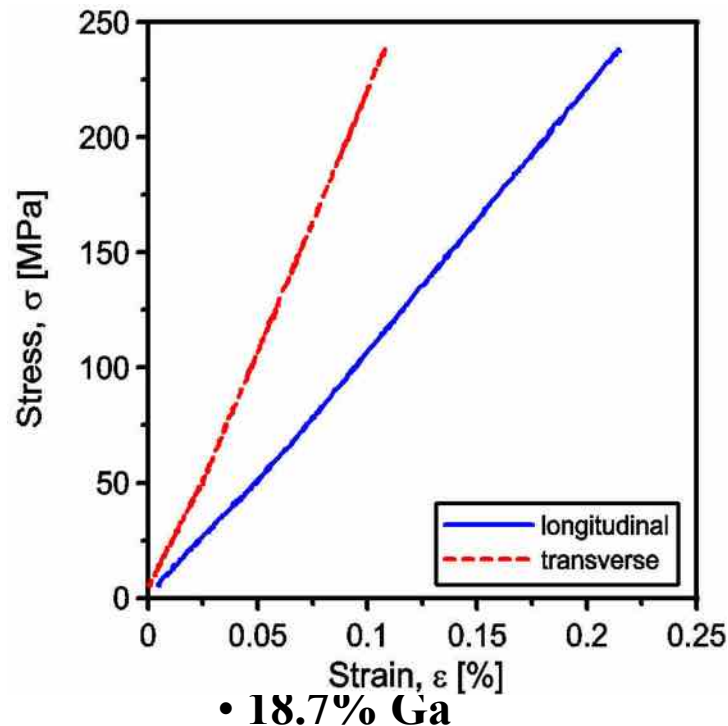
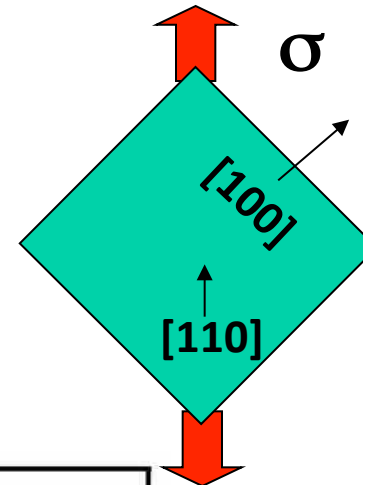
• 28.9% Ga

The test speed is 0.5 $\mu\text{m}/\text{sec}$ in each test with constant load limits.

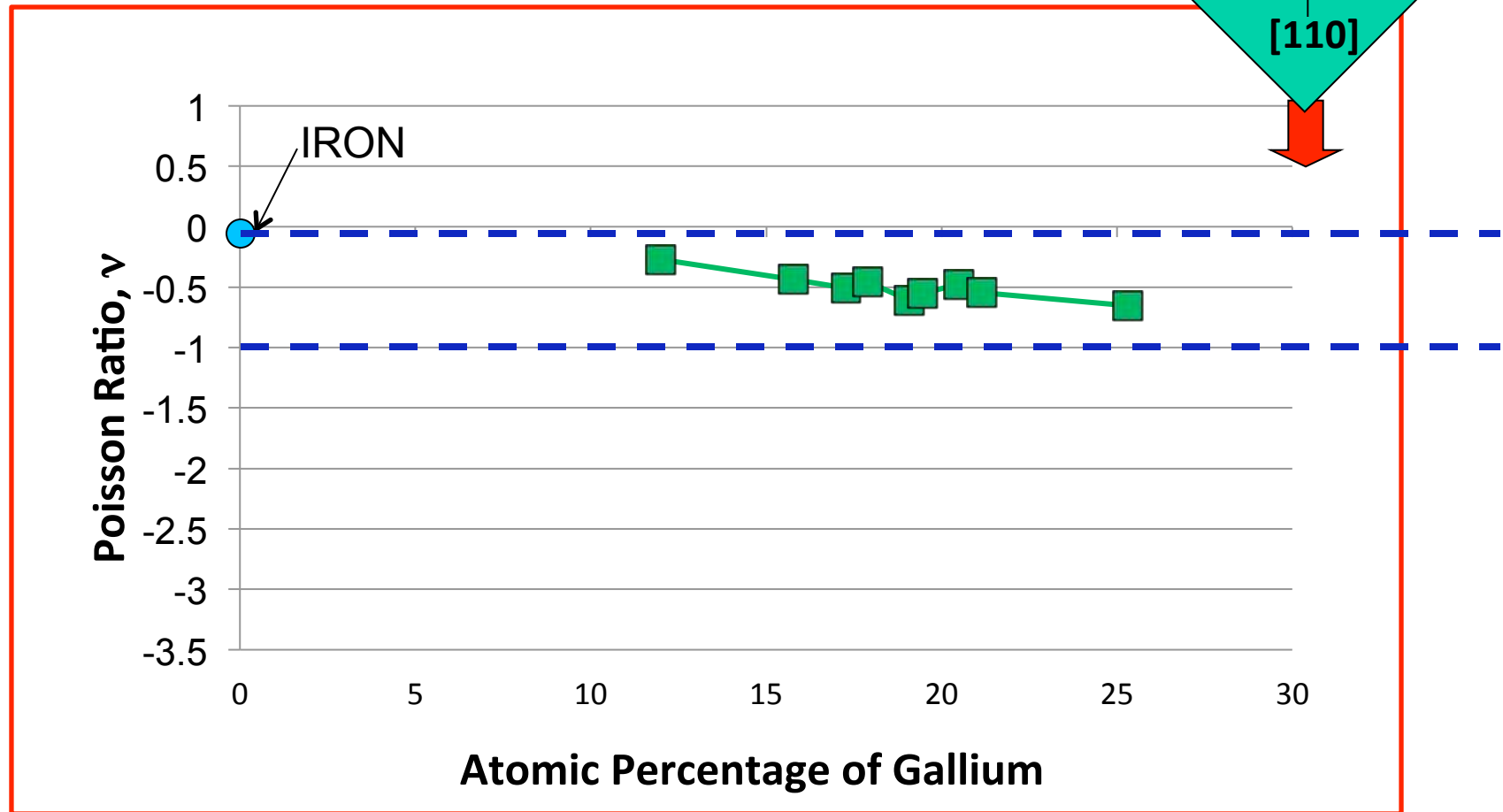
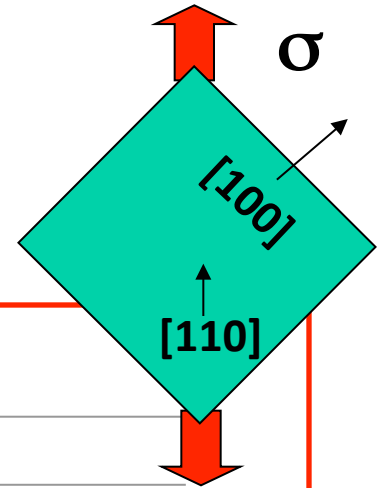
[110] Tension Test Experimental Results

- Load applied along [110] directions
- Samples get longer and wider (and really thin!)
 - Both stress-strain curves have a positive slope!!
- The alloys have a **negative Poisson ratio**

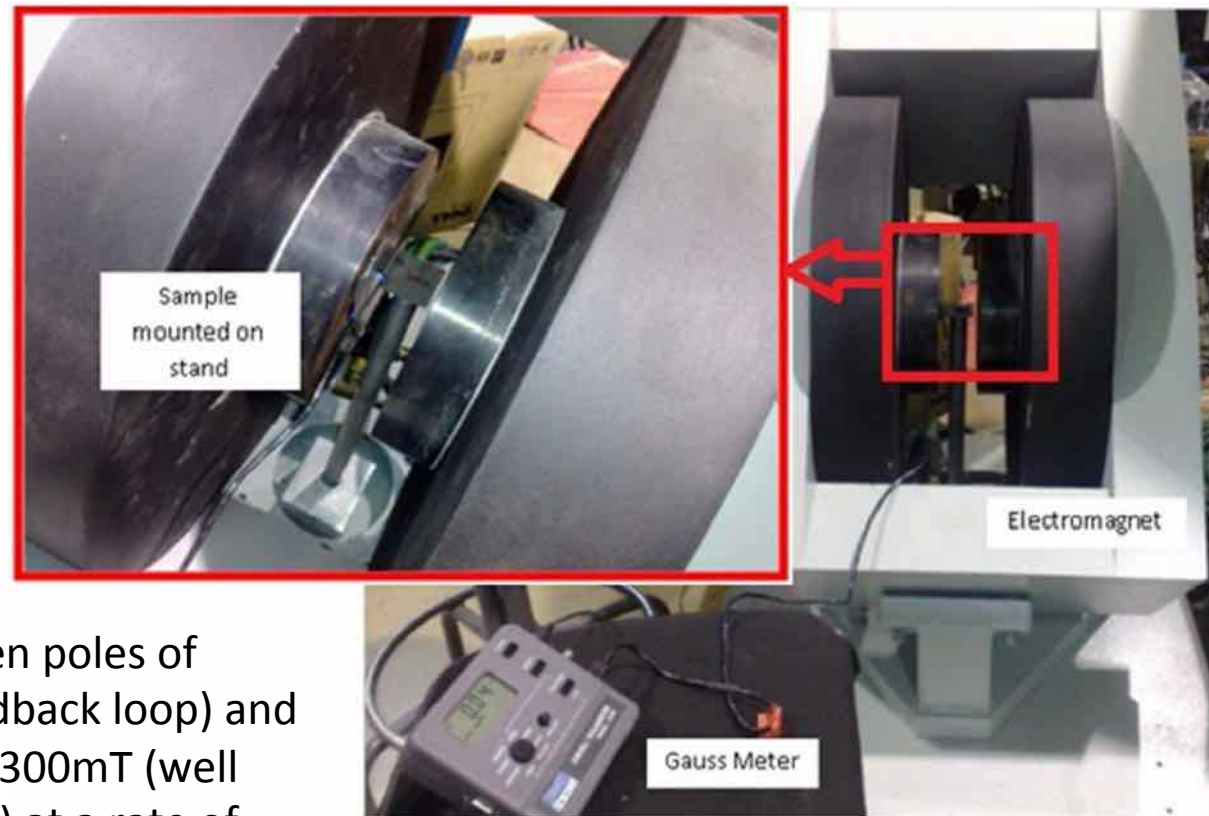
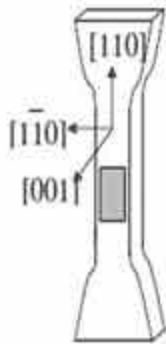
Alloys are **AUXETIC** in [110] directions



Auxeticity in response to applied mechanical stress



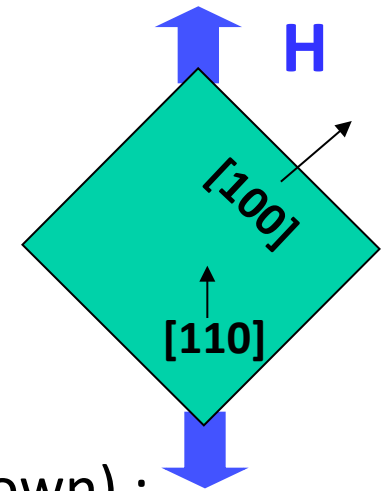
Magnetically induced auxeticity in Galfenol?



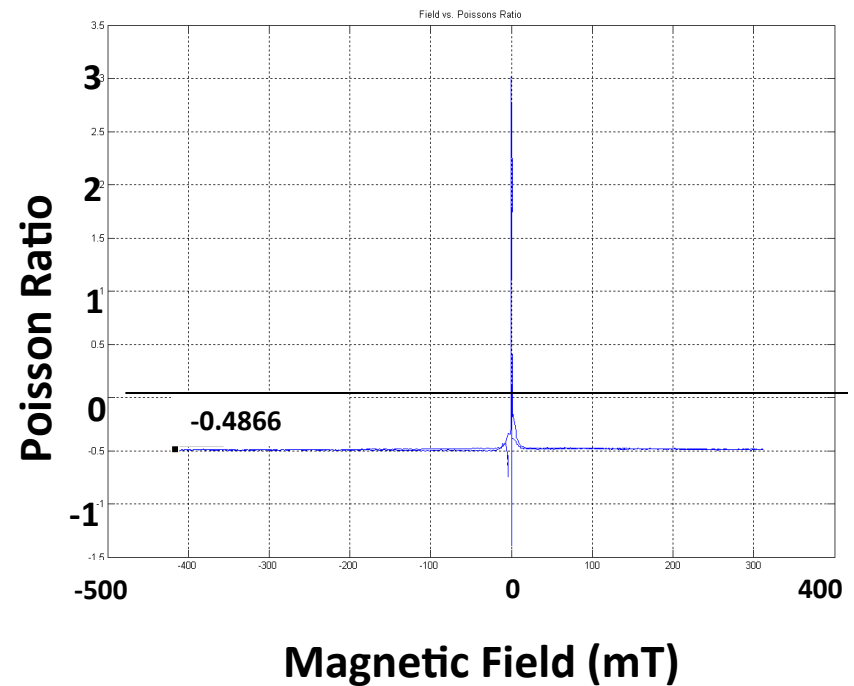
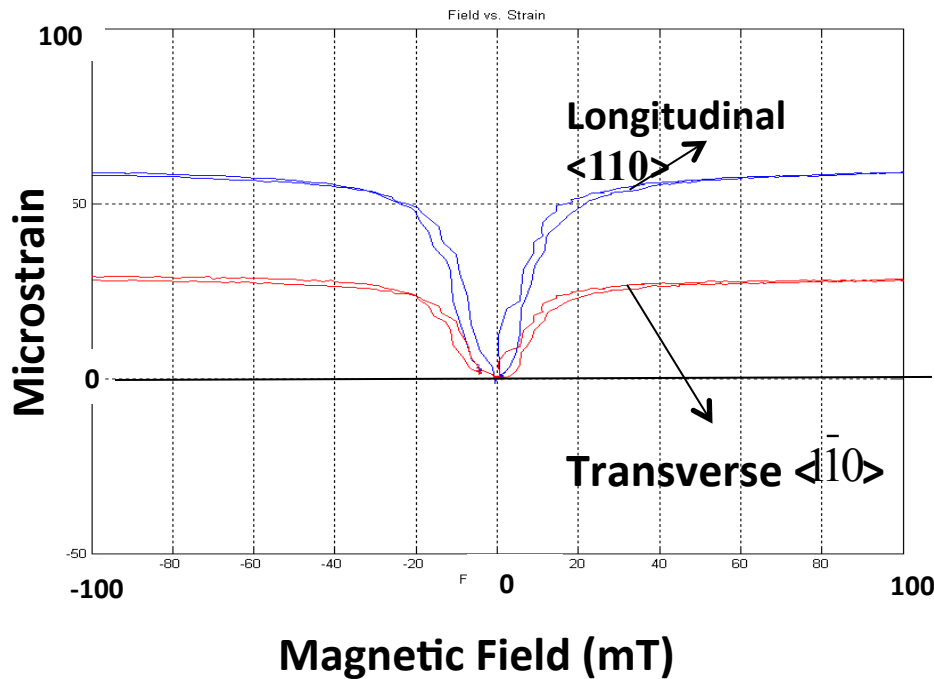
Sample mounted between poles of electromagnet (with feedback loop) and field was ramped up to $\pm 300\text{mT}$ (well past magnetic saturation) at a rate of $\pm 10\text{mT/s}$

...is there a Delta Poisson Ratio Effect?

Yes! Poisson Ratio (negative ratio of longitudinal to transverse strain) changes when a DC magnetic field is applied along the sample length



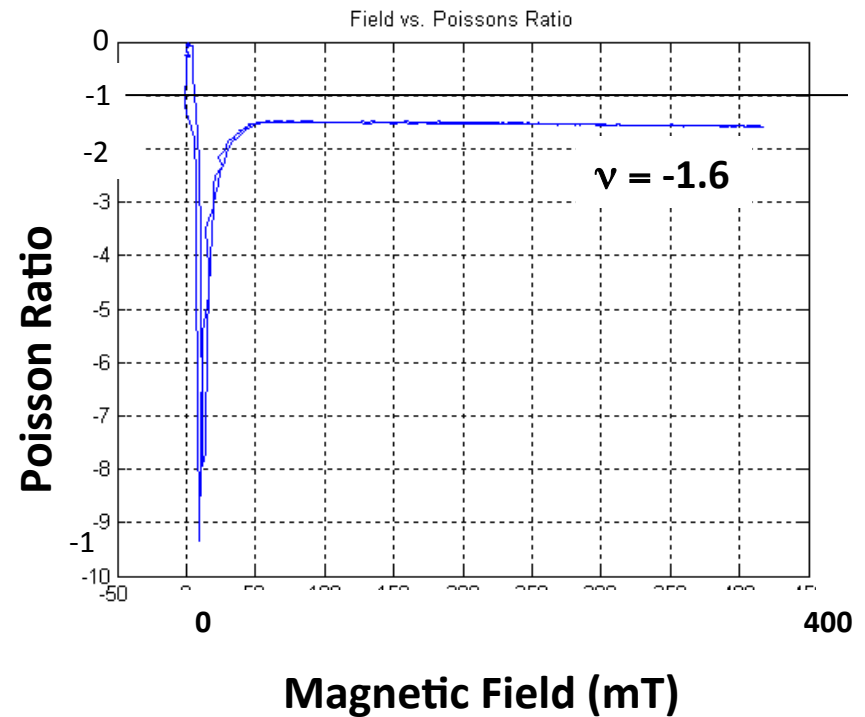
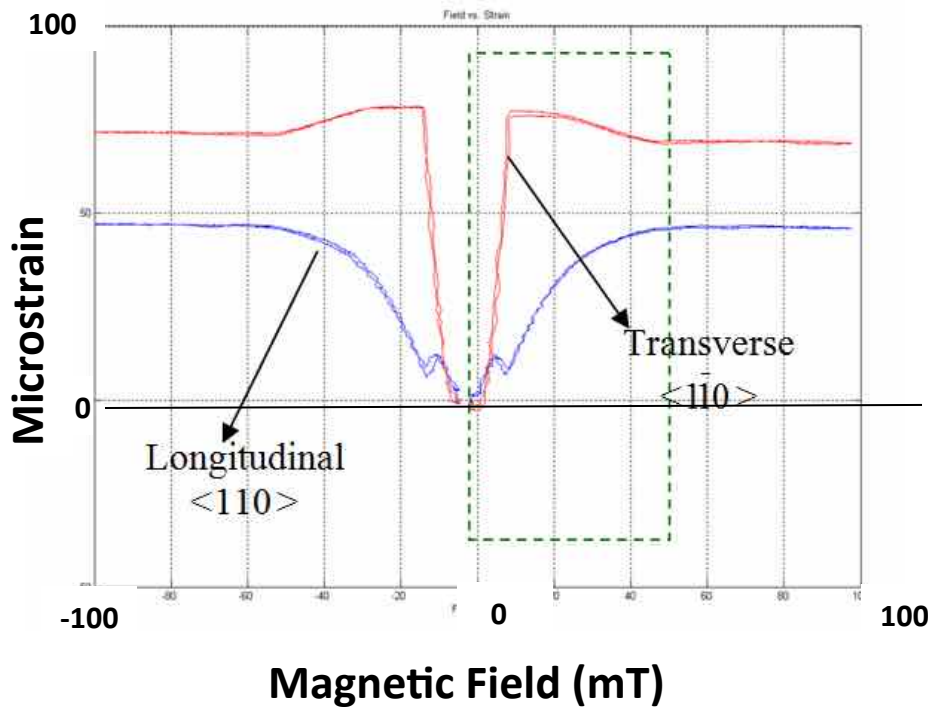
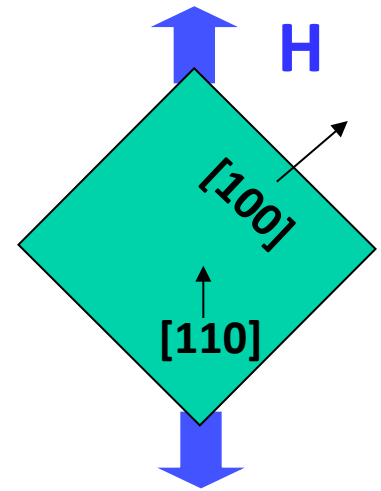
Typical results from [110] Galfenol Samples (31% Ga shown) :



For compositions of $<17\%$ Ga, sample width increases more than the length!

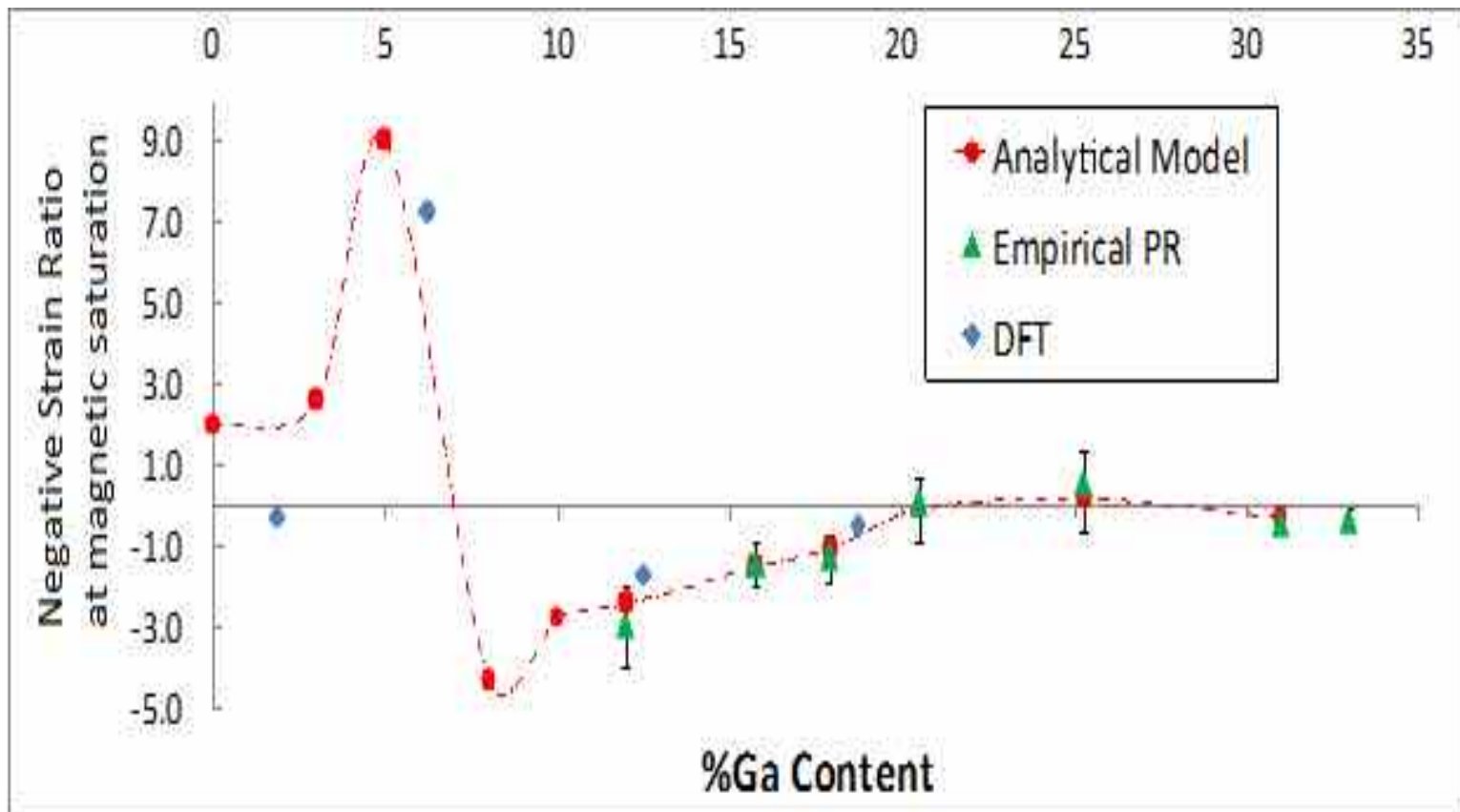
Poisson ratio is less than -1.0 !

Results from the 16% Ga $[110]$ Galfenol Sample:



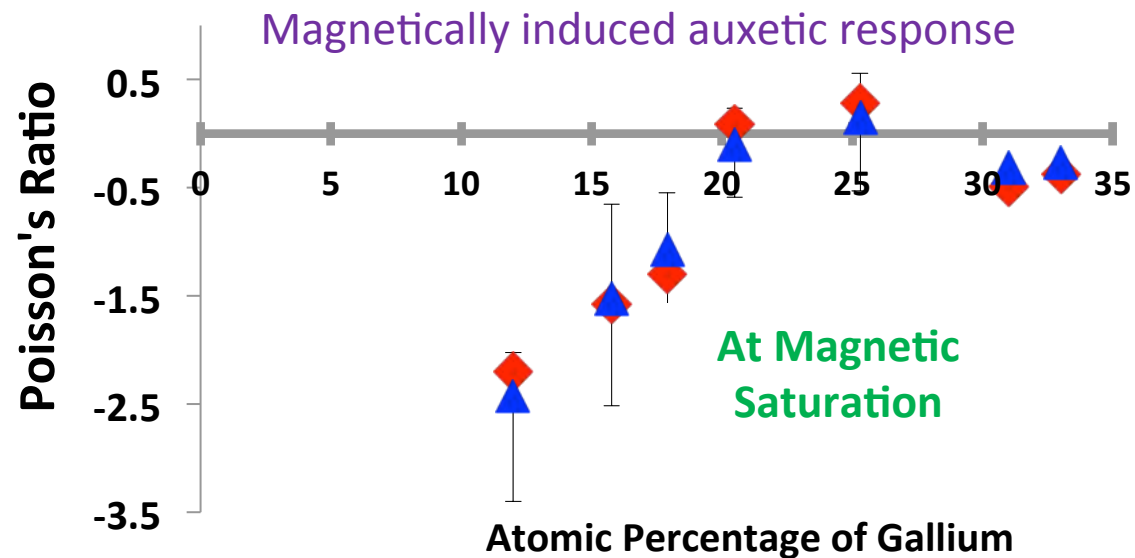
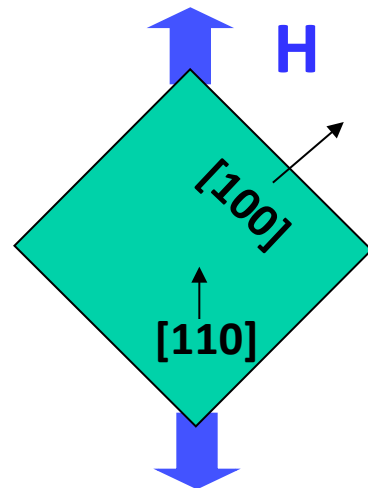
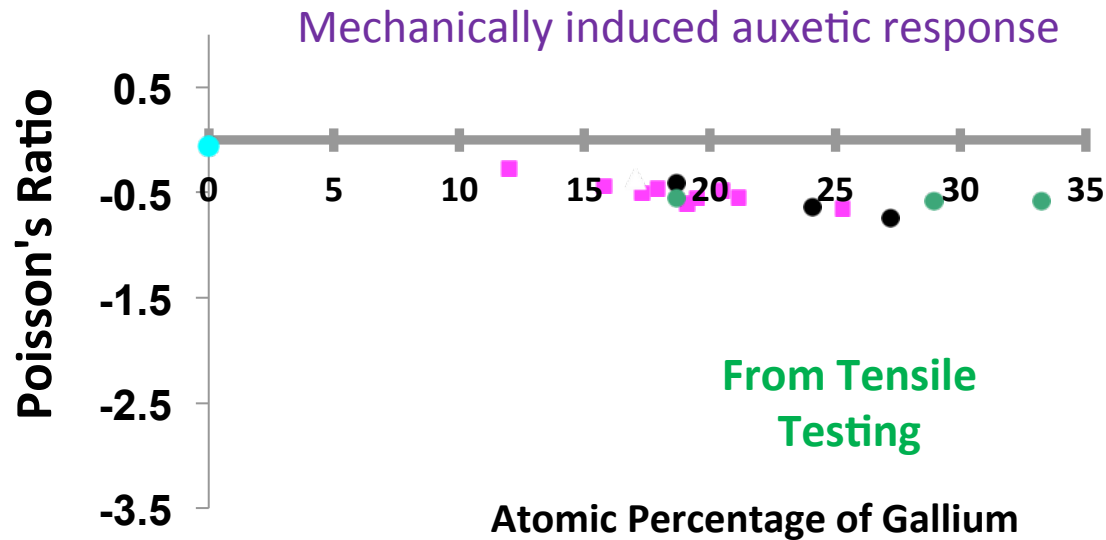
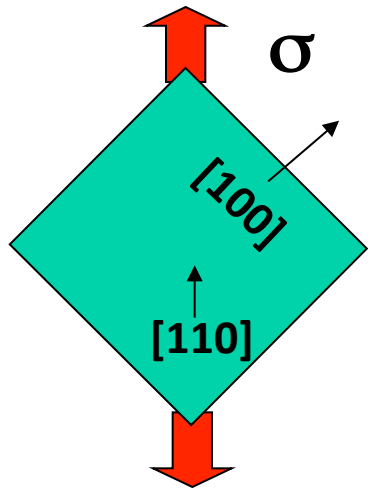
Comparison of models and experimental Poisson ratio data.

Poisson ratio values under a saturating magnetic field (400 mT) for different compositions of FeGa from an energy-based analytical model, density functional theory simulations, and ratios of measured strain values

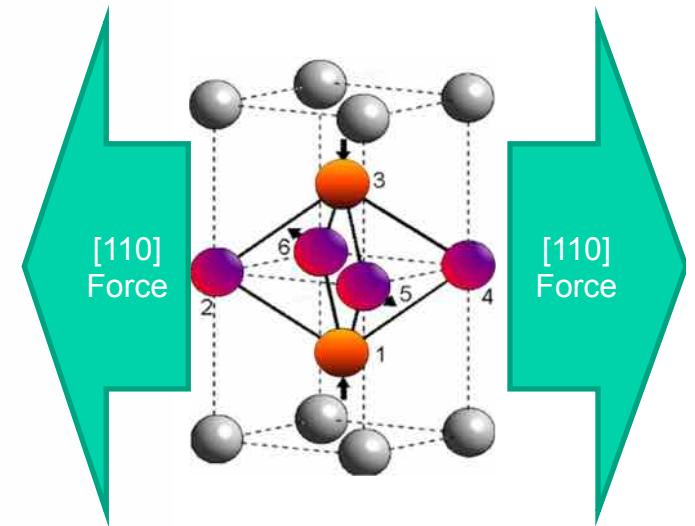
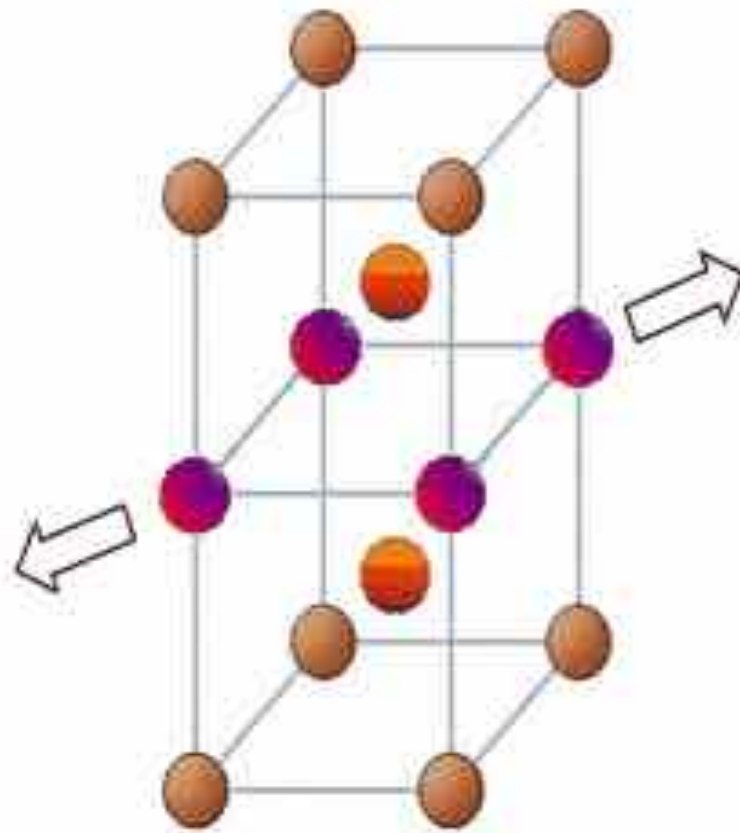


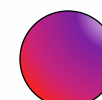



Poisson ratio data for Galfenol of different compositions



GAS MODEL FOR AUXETIC EFFECT IN BCC CRYSTALS



-  Atoms that move away from one another
-  Atoms that approach one another

Outline

Intro to Magnetostriction

Actuators: the “direct” effect

Sensors: the “inverse” (or Villari) effect

Structural Magnetostrictive Alloys

Magnetostrictive, magnetic & mechanical properties

Thin, highly textured rolled sheet

Introduction to auxetic behavior

Applications that use Galfenol

Bending sensor applications

Implantable wireless bone fixity sensor (Tech Univ. Dresden)

Nanowire sensors (Univ. Minn. & UMD)

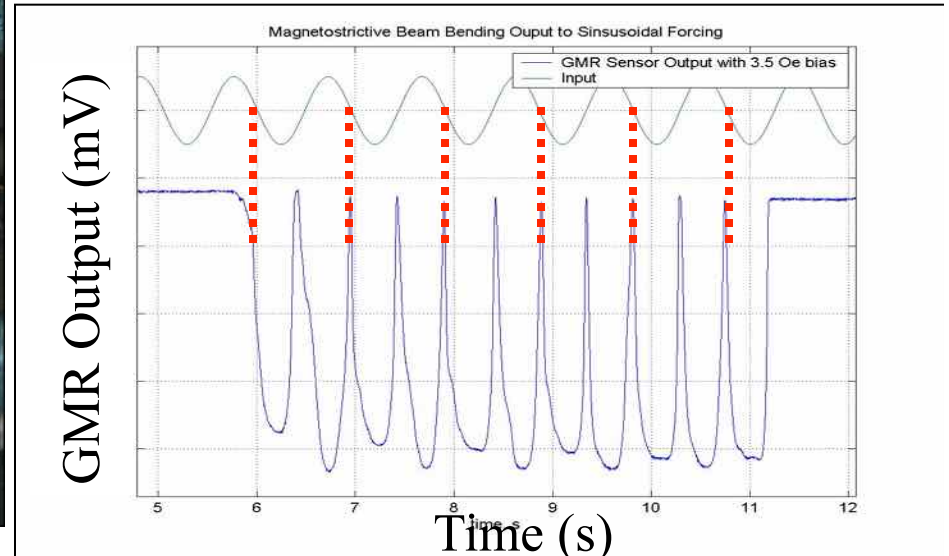
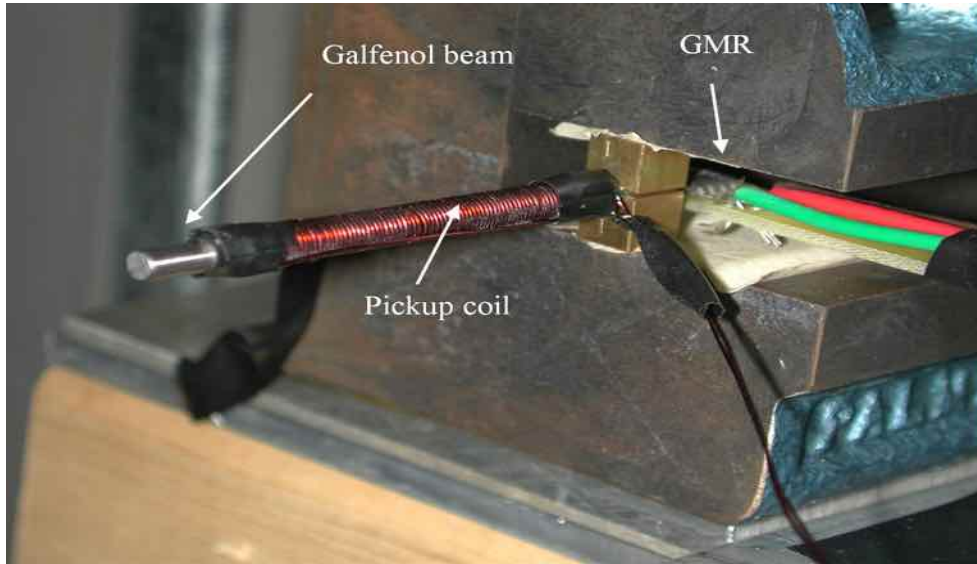
Applications for auxeticity?

Micro-motors (Kanazawa University, Japan)

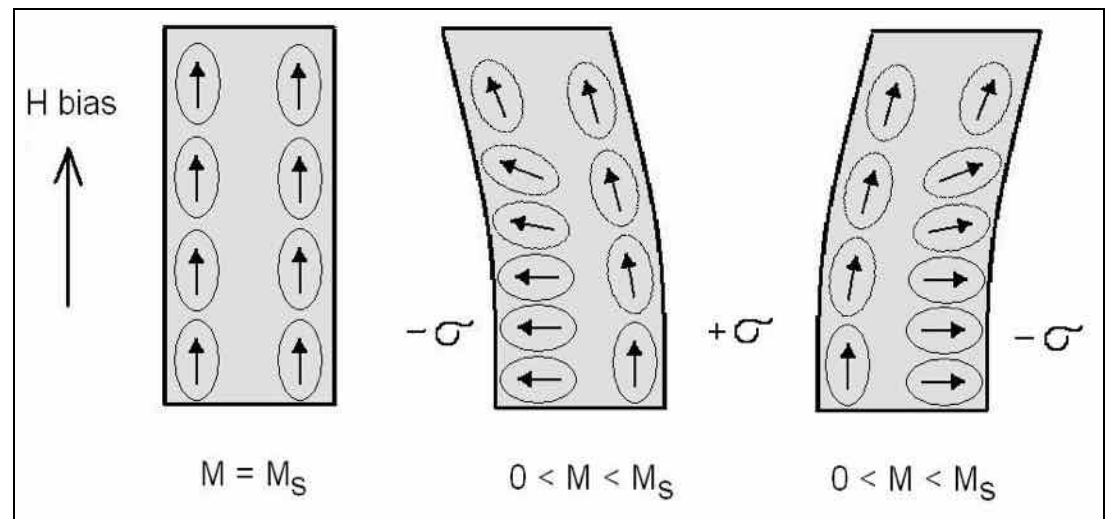
Energy Harvesting (Kanazawa Univ, UMD & Techno Sciences, Inc., Oscilla Power)

Summary

Early Bending Tests

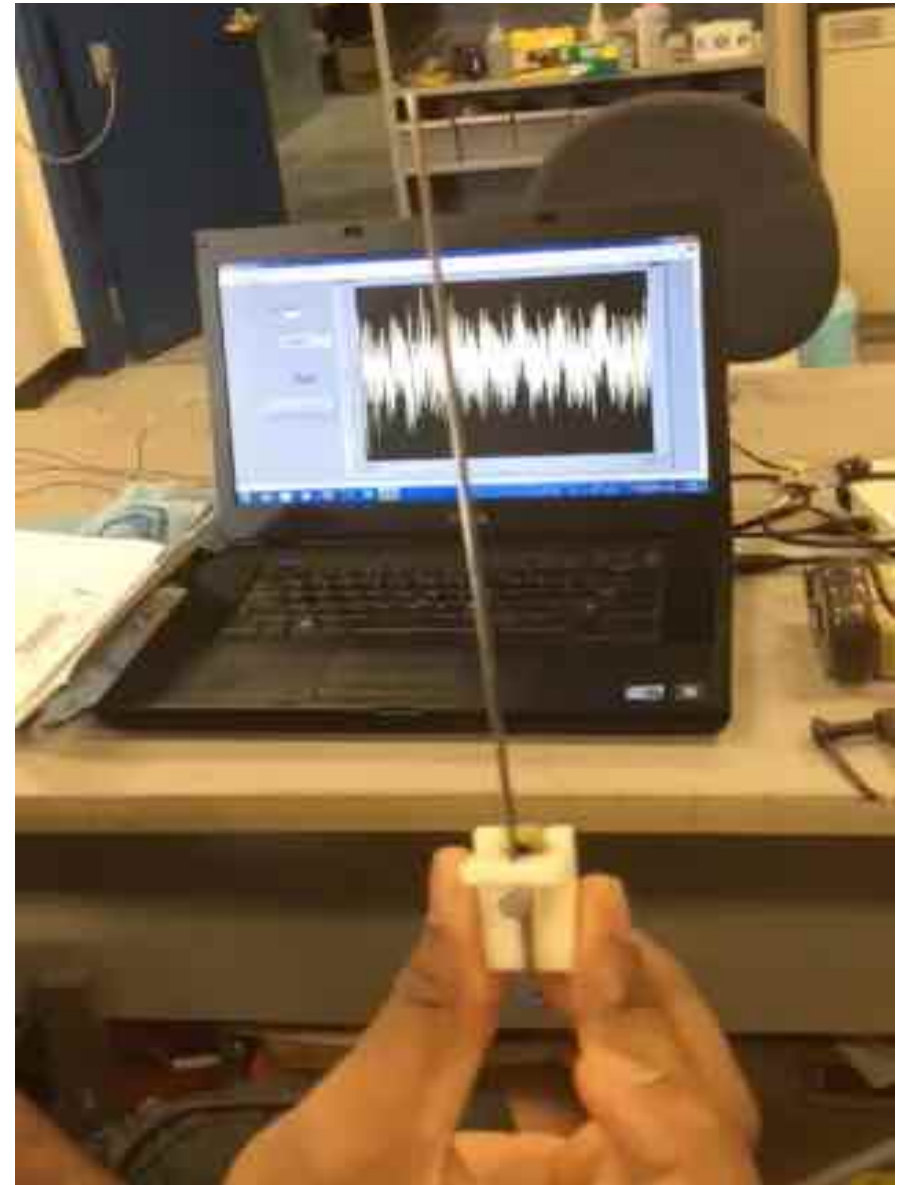
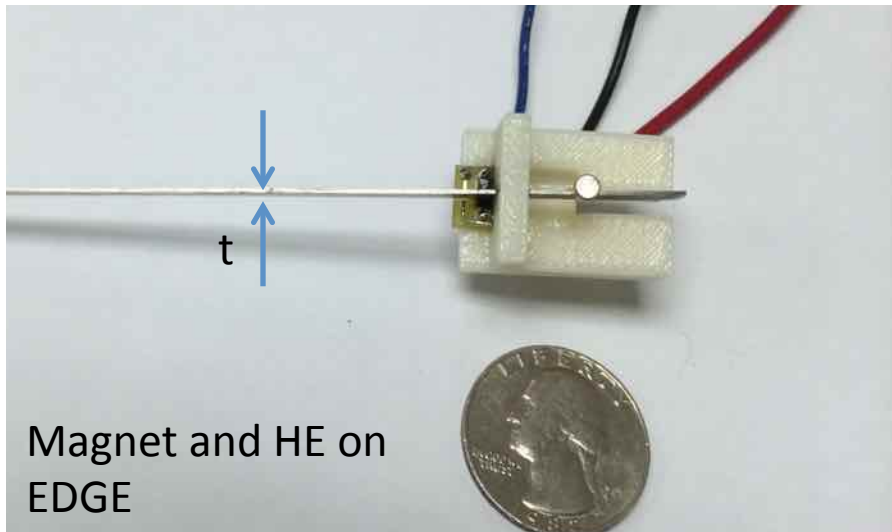


- Tensile stresses act trivially in same direction as bias field
- Compressive side of beam controls response
- Bias shifts where max coupling occurs
- GMR measures volume-averaged change in induction

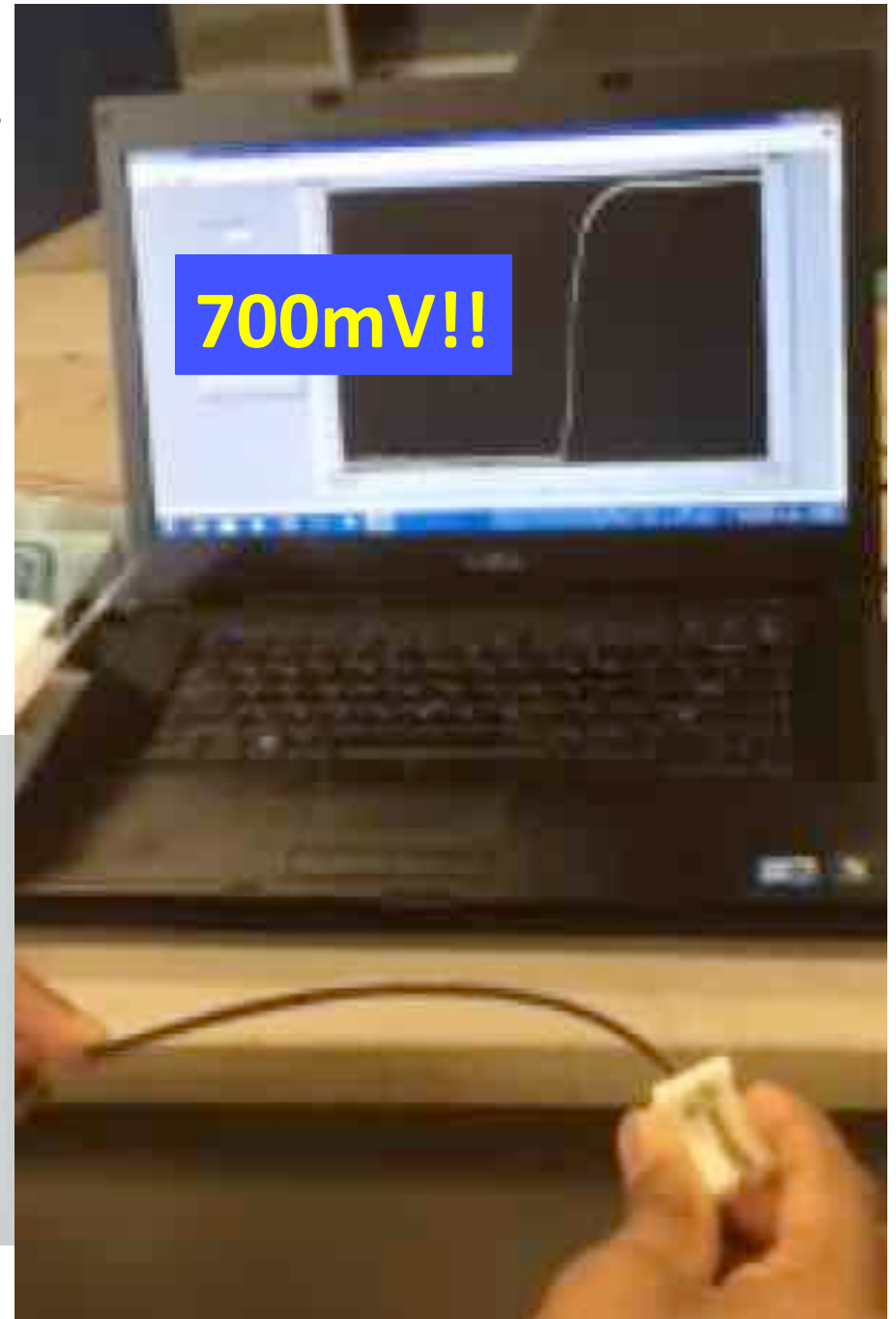
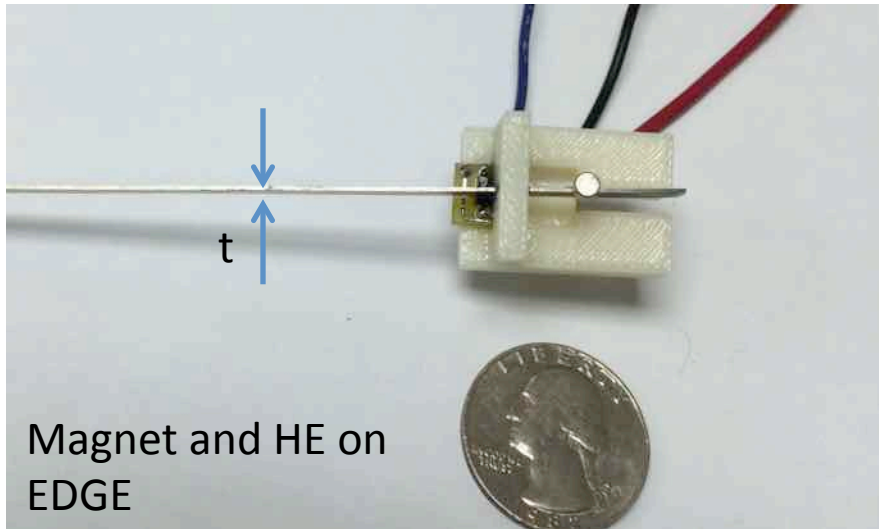


(NOTE: will show later these assumptions were only partly correct!)

Bio-inspired thin “whisker-like” bending sensors



Bio-inspired thin “whisker-like” bending sensors



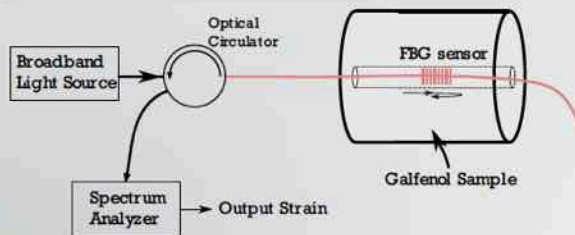
Magnetostrictive biased magnetic field sensor

Apicella, Caponero, D. Davino & C. Visone (2018); Univ. Sannio-Benevento, ITALY

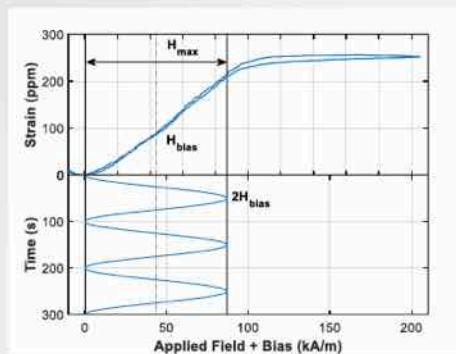
Smart Sensing Applications: Magnetic Field Sensor



Working principle

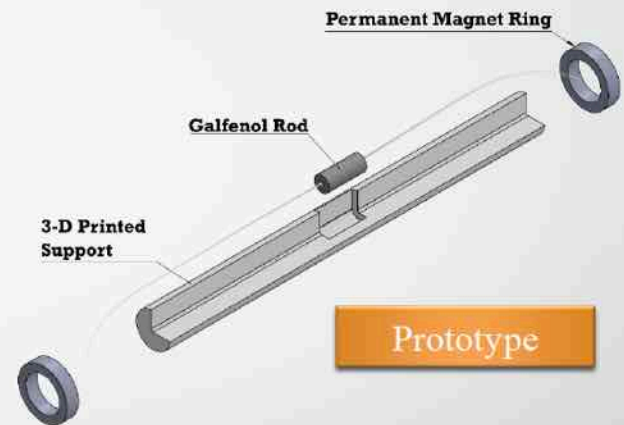
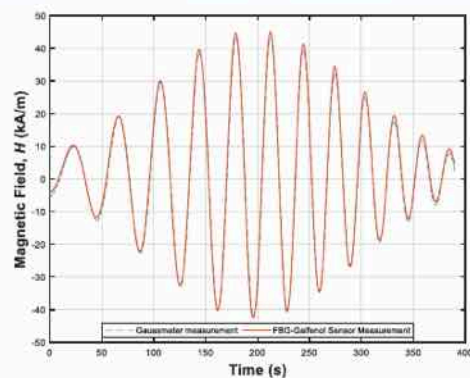


A Fiber Bragg Grating measures the magnetostriction, then related to the applied magnetic field.

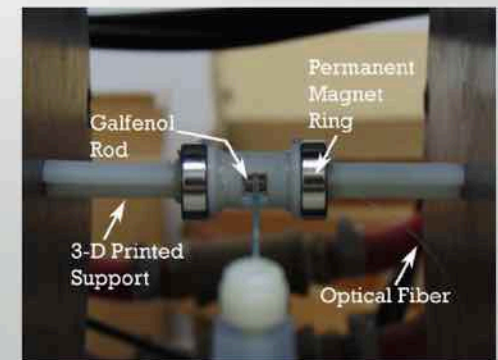


A magnetic bias system allows to detect both positive and negative magnetic fields.

Magnetic Field Reconstruction



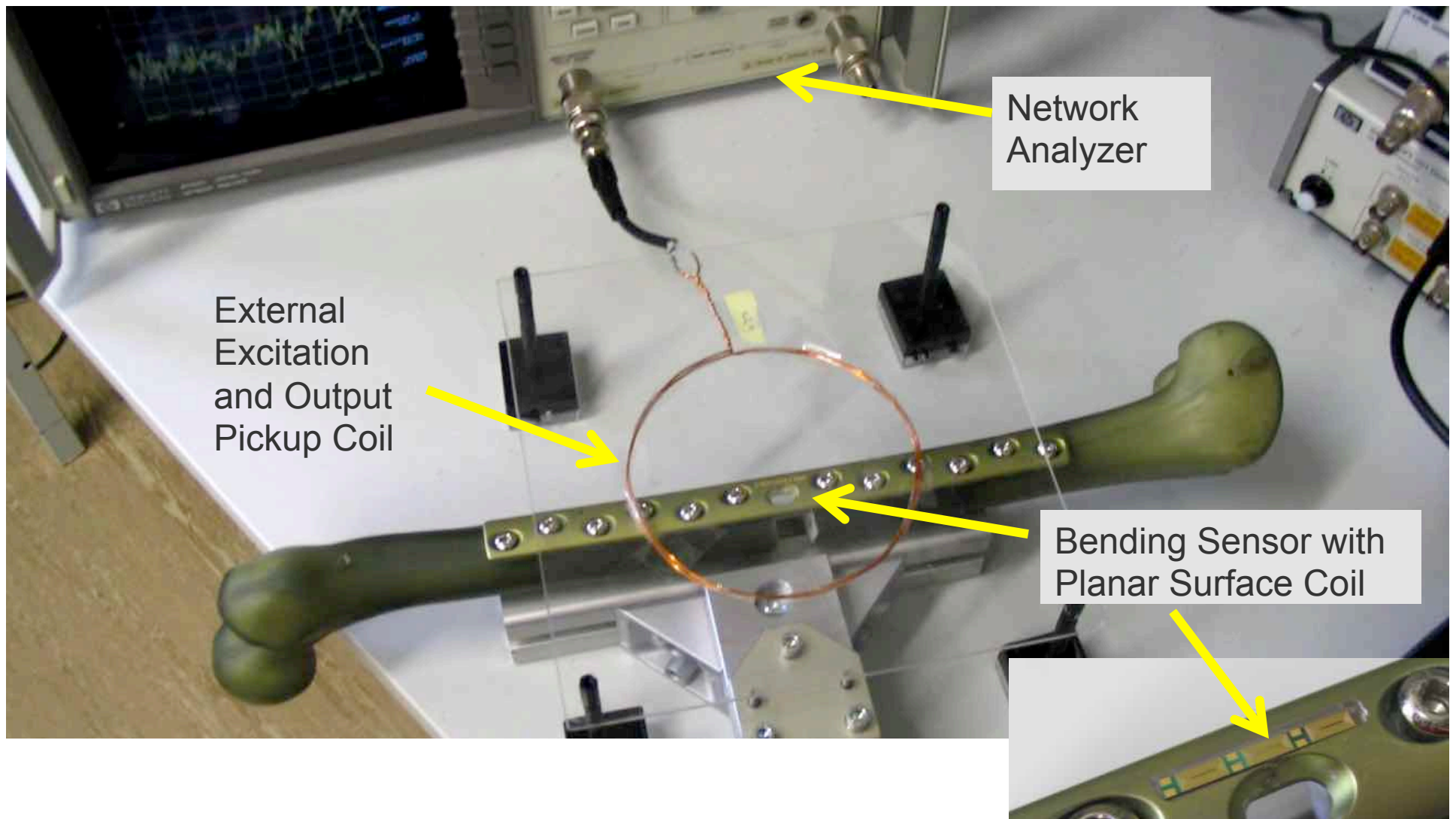
Prototype



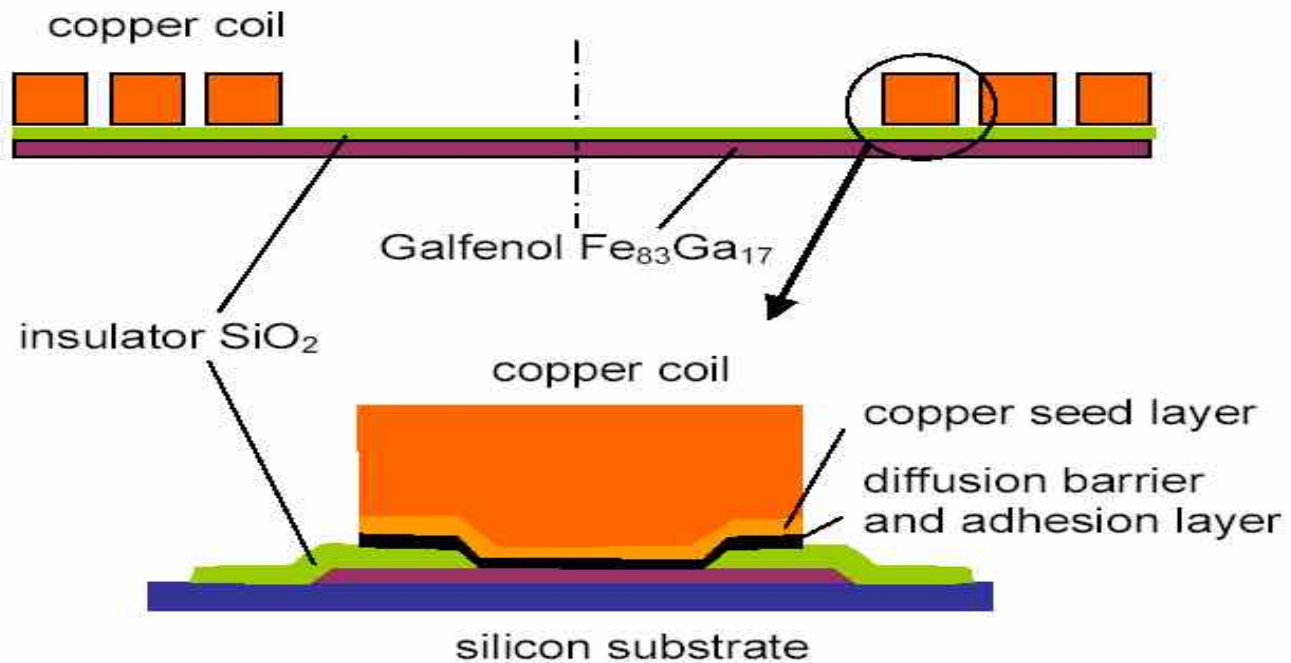
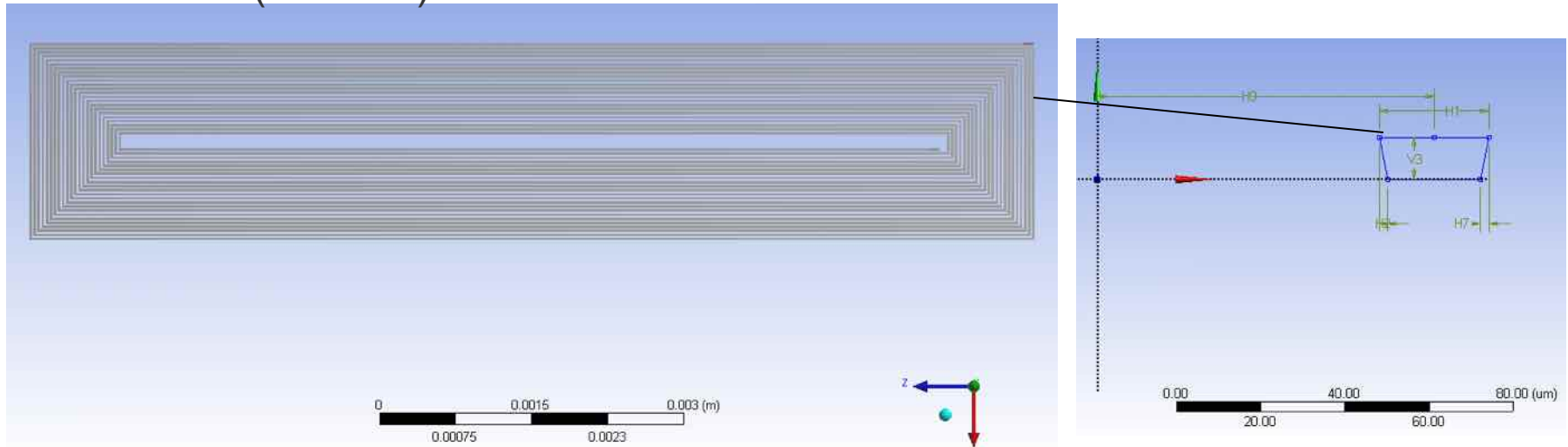
Apicella V., Caponero M. A., Davino D. and Visone C. (2018). A magnetostrictive biased magnetic field sensor with geometrically controlled full-scale range. *Sensors and Actuators A: Physical*.

Galfenol Resonant Sensor for Indirect Wireless Osteosynthesis Plate Bending Measurements

Fischer et al. (2009); Wentzel et al. (2009); Tech. Univ. Dresden



Planar coil (22 turns)

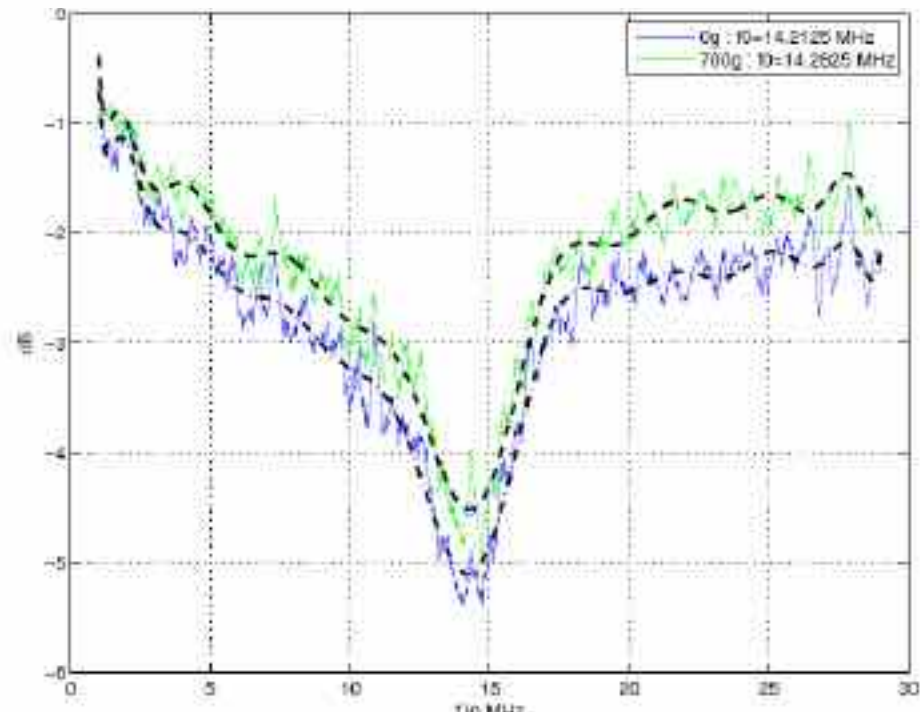


Fischer et al. (2009); Wentzel et al. (2009); Tech. Univ. Dresden

Stress induces a change in permeability. Changes resonance of planar coil

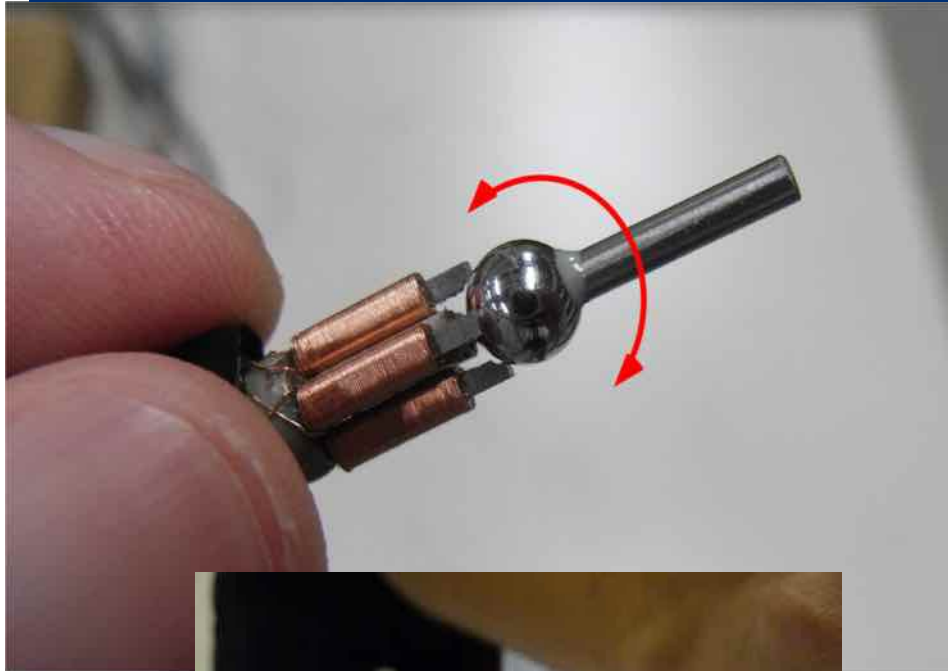
Excitation/pickup coil 1 cm above bone plate and 6 cm radially from center of $10 \times 2 \times 100 \text{ mm}^3$ sample

Loading of 700 grams produces a 70kHz shift in resonance



*Fischer et al. (2009); Wentzel et al. (2009);
Tech. Univ. Dresden*

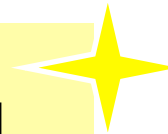
Micro spherical motor Prof Toshiyuki Ueno Kanazawa Univeristy, Japan



**Galfenol → drive element
and magnetic core**

Advantage

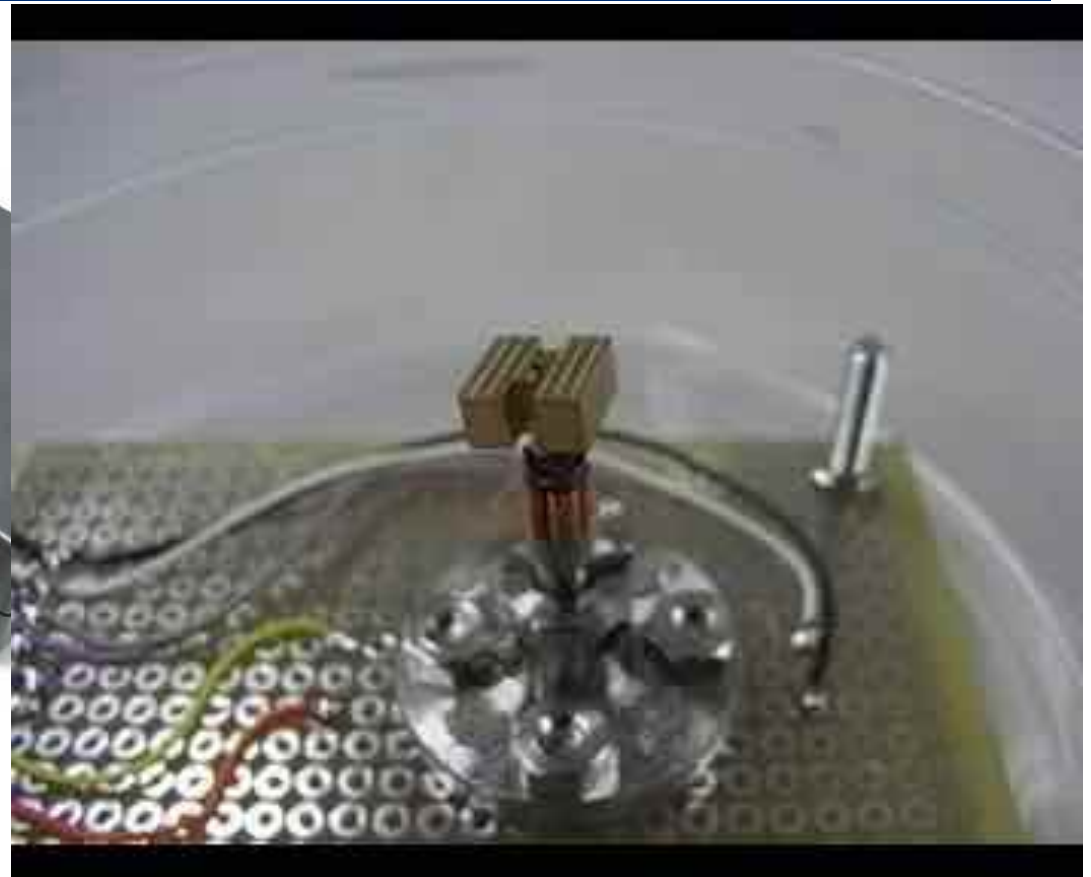
- Simple and small
- Holding mechanism
- Low voltage driving
by simple circuit



**used at endoscope
for e.g. minimally invasive surgery**

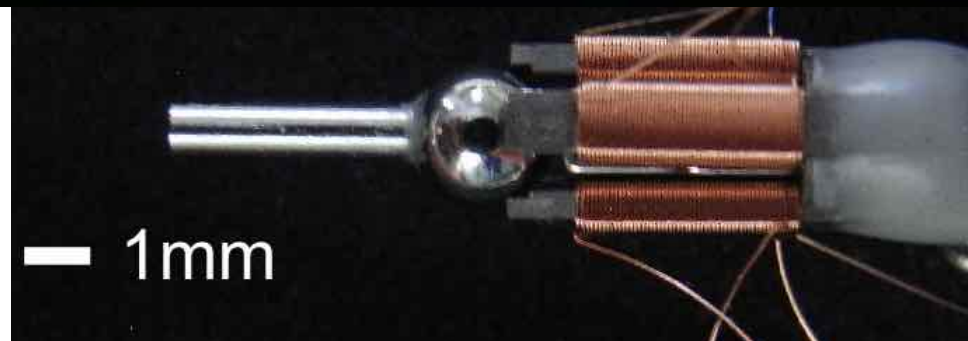
Joint of micro robot (amusement)

Movie of movement



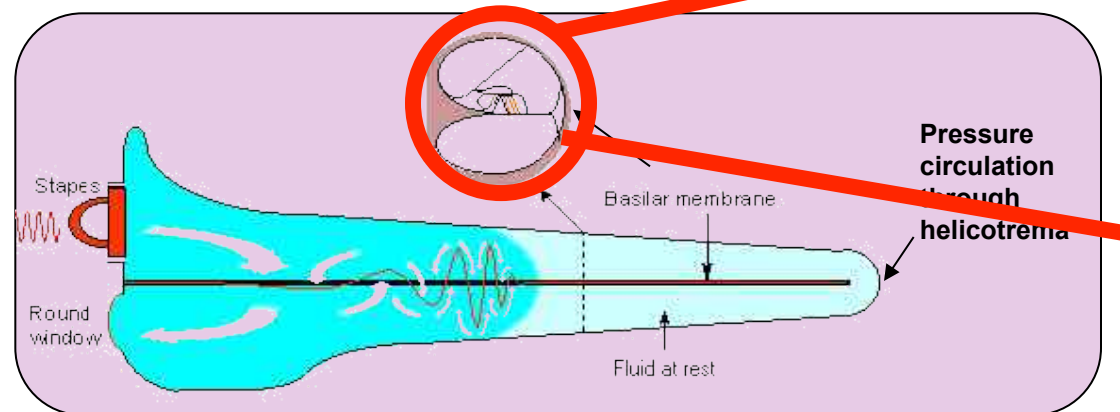
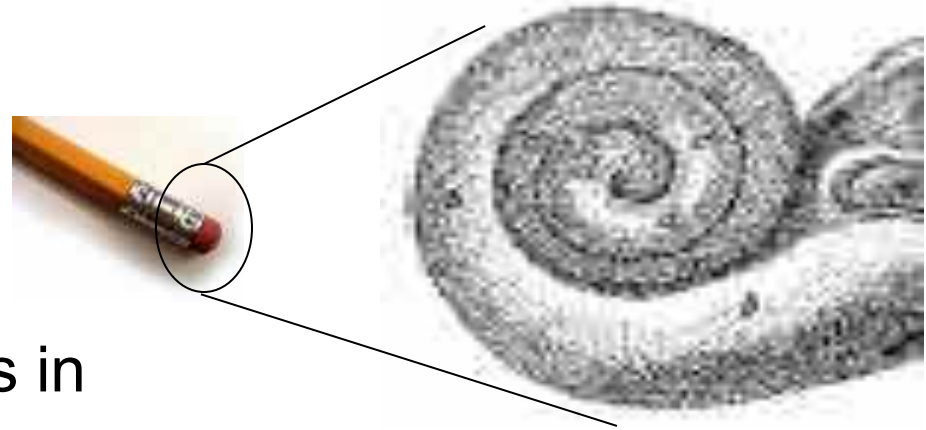
Driving condition: saw tooth
current $\pm 0.2A$ 2 kHz

DOF	2
Angle range	360°
Angle velocity	$50^\circ/\text{sec}$
Driving voltage	5V (USB)

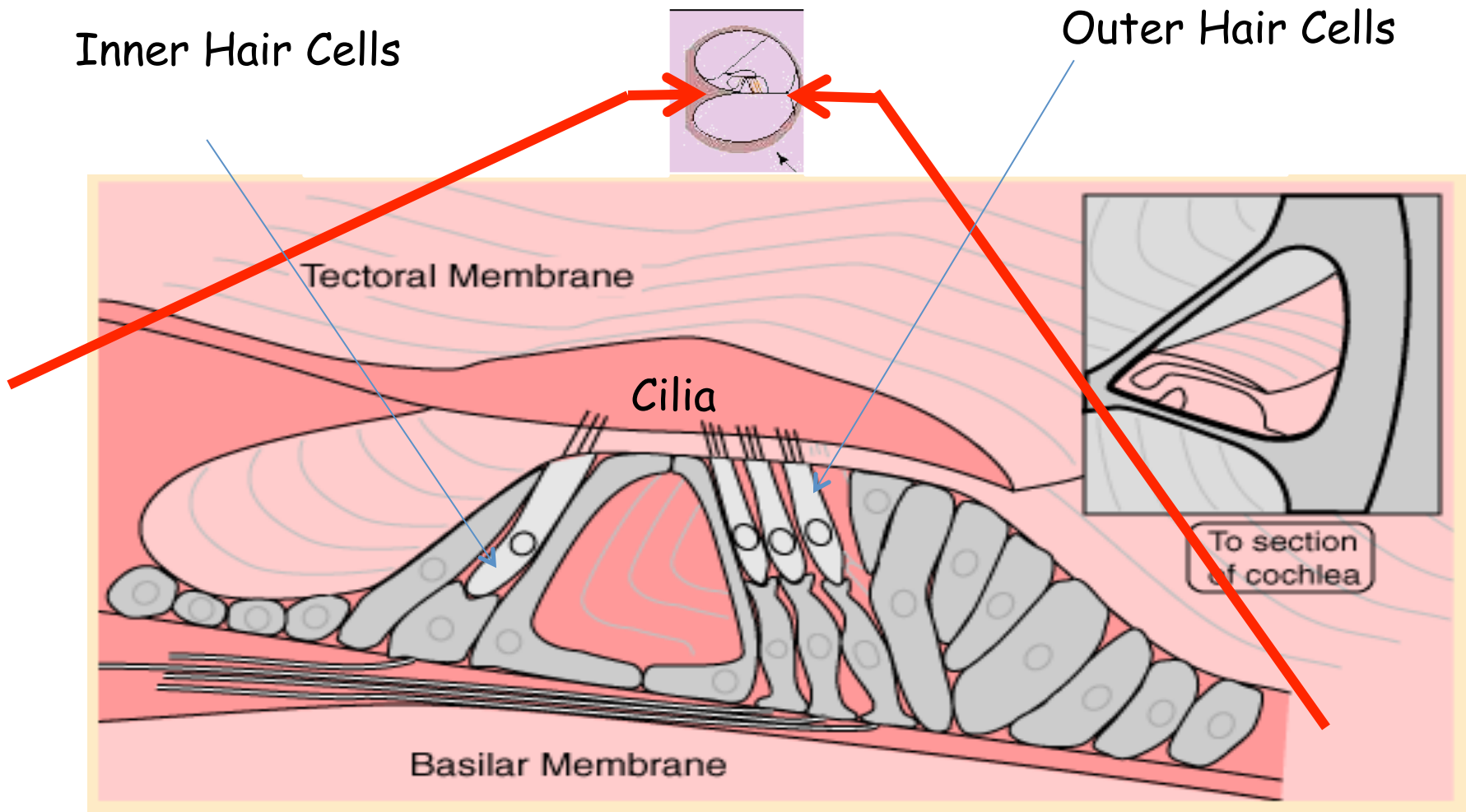


Cilia: Nano-scale transducers

- Human cochlea: $\sim 98\text{mm}^3$
 - $\sim 35\text{ mm}$ long with varied width & thickness.
- Basilar membrane increases in width and thickness with distance
- Cochlea acts as a low pass spatial filter, with high frequency response near stapes/oval window
- Location of maximum motion correlates to the detected frequency

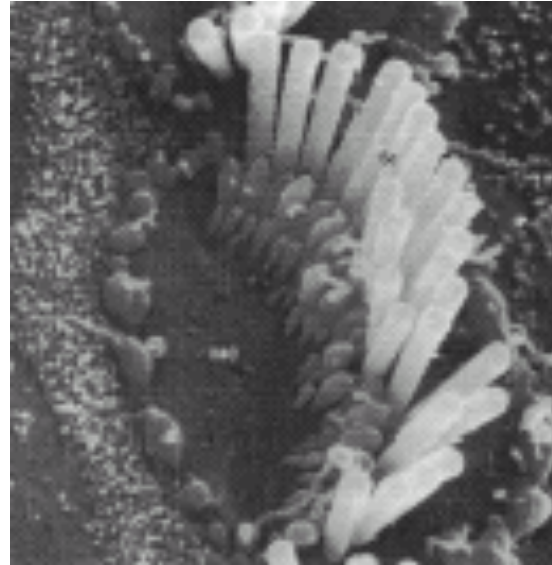


Schematic of the cross-section of the human-ear cochlea

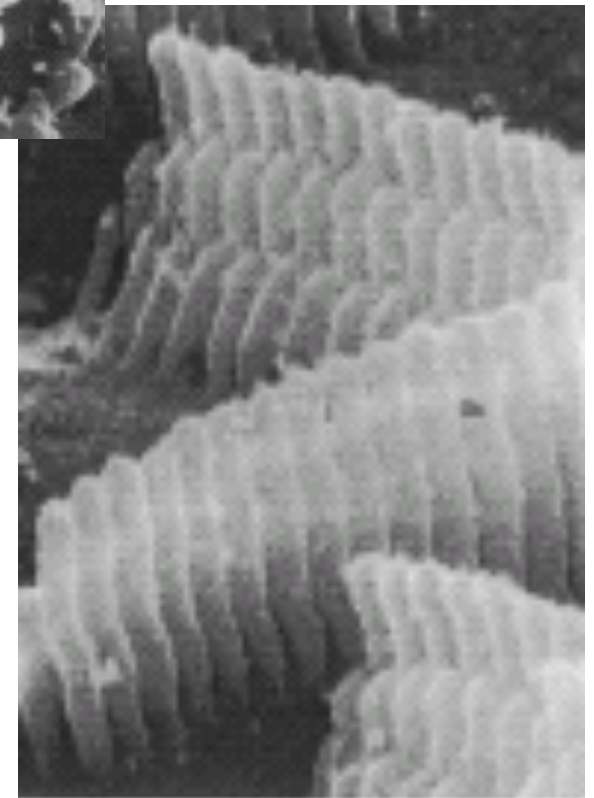


Cochlea/Cilia-based Sensors

- ~3500 inner hair cells with ~50 cilia/cell
- ~12,000 outer hair cells with ~150 cilia/cell
- Cilia dimensions:
 - ~2-6 μm long
 - ~100 nm at their base
 - ~250 nm at their tip (ohc)
- Cilia tips are tethered to neighboring cilia

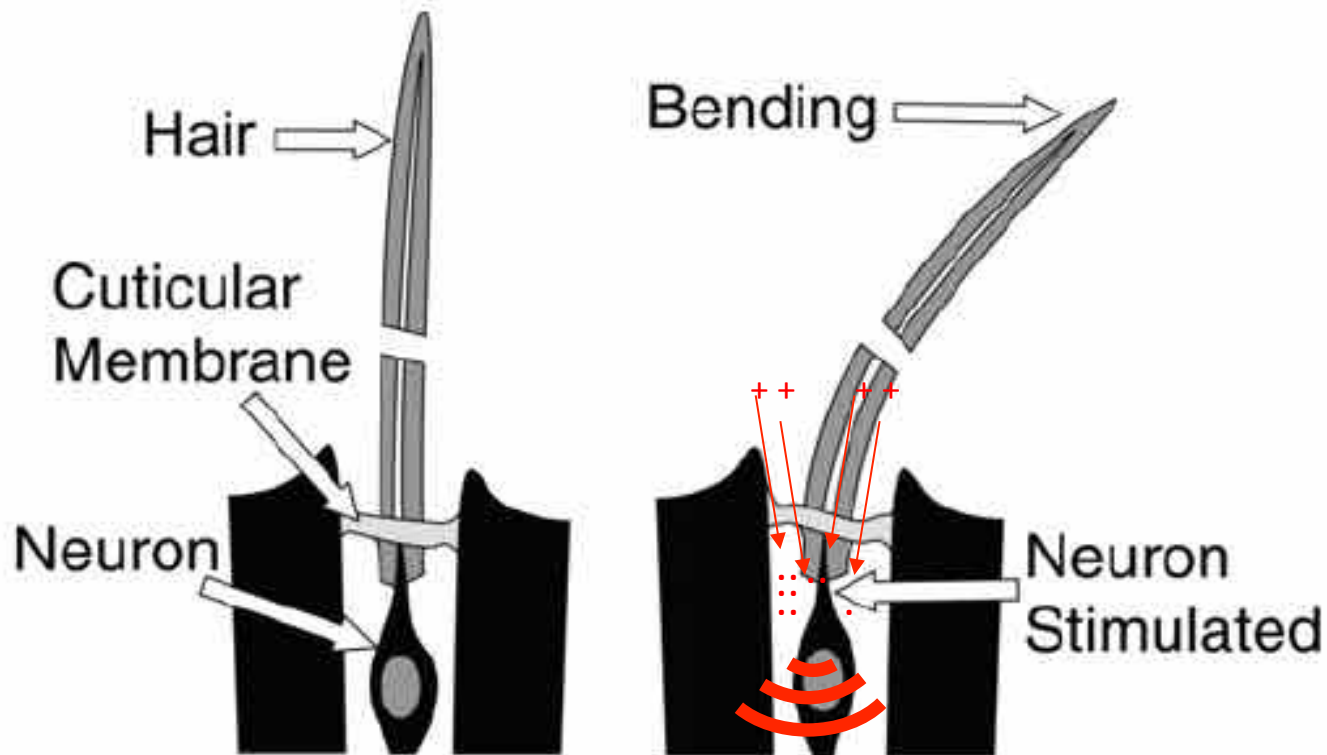
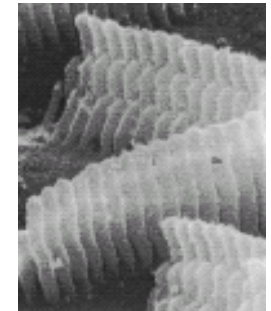


Cilia from inner hair cell



Cilia from outer hair cell

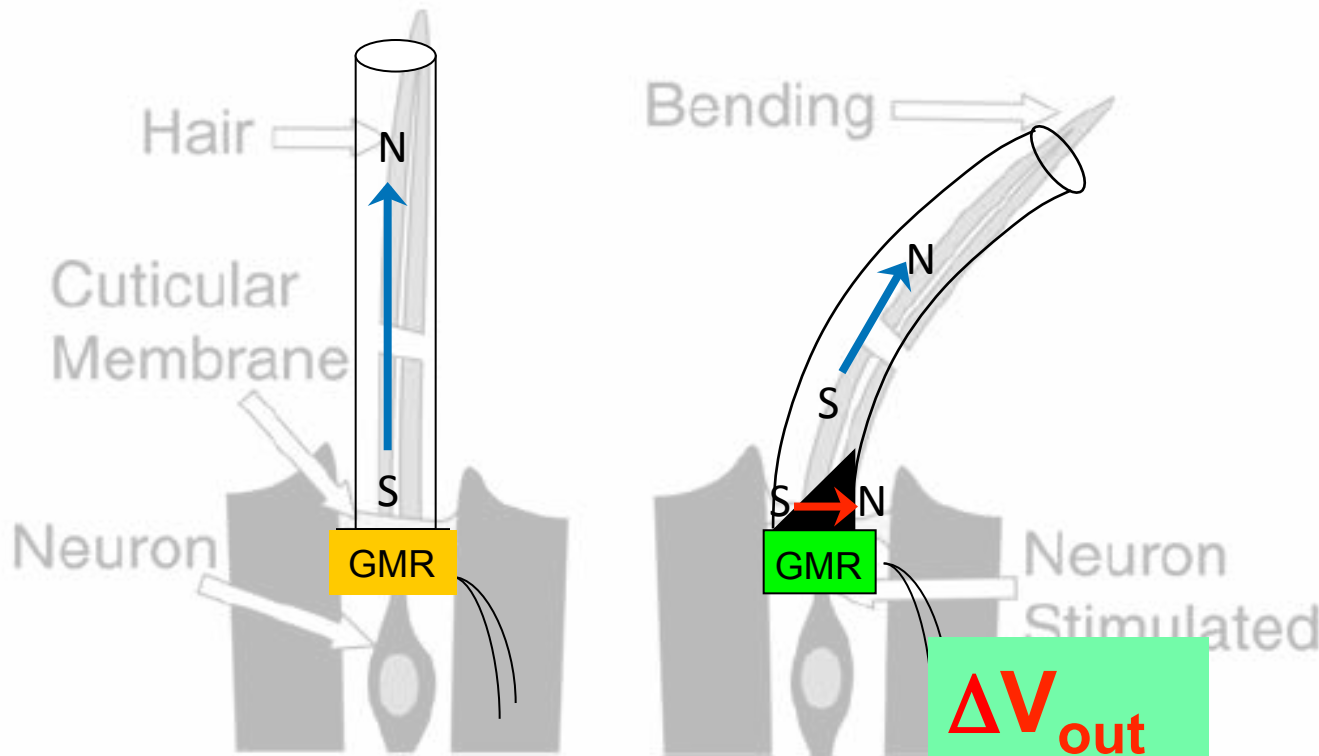
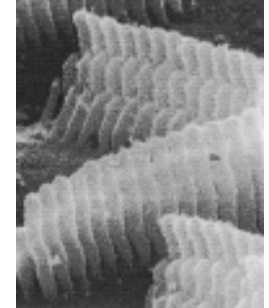
Cilia & Whiskers as sensors



Chen et al The 12th Solid State Sensors, Actuator, and Microsystems Workshop, June 2006. Hilton Head, SC, USA

Whisker deflection creates **chemical potential change** that **fires neuron**

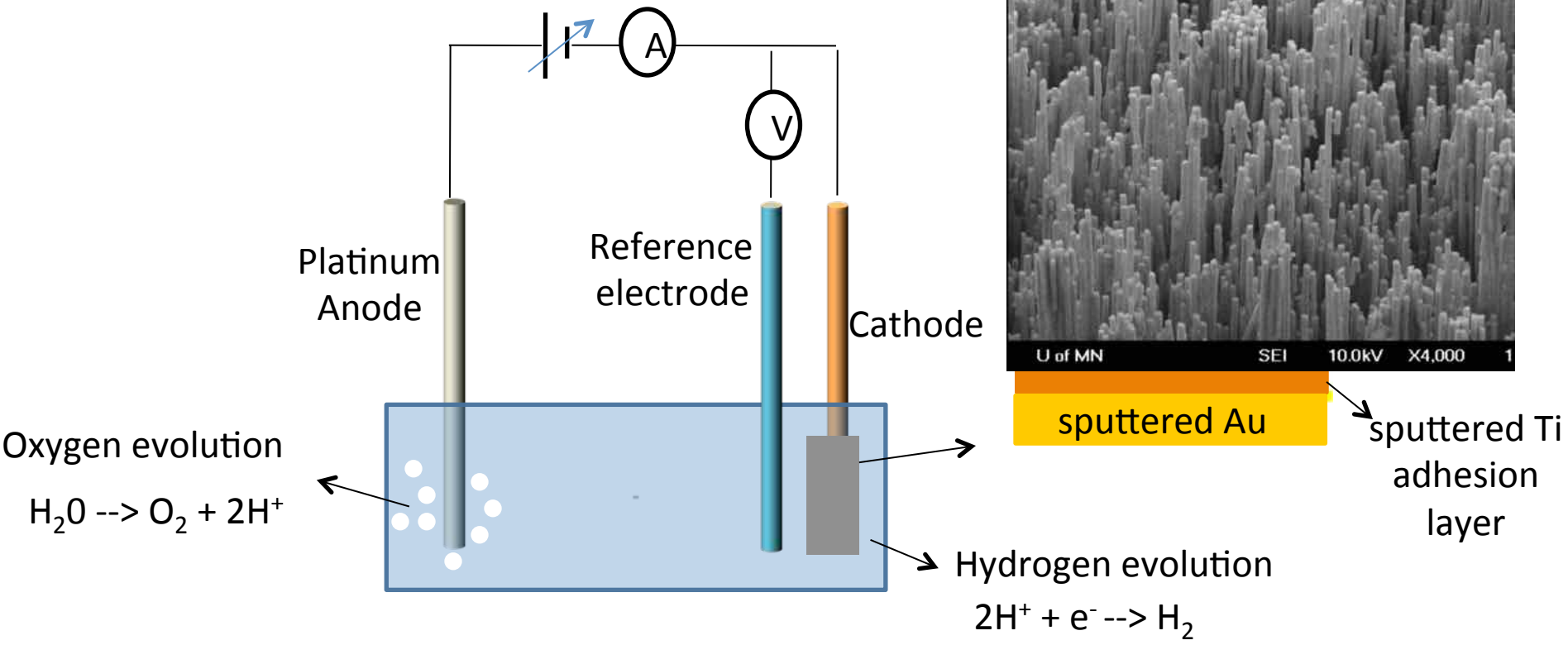
Magnetostrictive whisker sensors at the SAME nanoscale



Whisker deflection creates **chemical potential change** that fires neuron
Wire deflection creates **magnetization change** that changes GMR resistance

Fe-Ga NW: DC Electrodeposition

Electrochemical Cell



☐ FeGa nanowires are grown using a single bath containing Fe^{+2} and Ga^{+3} ions with Sodium Citrate as complexing agent.

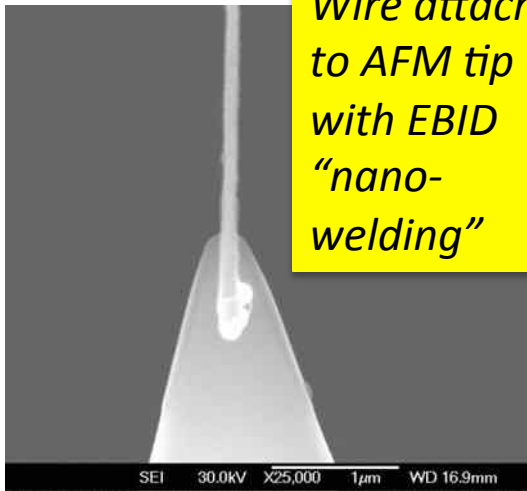
Mechanical properties of Fe-Ga NWs



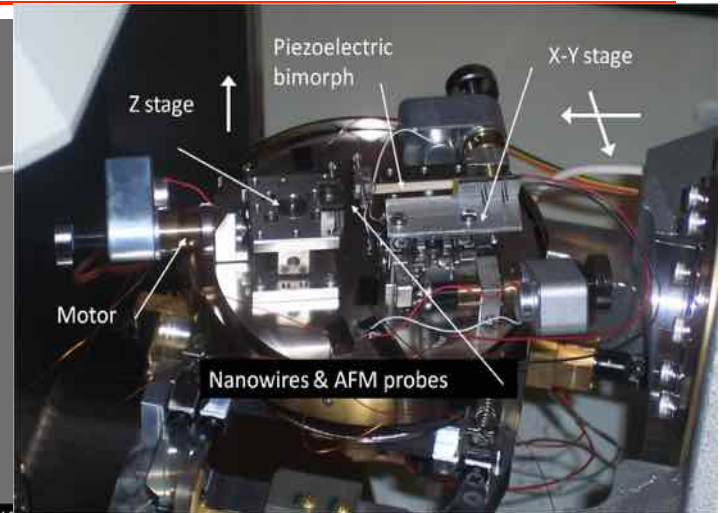
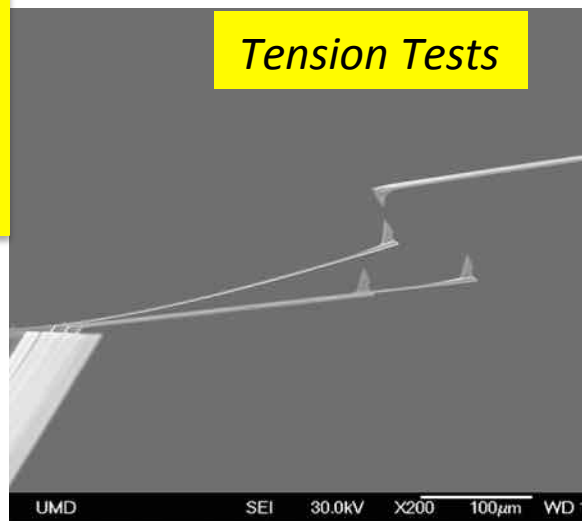
UNIVERSITY OF MINNESOTA



Wire attached to AFM tip with EBID "nano-welding"



Tension Tests

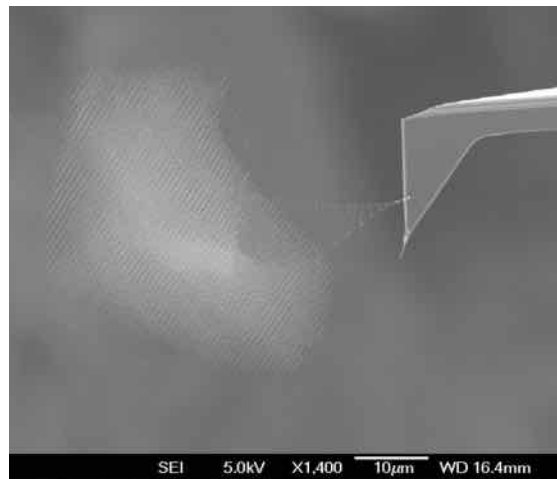
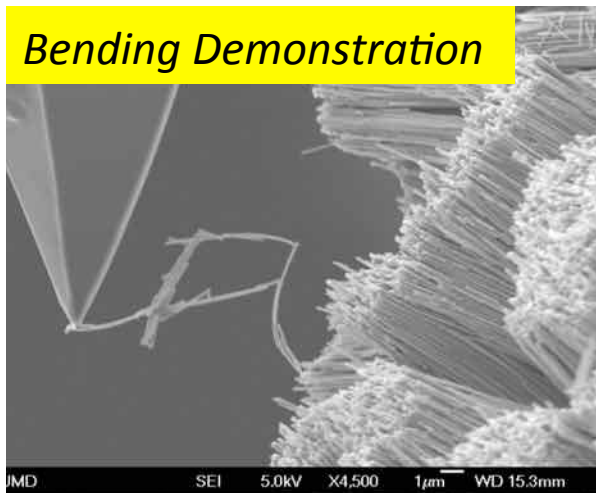


Nano-manipulator

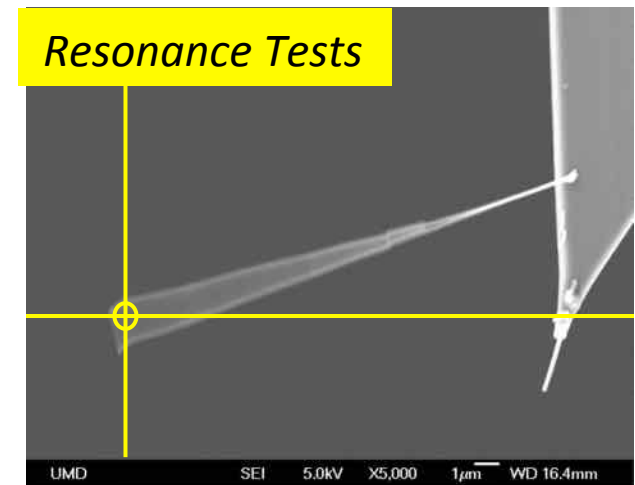
McGary et al. *J. Appl. Phys* 99 (2006)
Downey et al. *J. Appl. Phys* 103 (2008)

During testing the soft AFM cantilever deflects upward

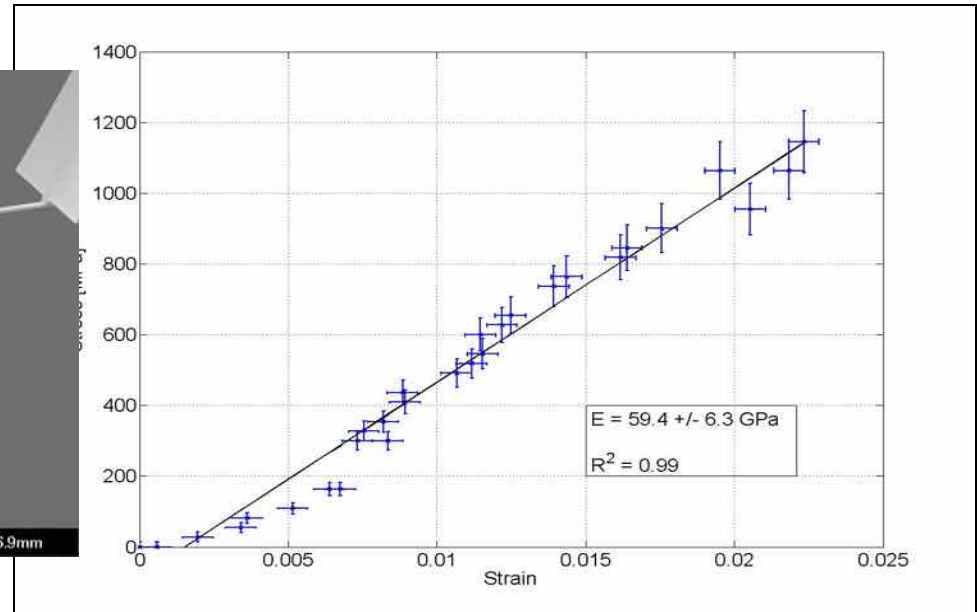
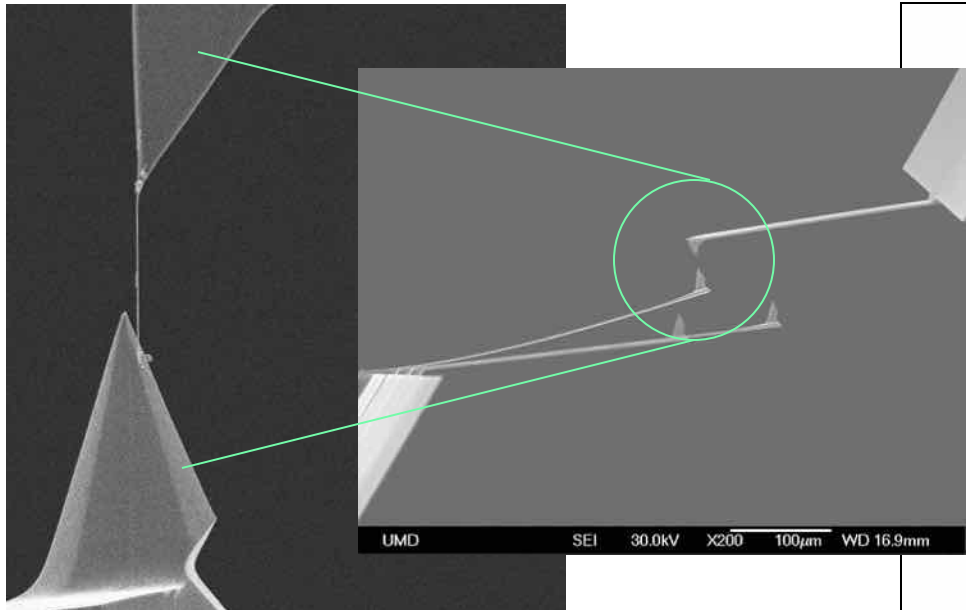
Bending Demonstration



Resonance Tests



Tensile Tests



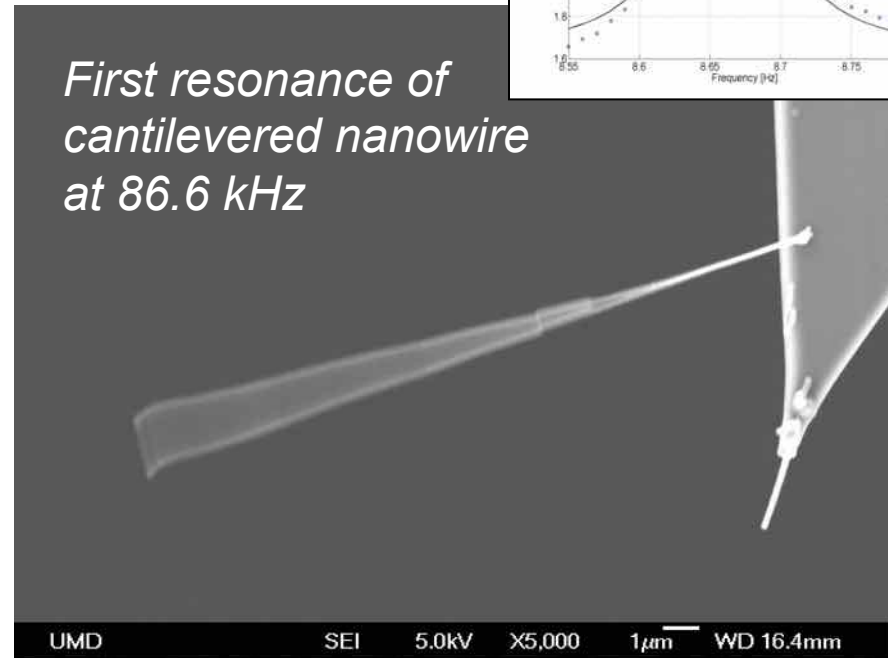
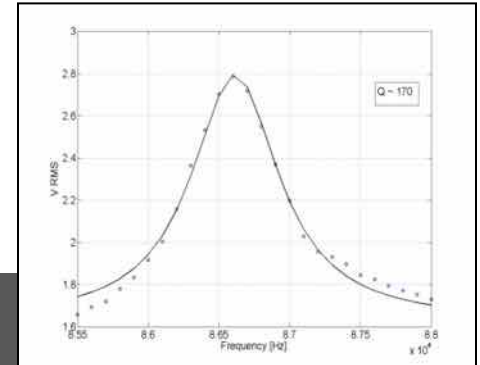
Wire #	Diameter (nm)	Length (μm)	Ultimate Strength (MPa)	Young's Modulus (GPa)
1	105 +/- 5	9.80 +/- 0.01	1232 +/- 147	58.3 +/- 6.0
2	135 +/- 5	13.8 +/- 0.01	1202 +/- 119	59.4 +/- 6.3
3	225 +/- 5	36.8 +/- 0.01	1084 +/- 60	54.9 +/- 7.1
4	130 +/- 5	7.55 +/- 0.01	1050 +/- 91	58.9 +/- 8.6
Bulk Fe₈₃Ga₁₇ [100] (Kellogg et. al, <i>Acta Mater.</i> 52, 2004)			500	65

Resonance Method Results

Wire attachment assumed fixed
 Frequencies swept with piezo
 Modulus related to resonance:

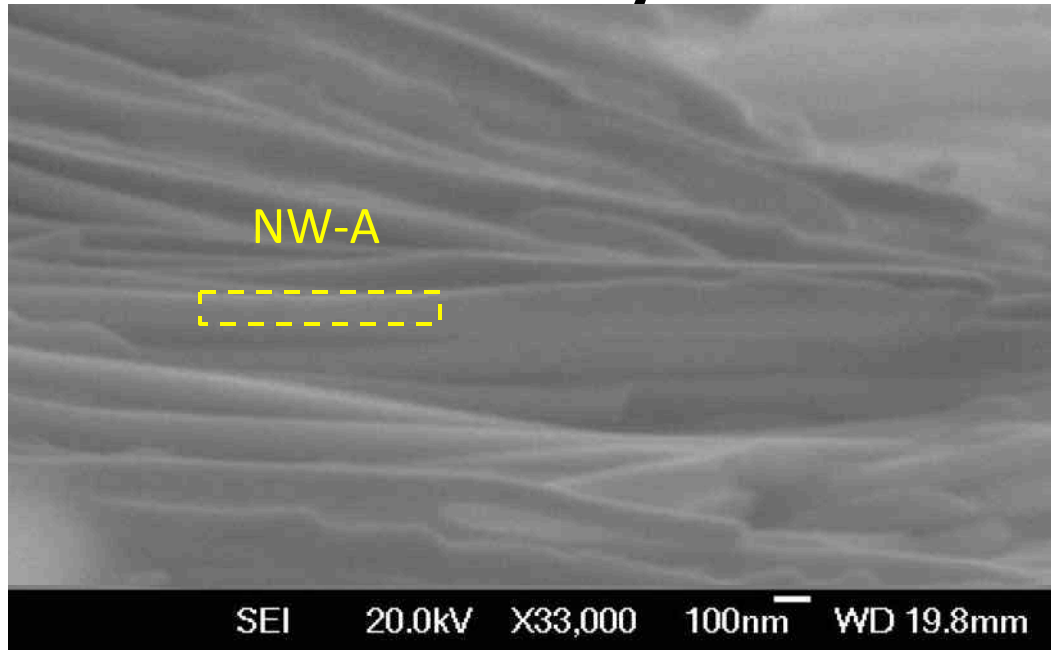
$$f_0 = \beta_0^2 / 2\pi \sqrt{(EI / mL^4)}$$

Results are lower bounds
 Two distinct values suggest a
 compositional variation

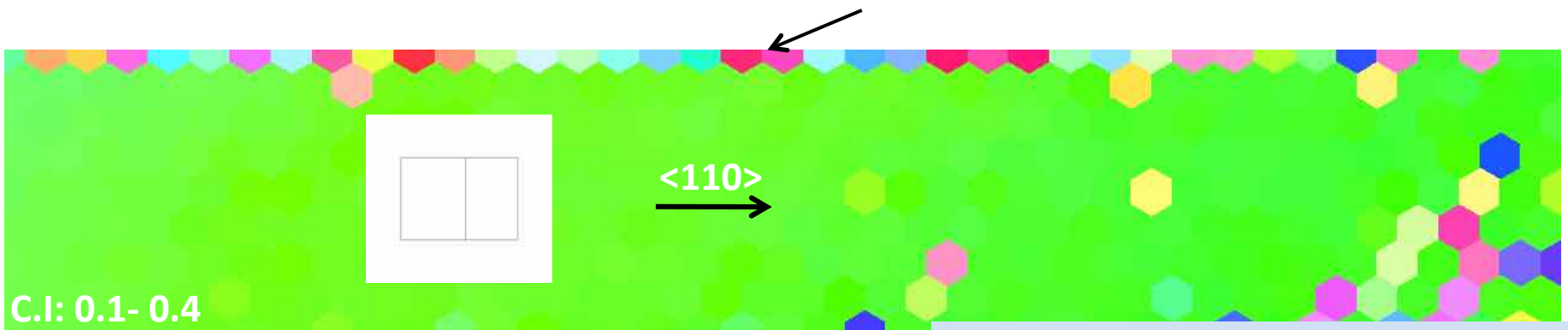
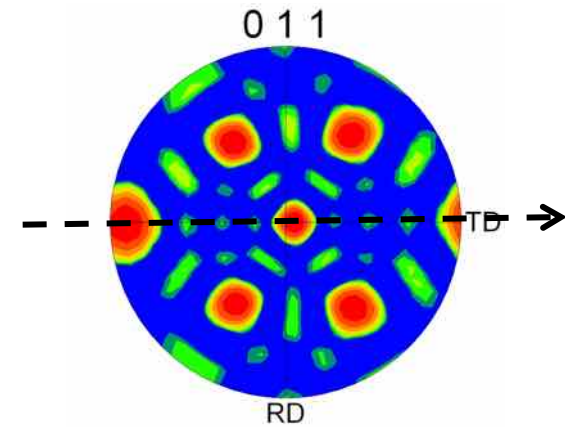


Wire #	Diameter (nm)	Length (µm)	Resonance Frequency (kHz)	Young's Modulus (GPa)
5	100 +/- 5	19.4 +/- 0.01	86.6 +/- 0.05	44.2 +/- 8.2
6	120 +/- 5	11.6 +/- 0.01	304.3 +/- 0.05	45.1 +/- 7.9
7	225 +/- 5	7.88 +/- 0.01	1781.1 +/- 0.05	93.1 +/- 8.3
8	125 +/- 5	4.43 +/- 0.01	3143.0 +/- 0.05	93.8 +/- 15

EBSD study on uniform FeGa NW



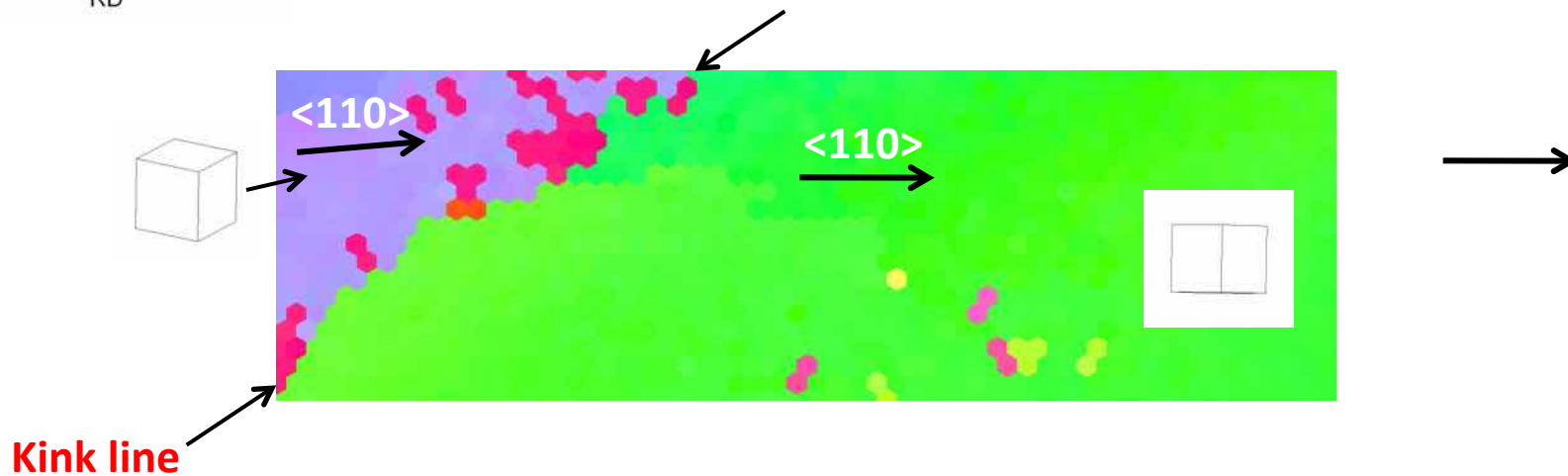
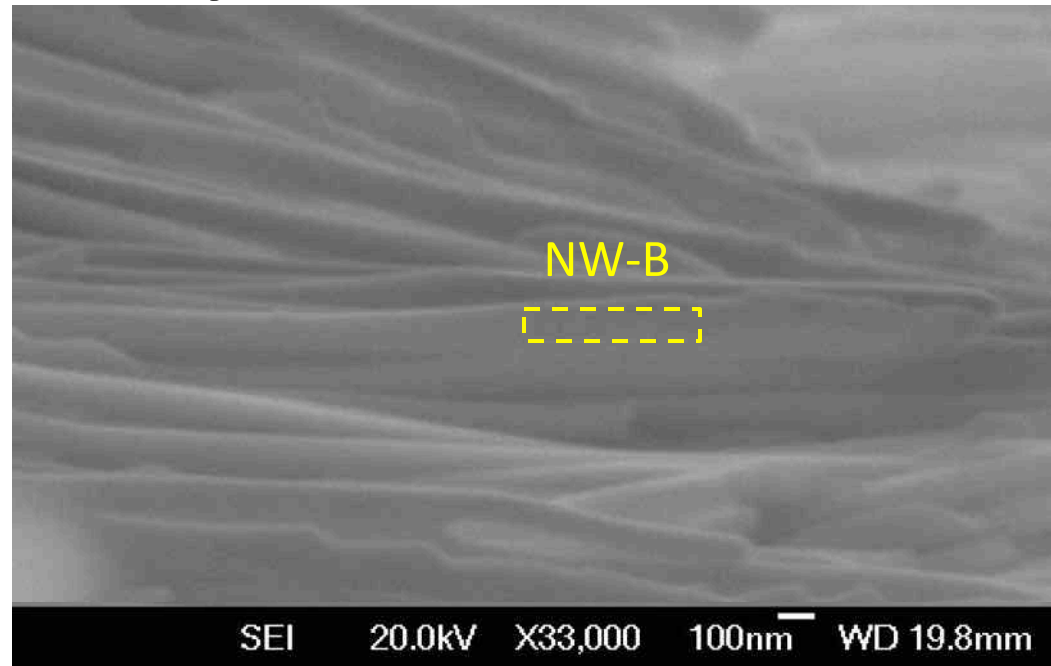
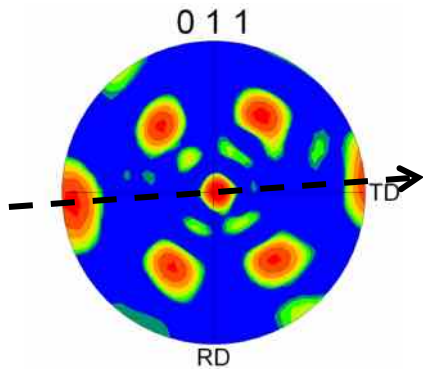
- Uniform FeGa NW ($\phi \sim 150$ nm)



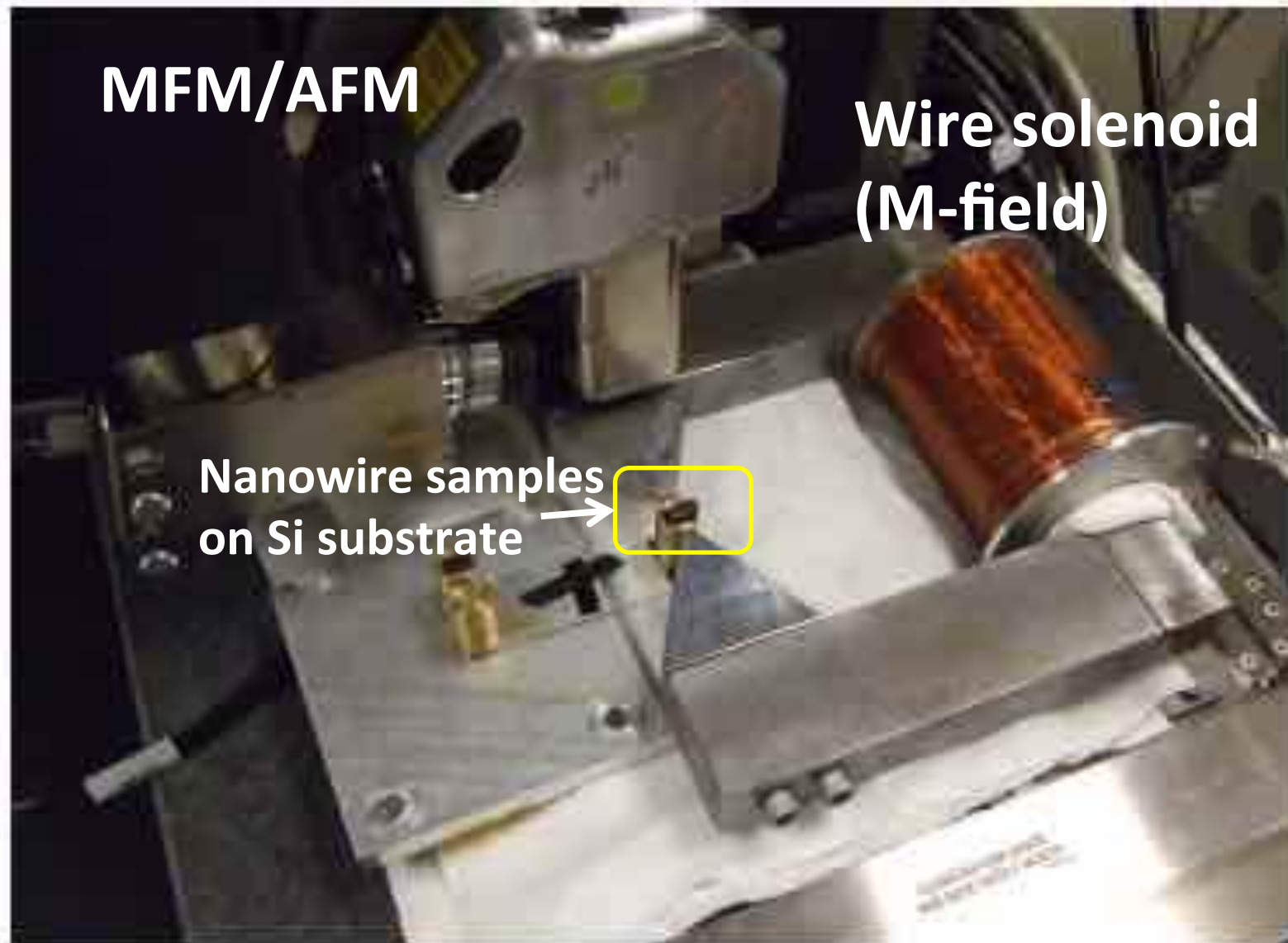
$\langle 110 \rangle$ orientation along NW length

EBSD study on FeGa nanowire

- Uniform FeGa NW
- $\langle 110 \rangle$ orientation along NW length



Magnetic studies of Fe-Ga NW



Magnetic studies of Fe-Ga NW



UNIVERSITY OF MINNESOTA



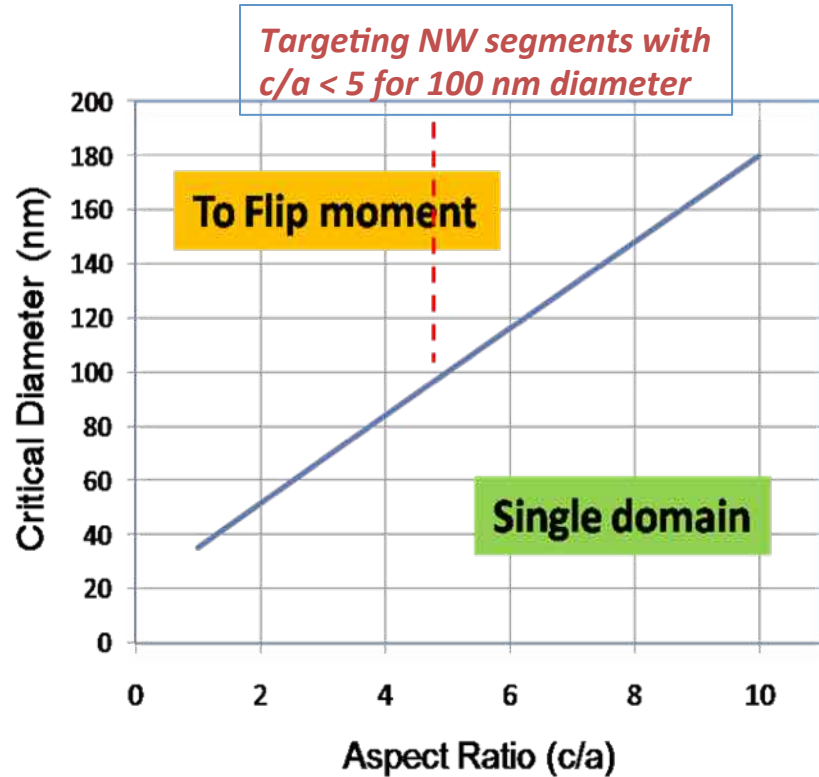
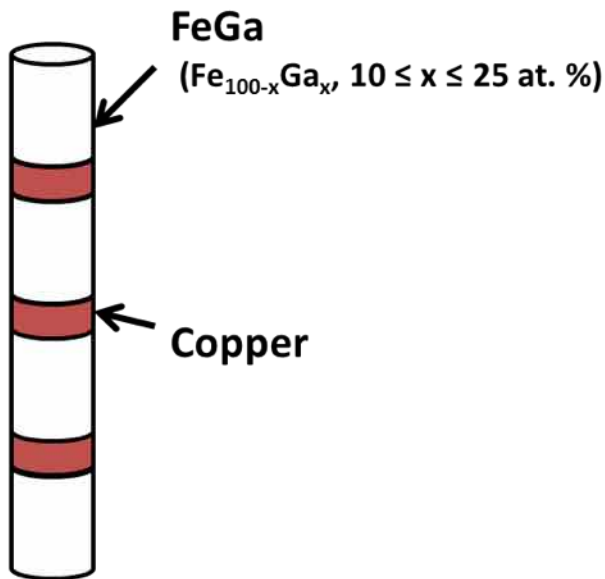
Scale bar: 0.5 μm

Energy term	Maximum cost [erg/ cm^3]
Exchange coupling	3×10^4
Magnetocrystalline anisotropy	3×10^5
Magnetoelastic	$2.5 \times 10^3 / \text{MPa}$
Shape anisotropy	7×10^6

Magnetic studies of Multilayer Fe-Ga/Cu NW



UNIVERSITY OF MINNESOTA



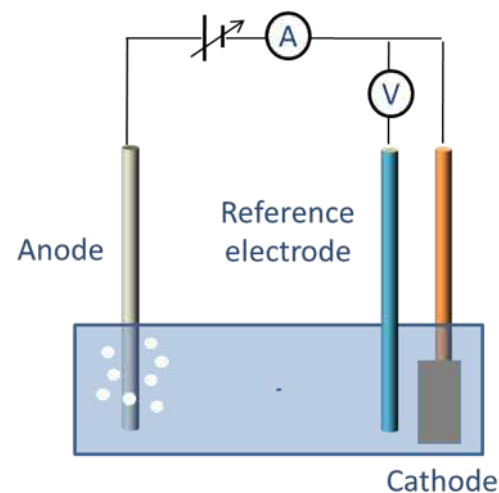
Scale bar: 0.5 μm

Fabrication of Multilayer Fe-Ga/Cu NW

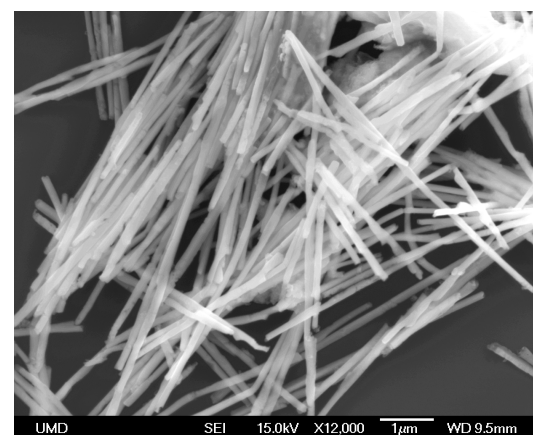
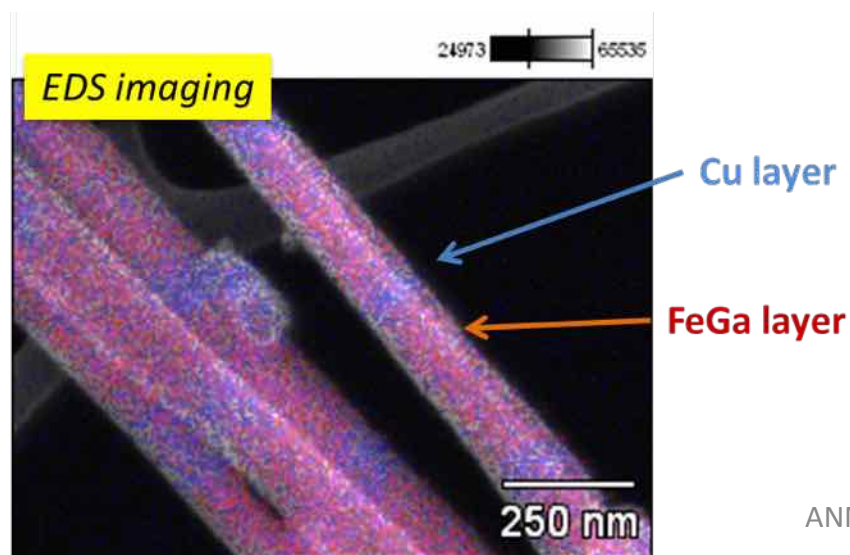


Electrodeposition

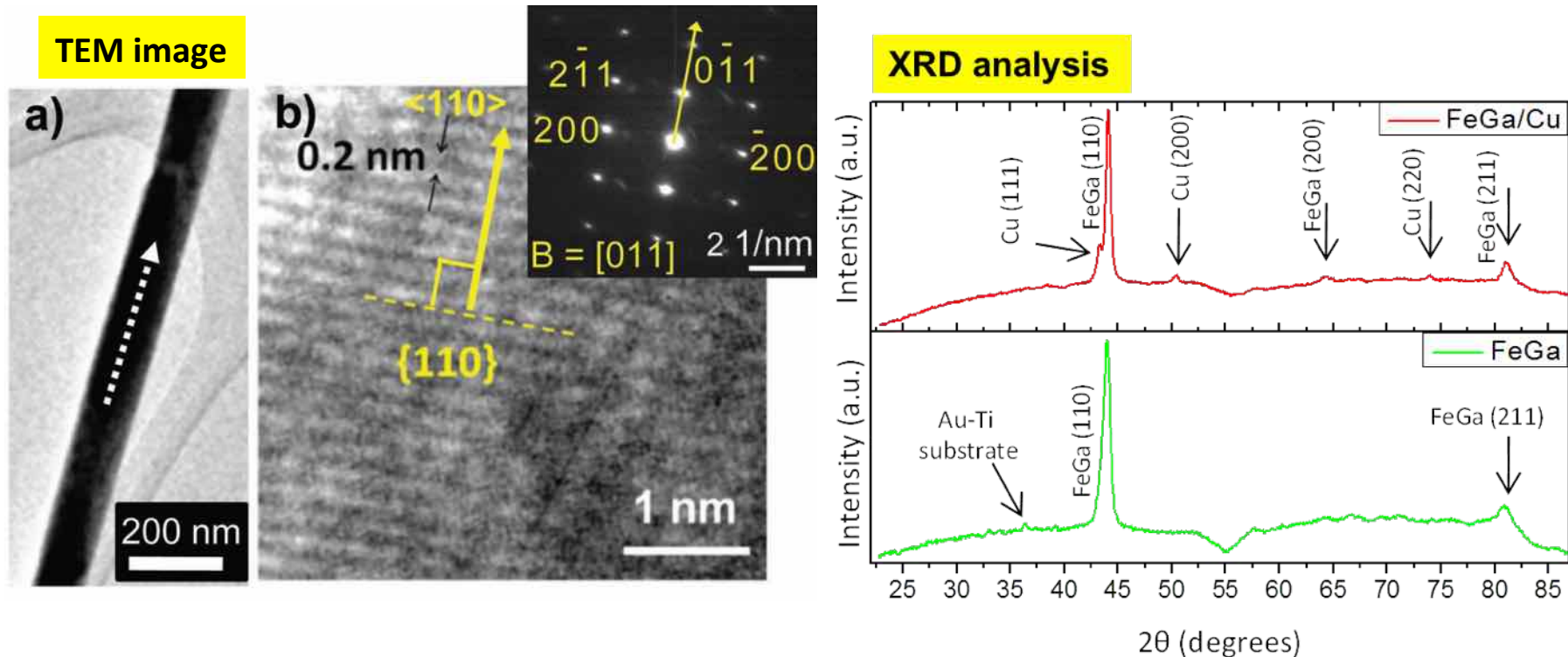
- Fe/Ga/Cu plating bath
- Deposition potential of -1.12V and -0.8V
- Grown in Anodized Aluminum Oxide (AAO) templates
- 150nm diameter, 200nm spacing



Nanowires separated and Isolated

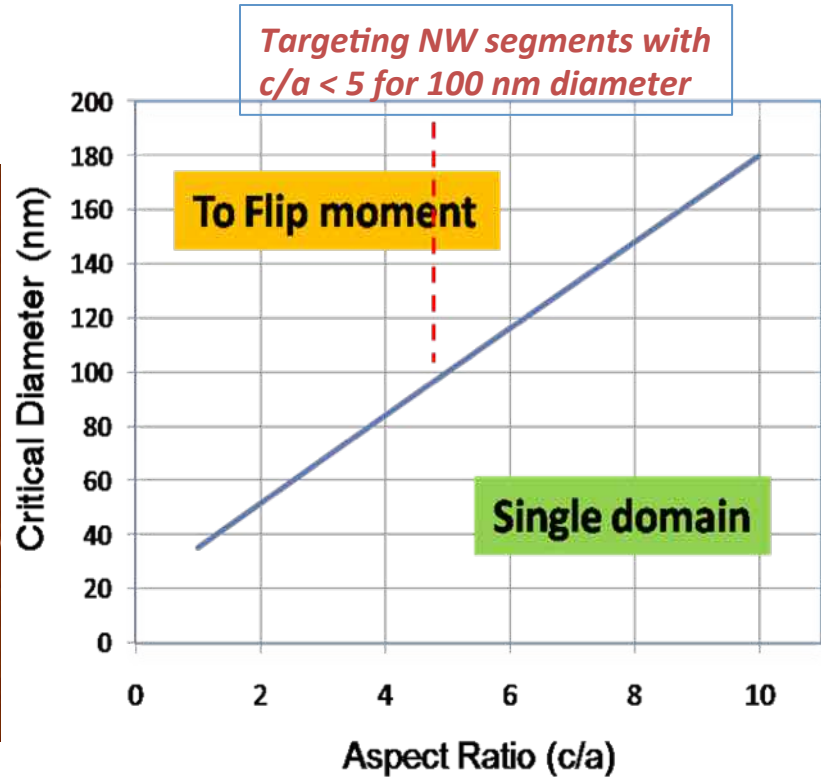
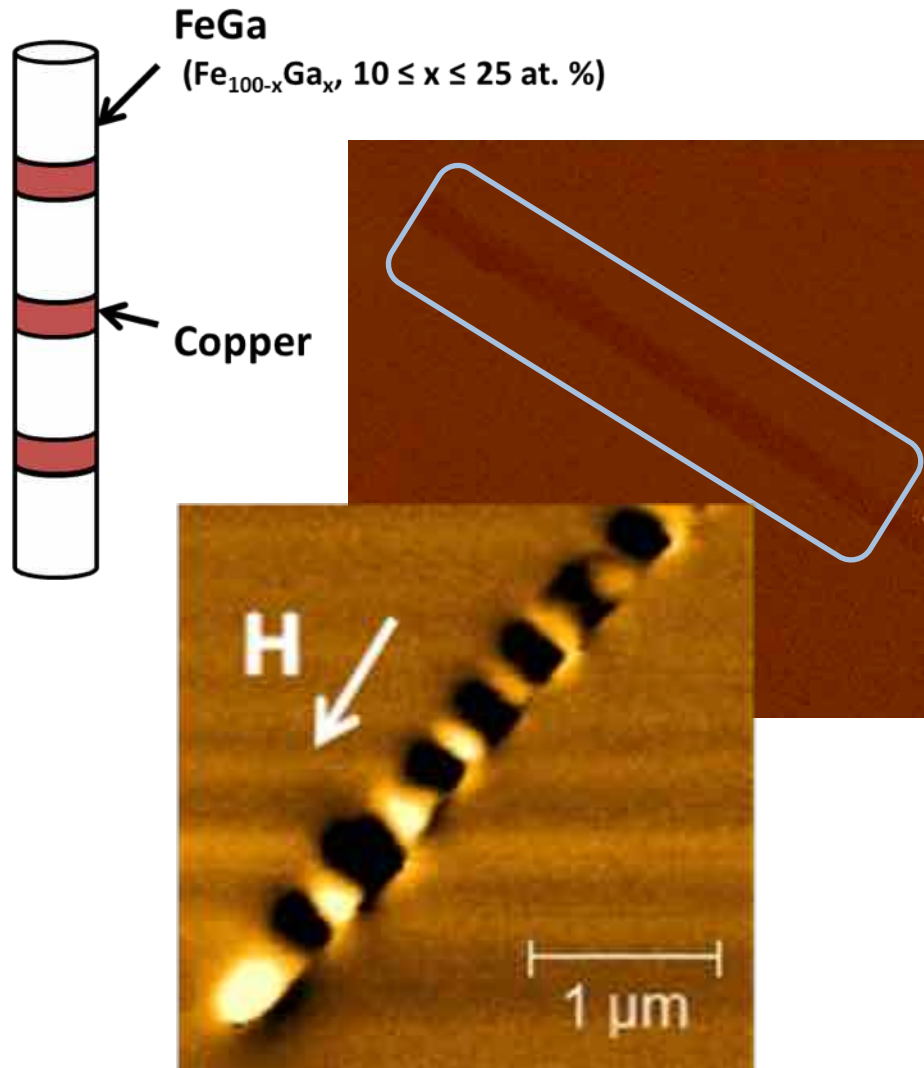


FeGa/Cu NW: Structural characterization



- ✓ Use of citrate baths for electrodeposition; highly textured growth even for FeGa-Cu multilayered nanowires. => high magnetostriction
- ✓ Extensive structural characterization by XRD and TEM reveals a strong $\langle 110 \rangle$ textured $\text{Fe}_{1-x}\text{Ga}_x$

Magnetic studies of Multilayer Fe-Ga/Cu NW



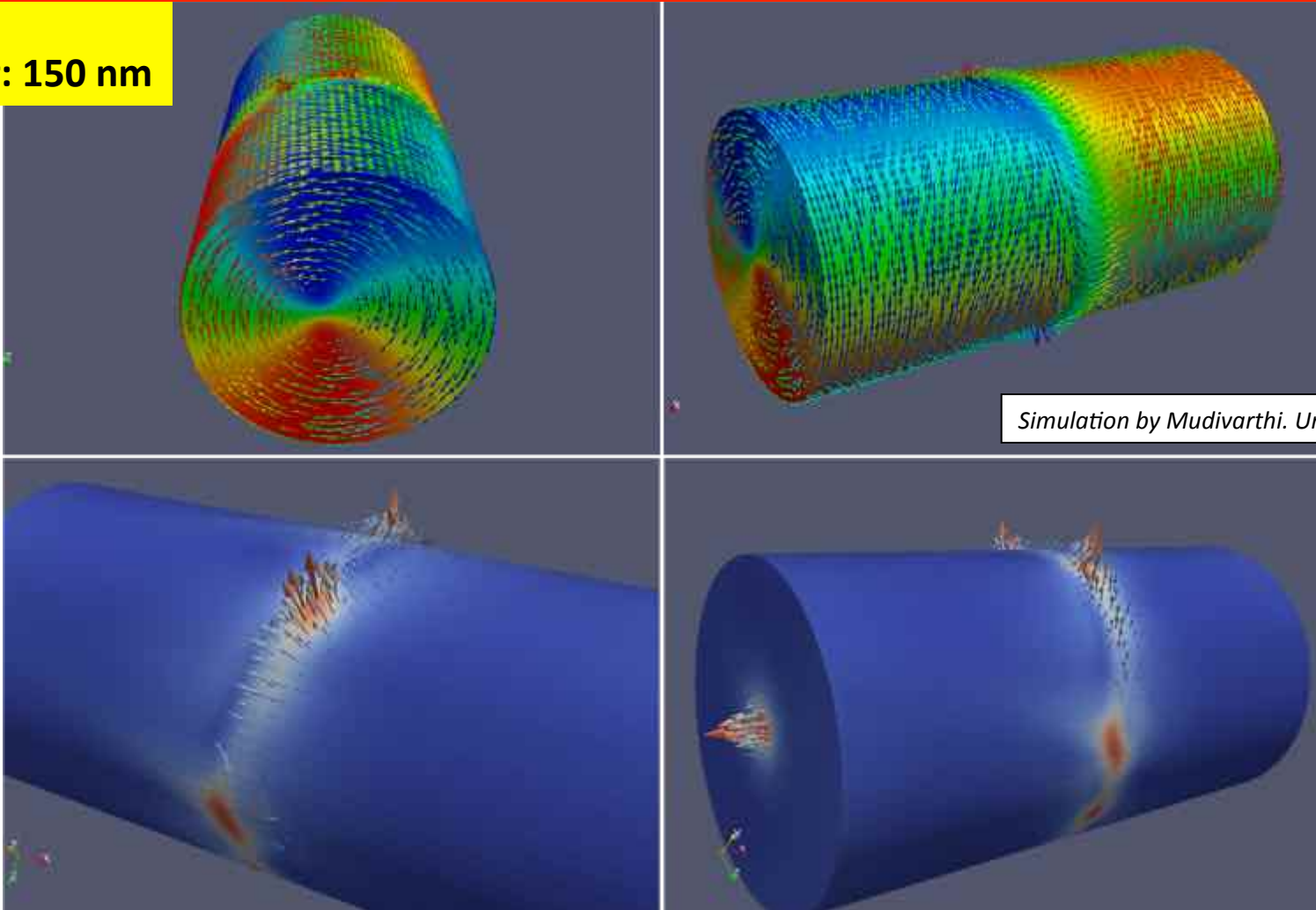
FEM (Magpar) of Fe-Ga segment



UNIVERSITY OF MINNESOTA



$c/a = 2$
Diameter: 150 nm

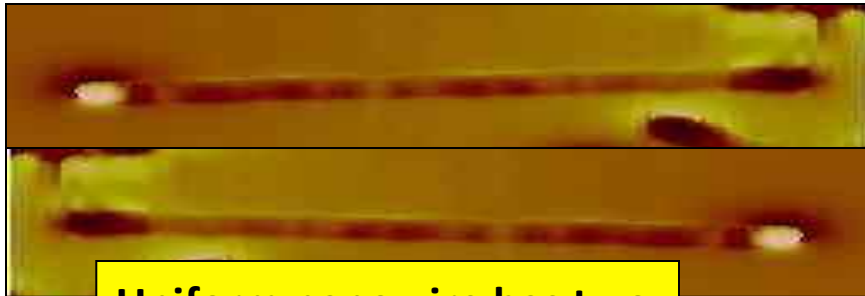


Simulation by Mudivarthy. Univ. of Maryland

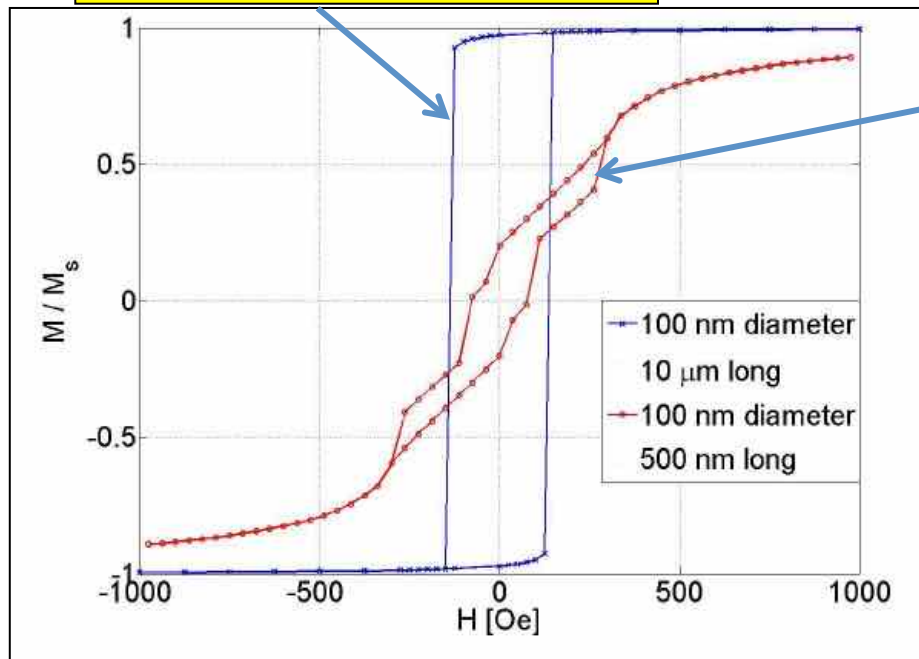
FEM predicts that at remanence, a nanowire with aspect ratio of two actually forms two opposite vortex domains at each end separated by a domain wall near the center.

Moment rotation in Fe-Ga NW and in Fe-Ga/Cu NW

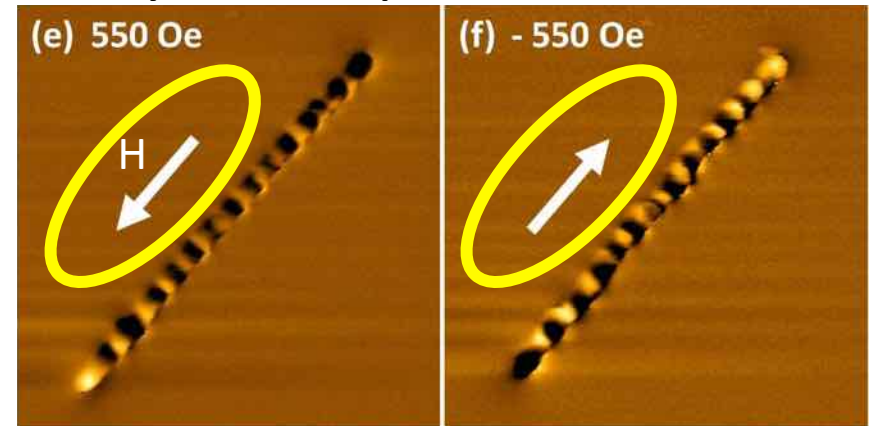
Magnetic force microscopy (MFM)



Uniform nanowire has two axial magnetization states



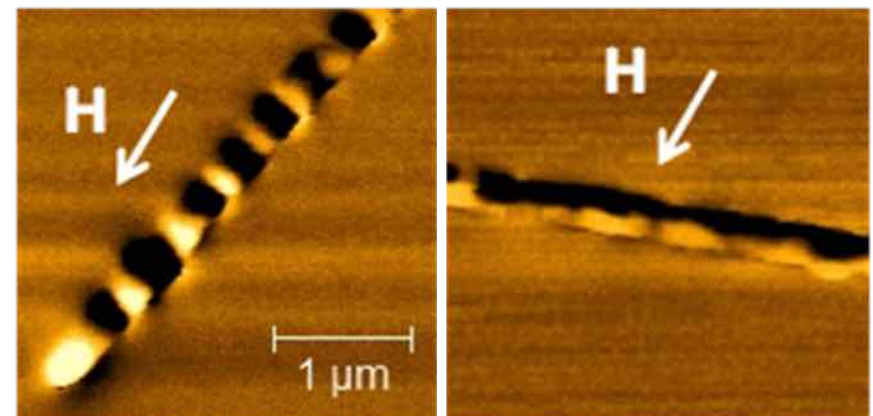
Multilayered, low aspect ratio nanowires



Multilayered, low aspect ratio nanowire has multiple domain structures / magnetization states

($H \sim 550$ Oe) $\sim 5^\circ$

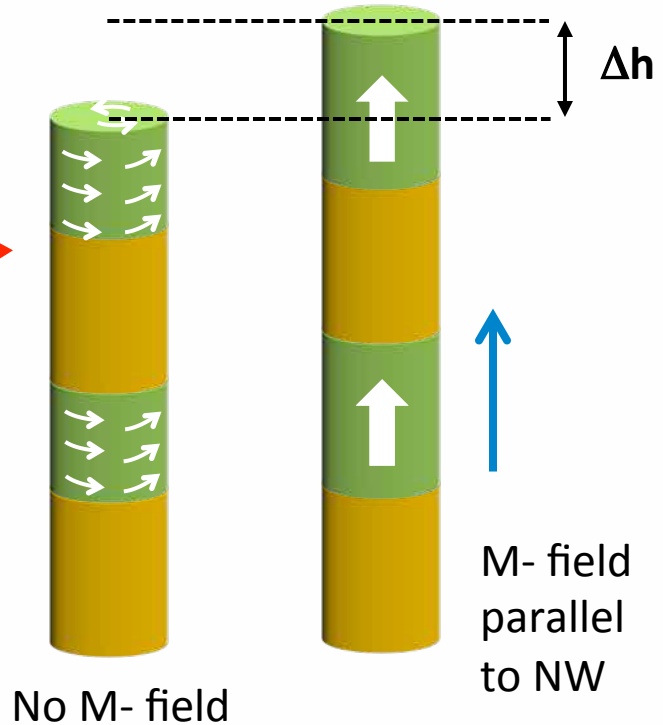
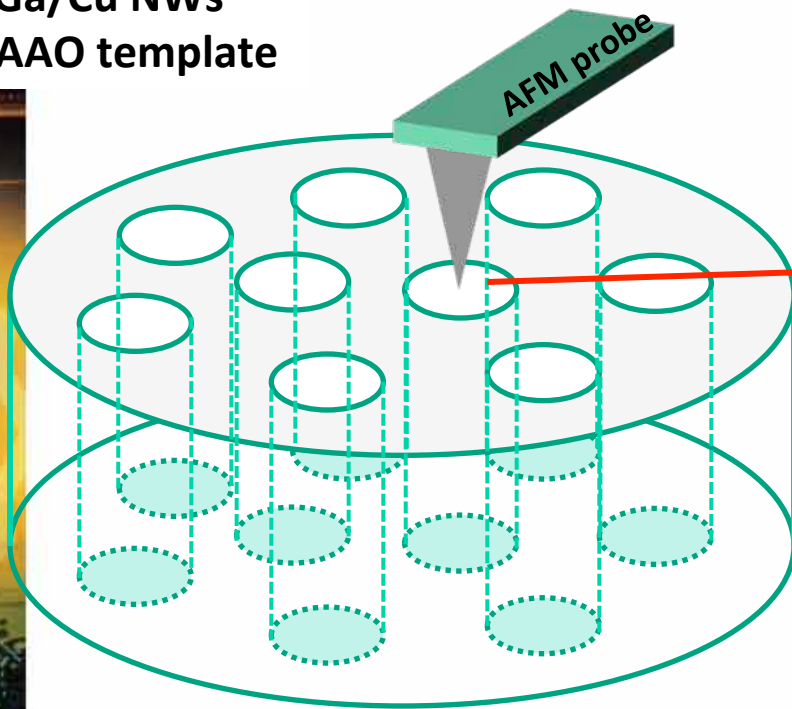
$\sim 105^\circ$



Magnetostriction of Fe-Ga/Cu NW



FeGa/Cu NWs
in AAO template

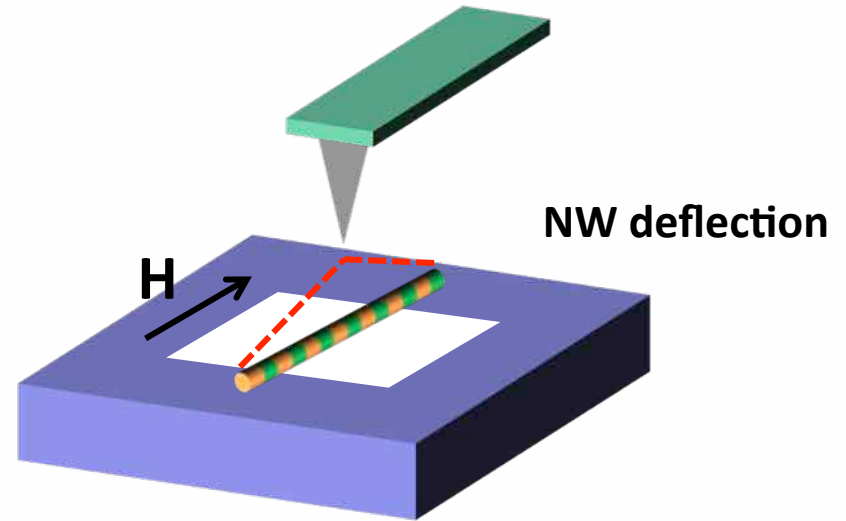
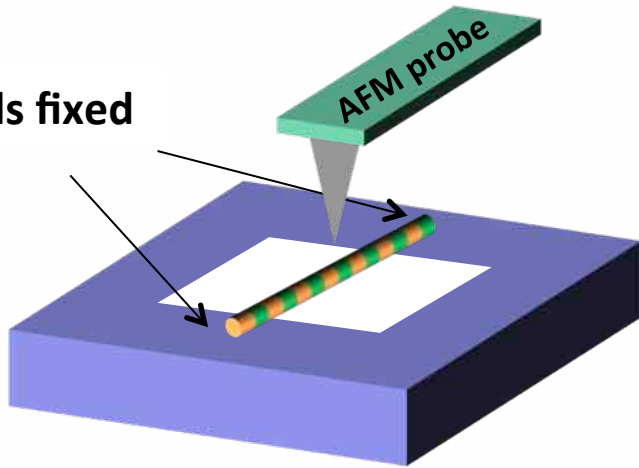


The expected length changes of 10 μm long multilayered (50:50) Fe-Ga:Cu NW with a magnetostriction of ~ 50 ppm along $\langle 110 \rangle$ are estimated to be in **range between 0.1 nm and 0.25 nm** = below the vertical resolution of our AFM system.

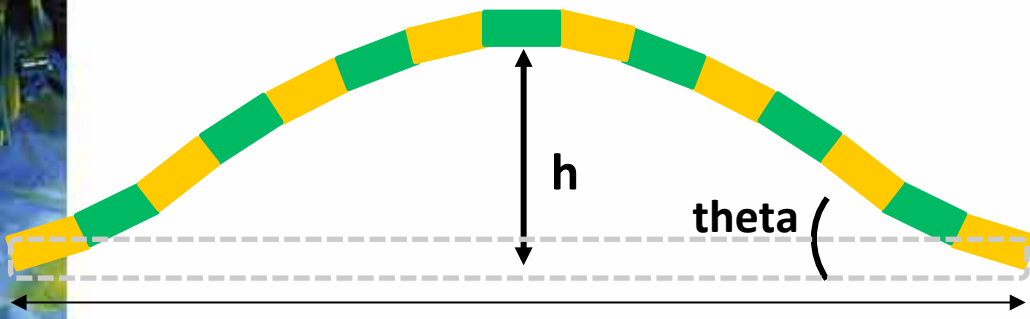
Magnetostriction of Fe-Ga/Cu NW



Both ends fixed



Magnetostriction generates a compressive buckling stress in the NW → Deflection of NW



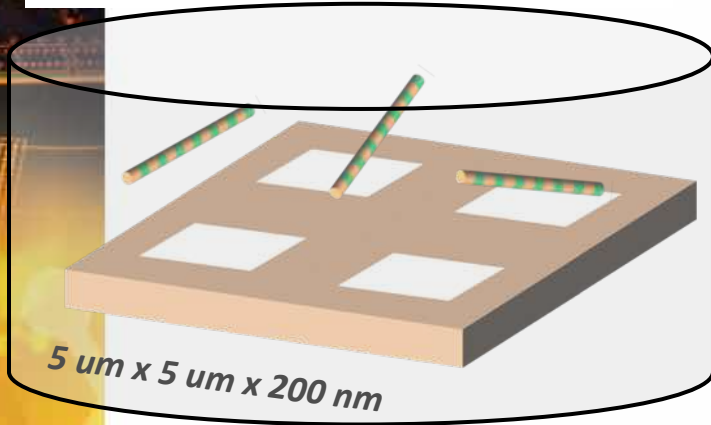
ppm	Delta L	$h = \sin(\theta) * L/2$
20	0.1(nm)	~22 (nm)
100	0.5	~50
200	1	~70
300	1.5	~86

Large enough to be measured by AFM

Sample preparation and AFM measurement



NW placement in isopropanol



AFM with external magnetic field

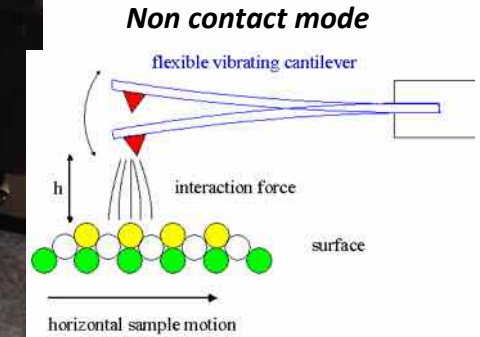
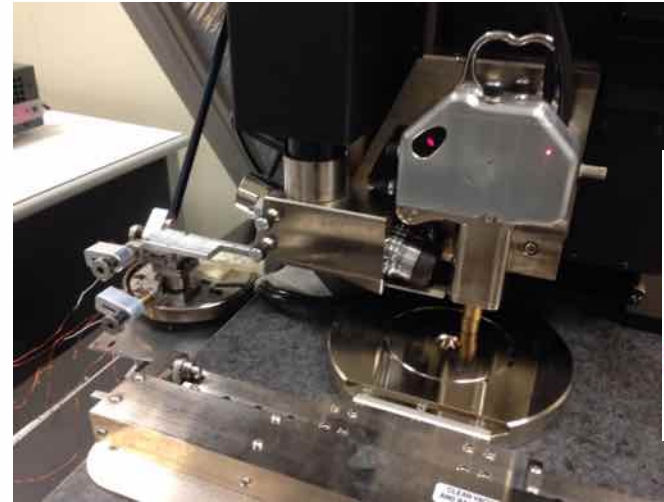
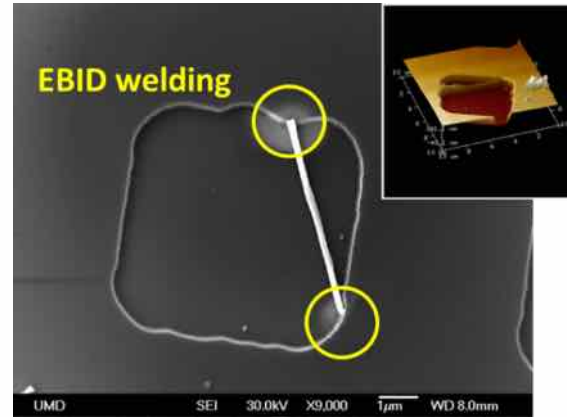
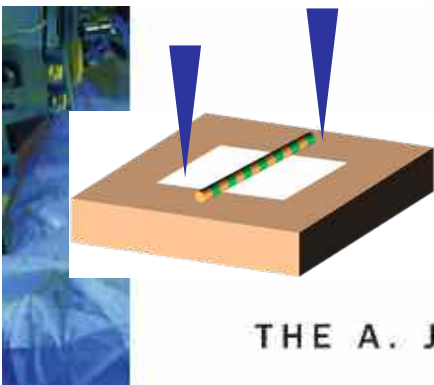
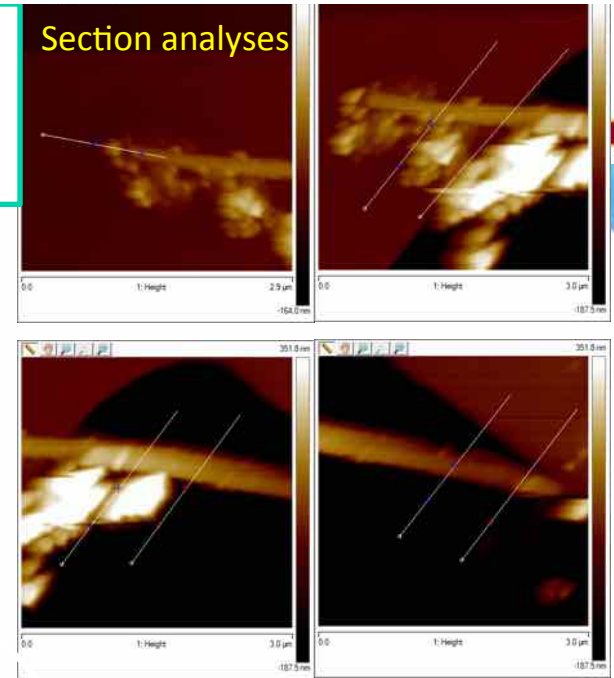
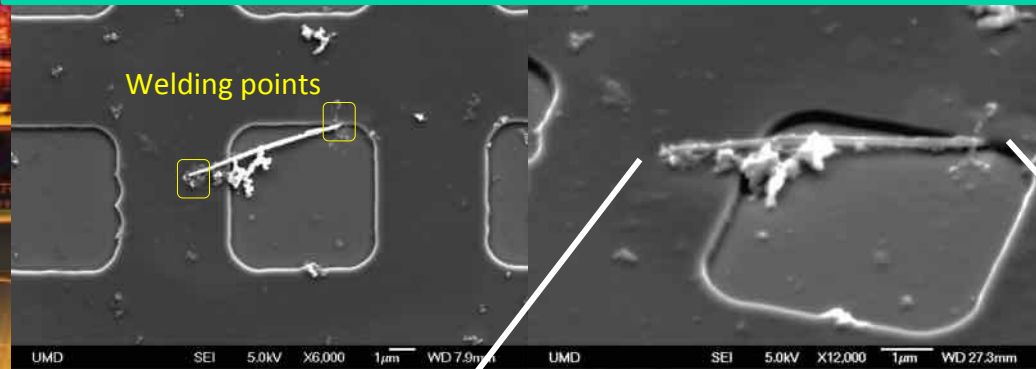


Image from webpage of Max Planck institute

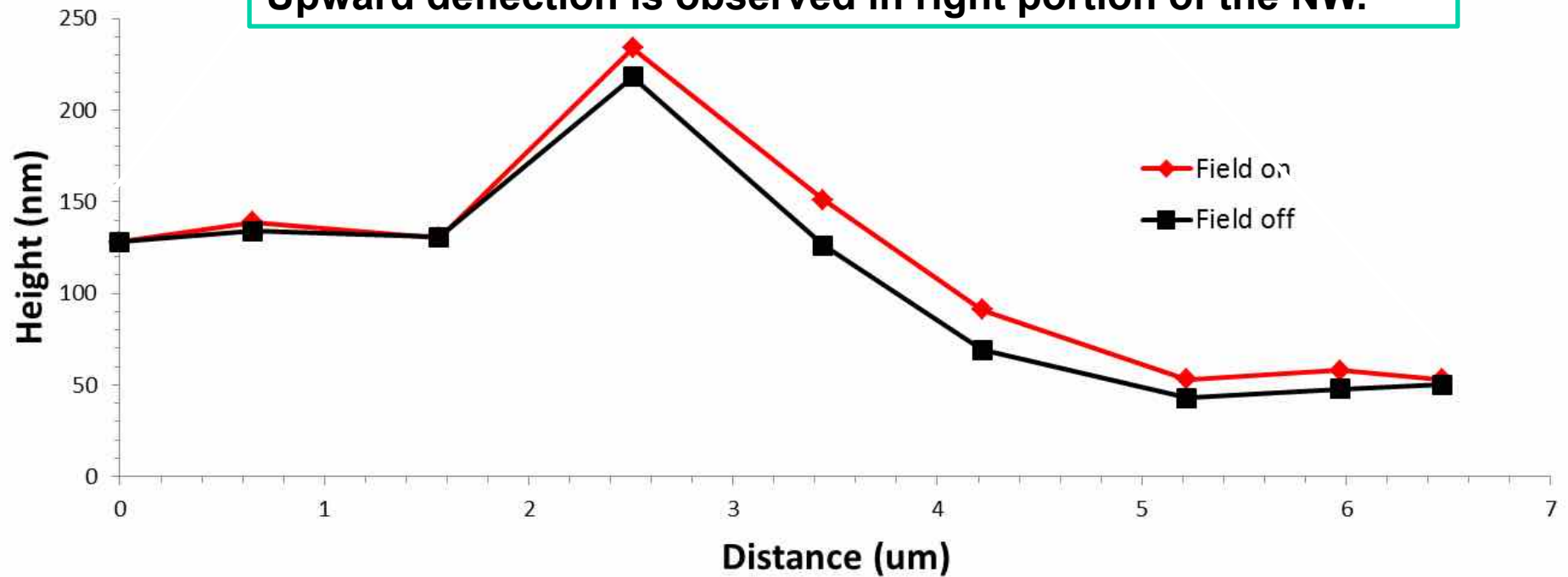
NW welding (EBID)



Height profile measurement along NW

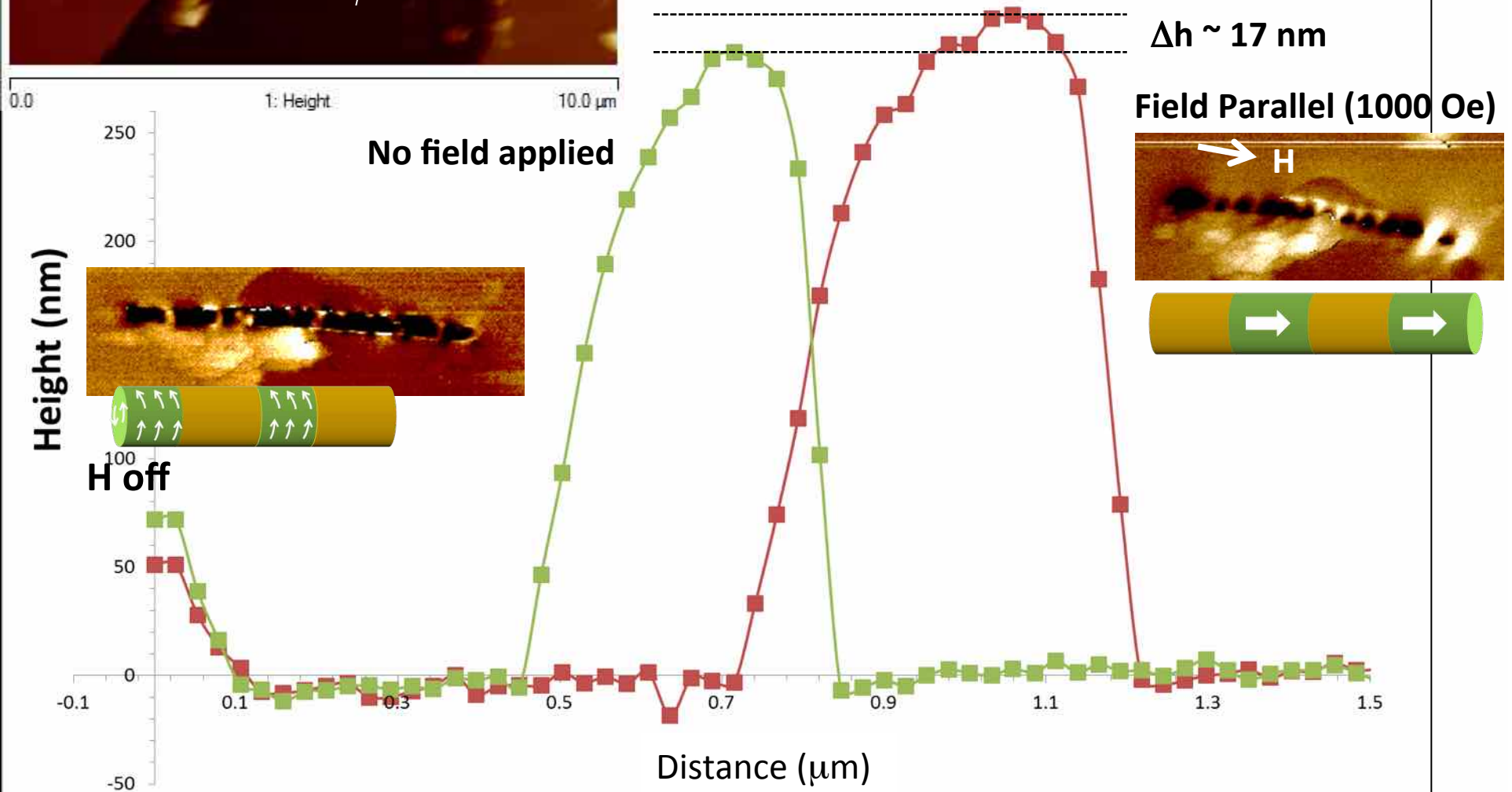


Upward deflection is observed in right portion of the NW.



Section analysis

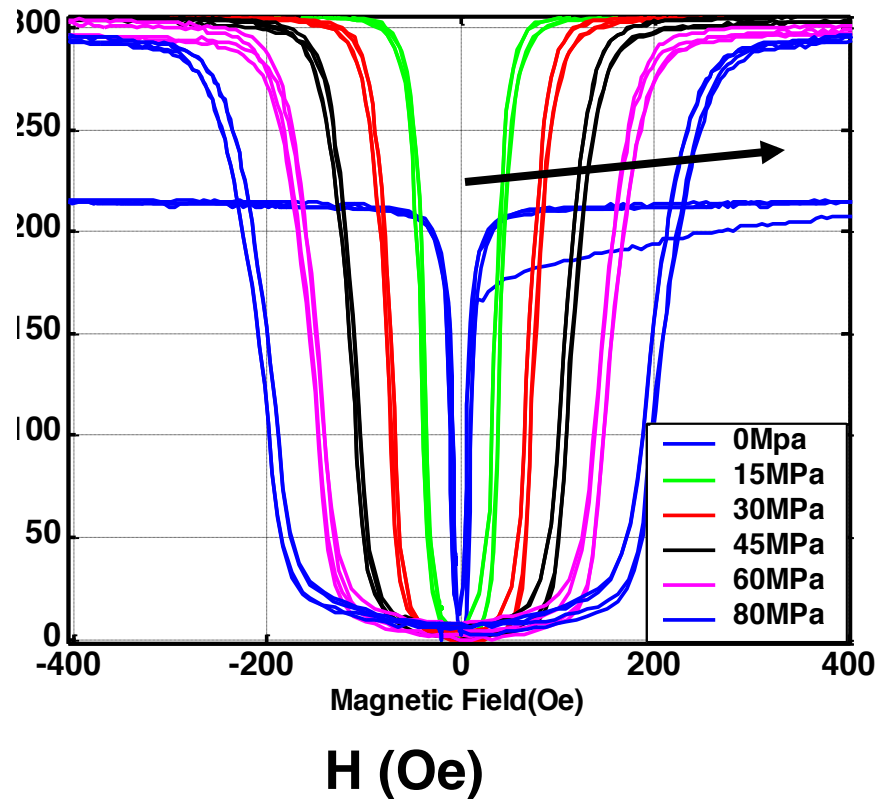
Field parallel to NW axis vs. No field



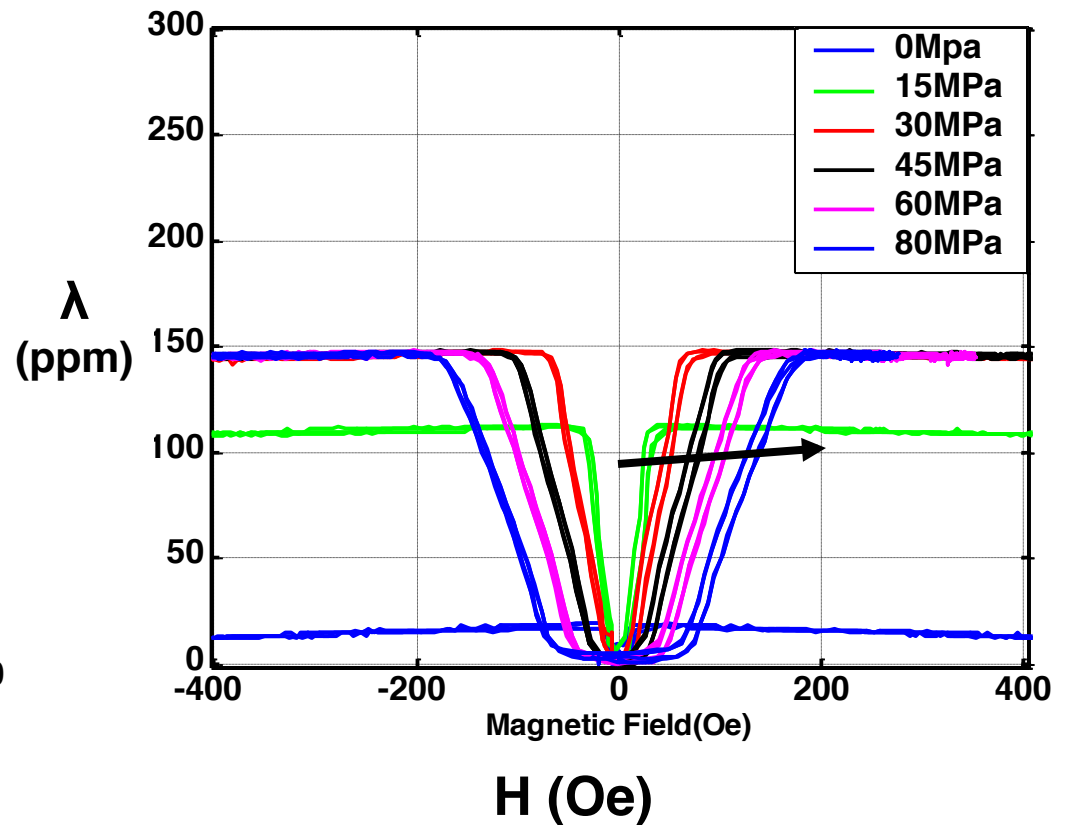
Parallel field elongated NW indicates magnetostriction of $\sim 20 \text{ ppm}$ compares well with reported values of $\lambda_{\text{sat}} = \sim 20 \text{ to } 50 \text{ ppm}$ in bulk alloy

Direct Effect λ -H along $\langle 100 \rangle$ and $\langle 110 \rangle$

$\langle 100 \rangle$, 19 at. % Ga

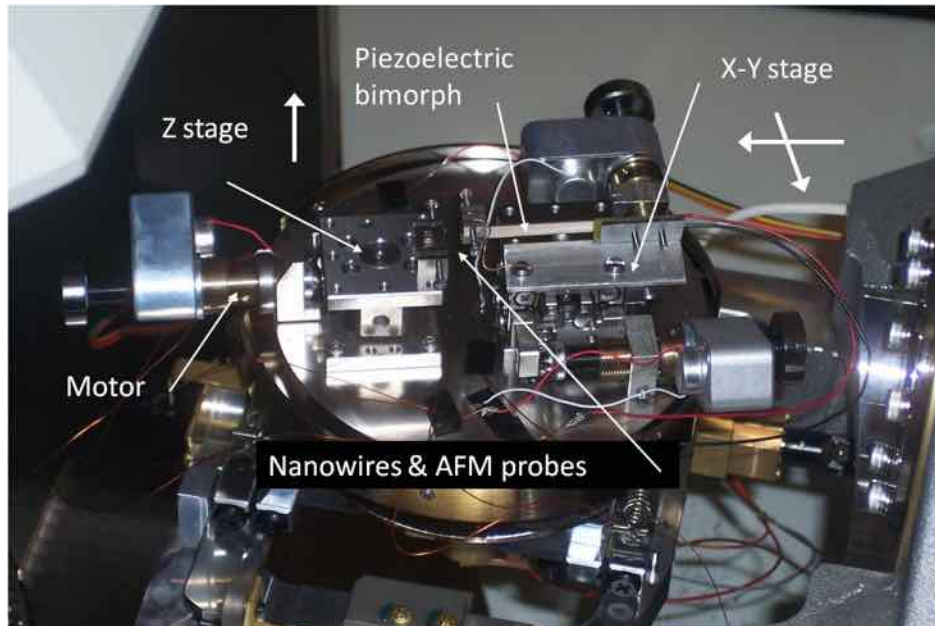


$\langle 110 \rangle$, 18 at. % Ga

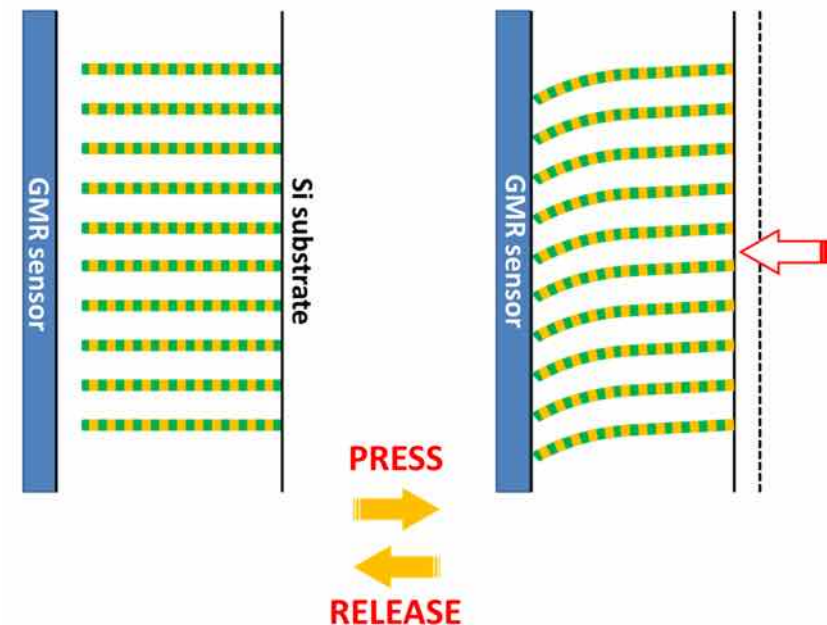


18-19 at. % Ga, single crystal

Pressure sensing: GMR sensing of magnetostrictive NW array



Schematic GMR sensing process



Partially etched AAO allows free standing NW array which is attached on a top substrate.

We would like to observe contact between NWs to GMR surface in SEM, using a nano-manipulator.

- *Minimize stress on GMR sensor*
- *Appropriate NWs contact on GMR surface*
- *NW deformation*

=>Controlled experiment

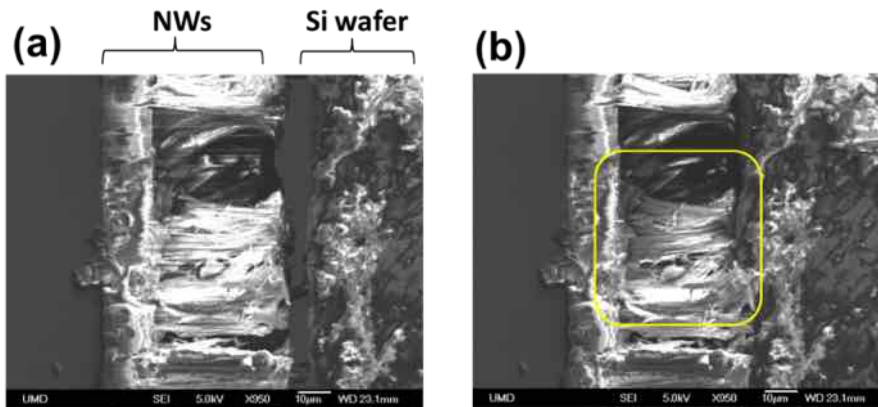
Magnetostrictive Fe-Ga/Cu Nanowires for Sensing Applied Pressure



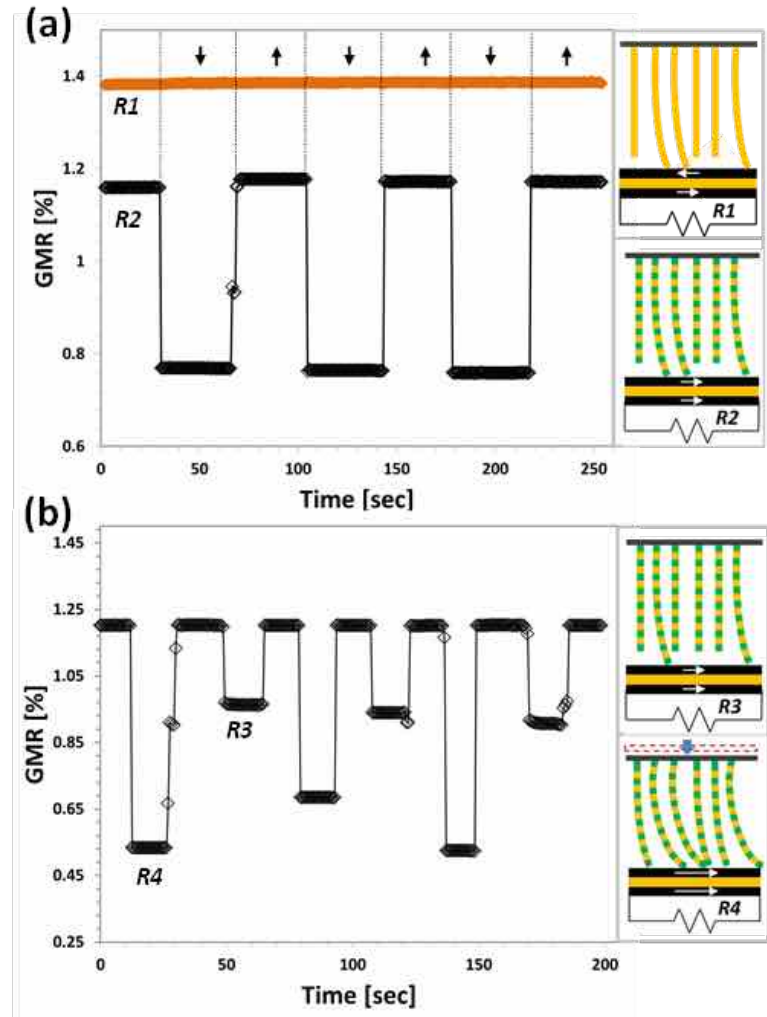
UNIVERSITY OF MINNESOTA



SEM: nanowire array compression



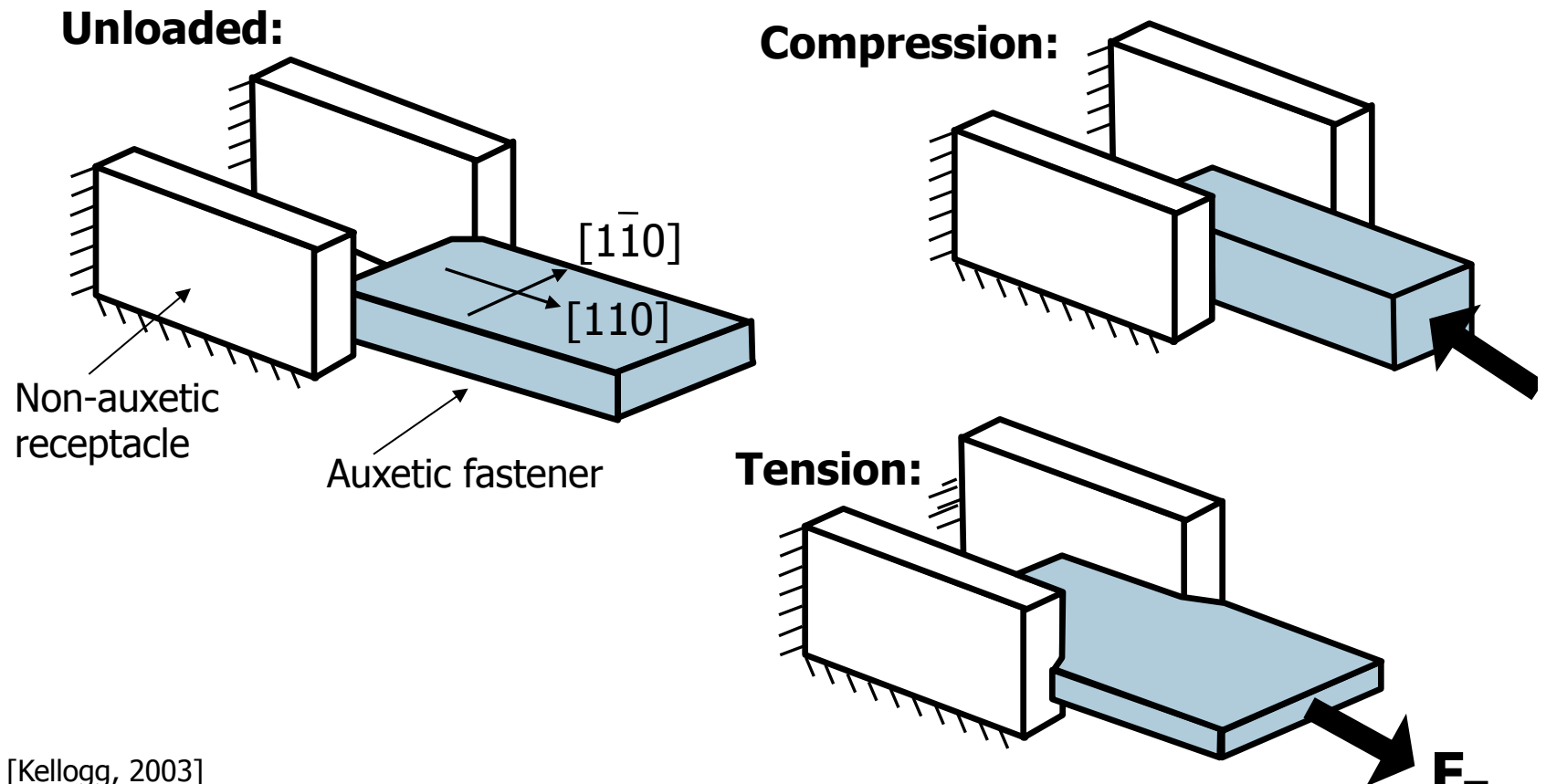
- No resistance change was observed by Cu NW array sample.
- The coarse step ($\sim 1 \mu\text{m}$) causes 2 times larger GMR % value change (0.5 – 0.65%) than the value change (0.2 – 0.3%) caused by the fine step ($\sim 100 \text{ nm}$).
- Estimated values of sensor sensitivity are $1 \sim 4 \text{ m}\Omega/\text{kPa}$.



$$[GMR\% = ((R(H) - R(H_{max}))/R(H_{max}))\%]$$

Applications for Auxeticity include:

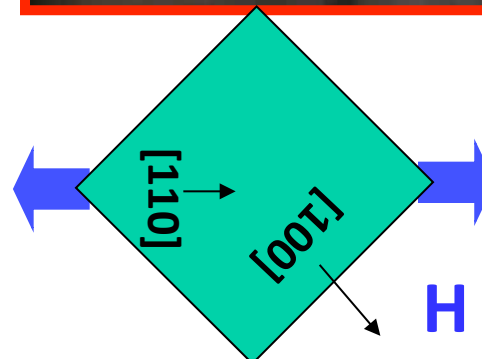
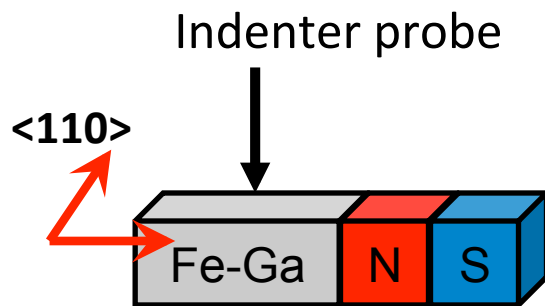
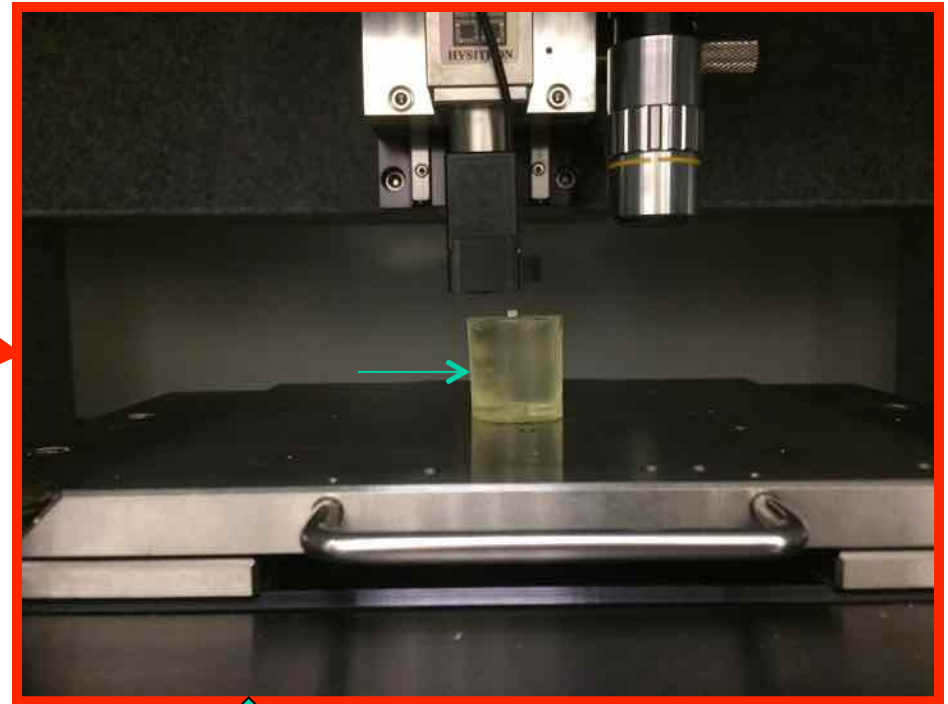
- Impede crack propagation
- Increased indentation resistance
- Reduced fiber pull-out
- Press fit fastening devices – control actively with Galfenol?





Nano indenter experiment to visualize effect of “magnetically tunable” auxeticity

Hardness is proportional to $1/(1-\nu^2)$





NANO INDENTATION DATA: HARDNESS AT 18% Ga Galfenol

Vicker's Hardness ~ 600 MPa in Iron

Without magnetic field:

Hardness ~ 400 - 700 MPa

Average Hardness ~ 550 MPa

Applied force of 0-980 microNewton
Displacement scale is 0-300 nm

With a DC magnetic field ~ 150 mT

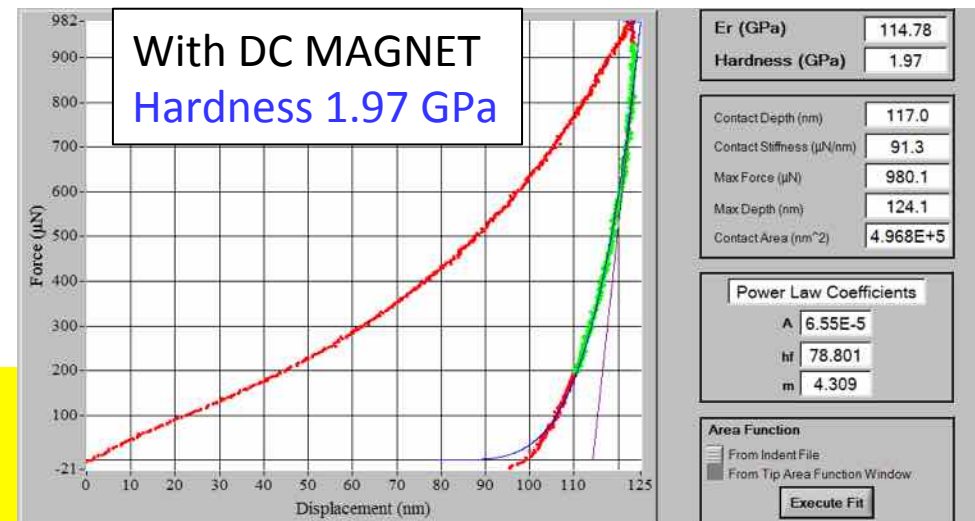
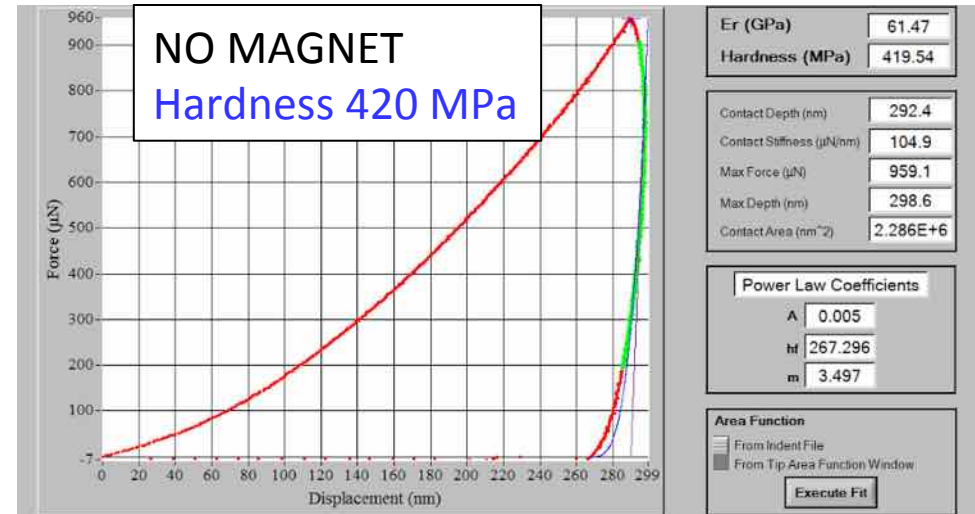
($>H_{sat}$):

Hardness ~ 0.95 - 2 GPa

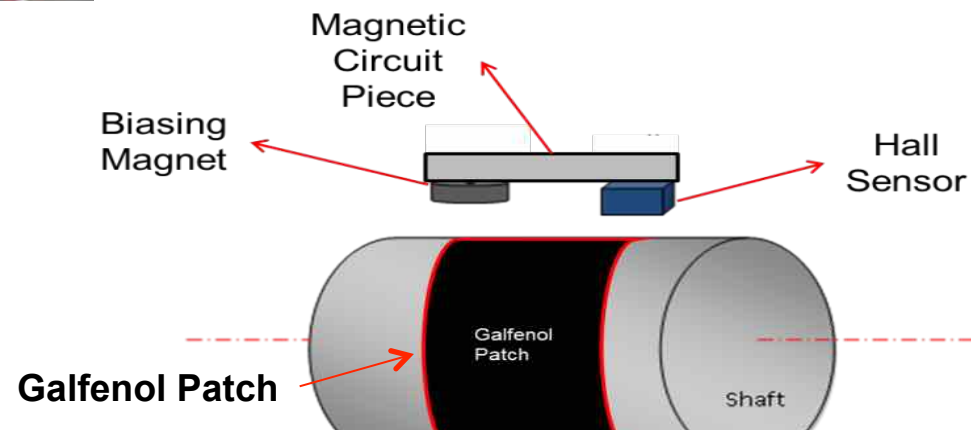
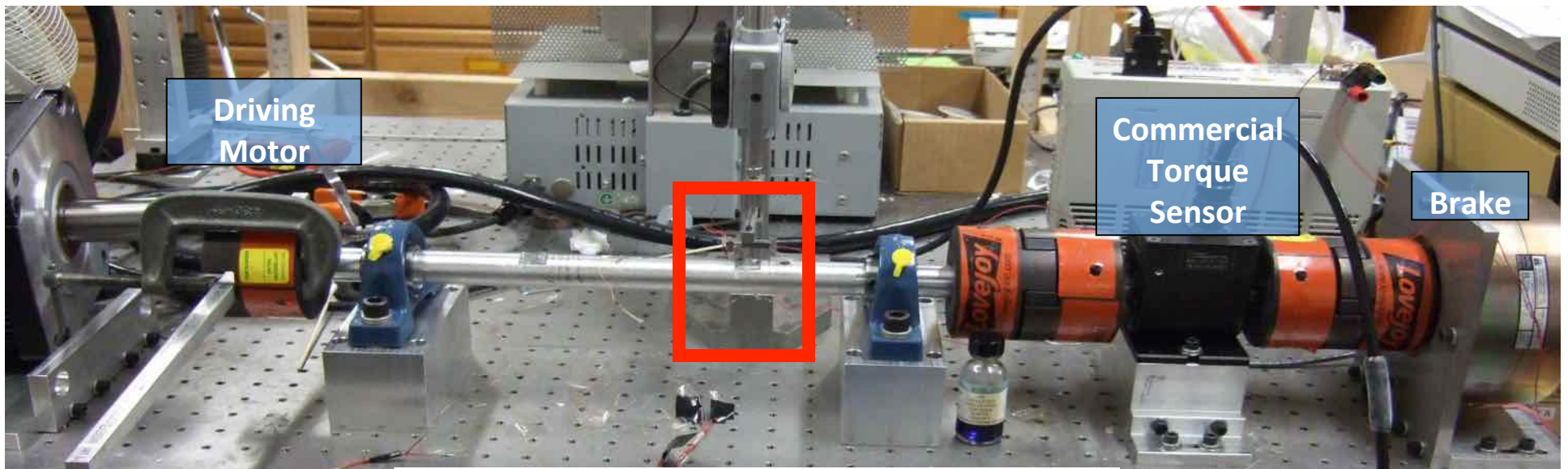
Average Hardness ~ 1.5 GPa

Applied force of 0-980 microNewton
Displacement scale is 0-125 nm

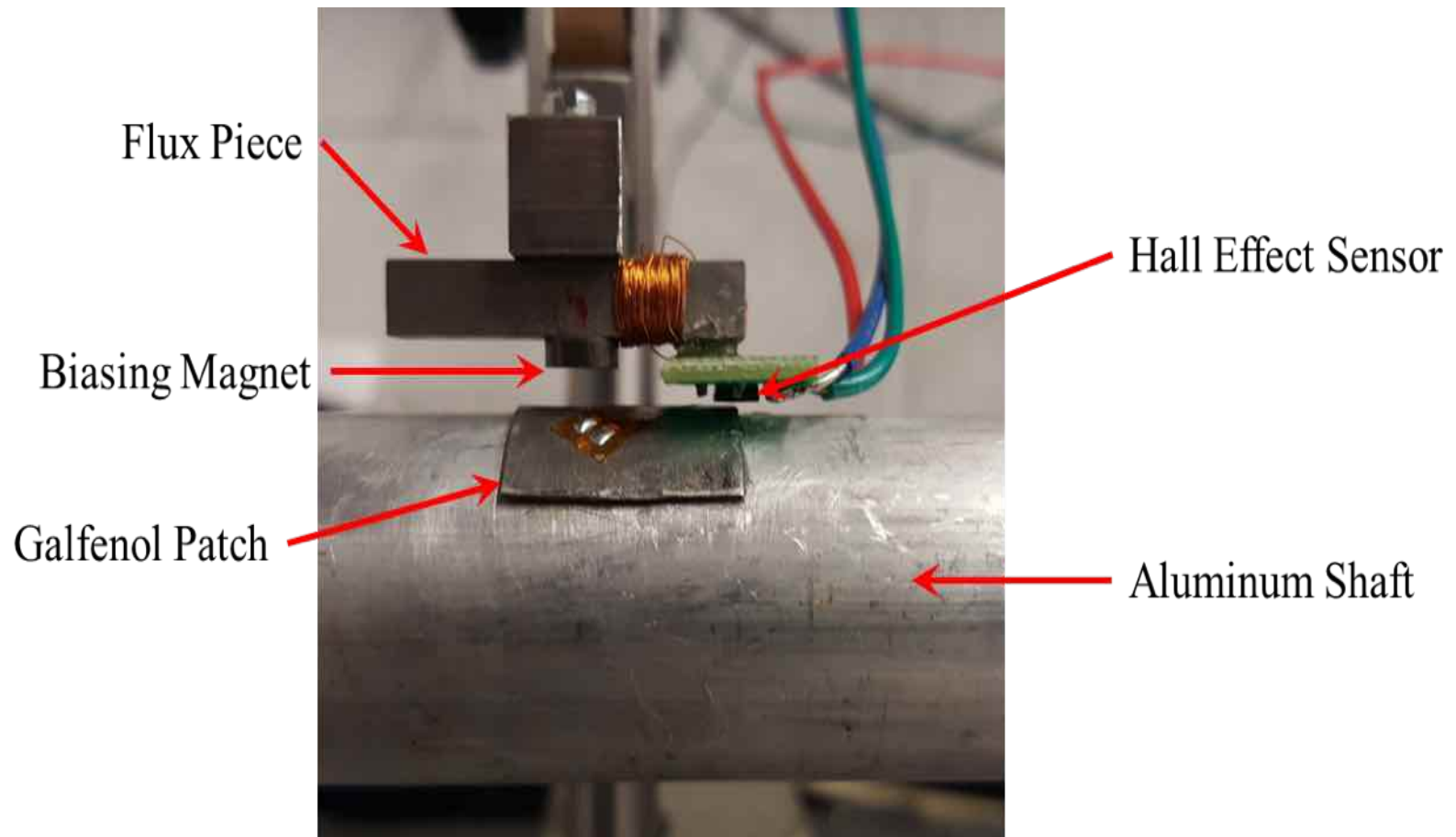
Measured Hardness Ratio 2.72
Predicted Estimate of 2.51!!



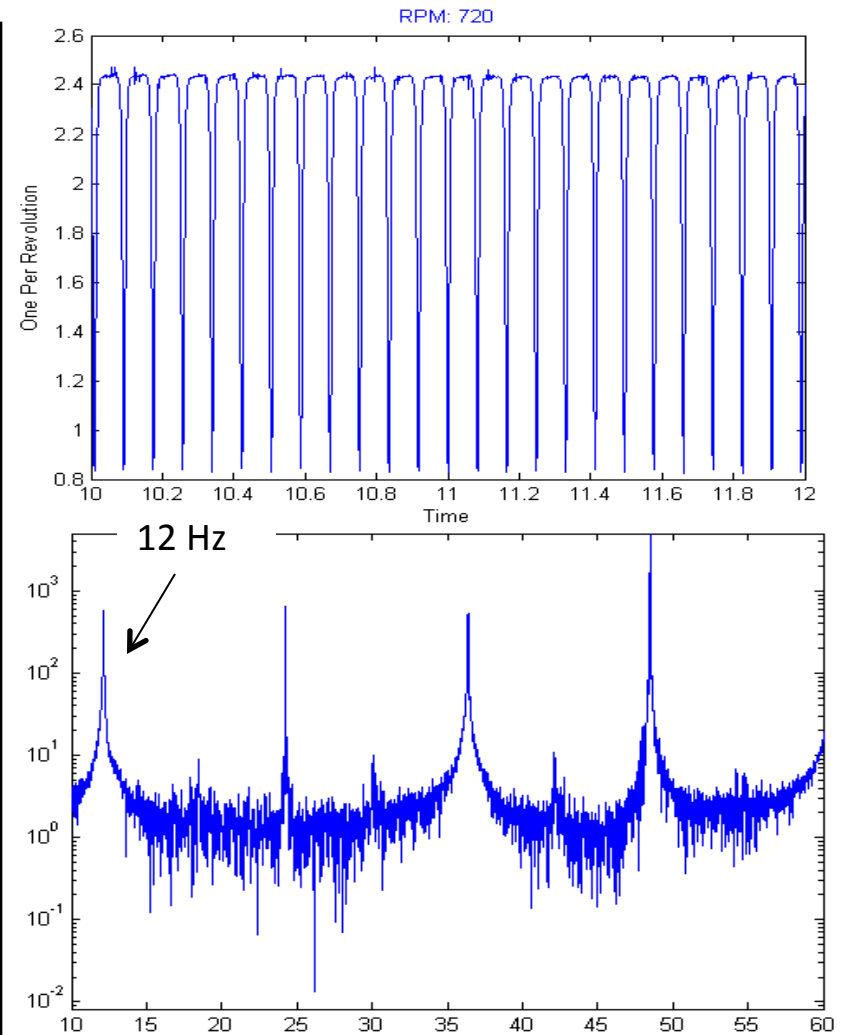
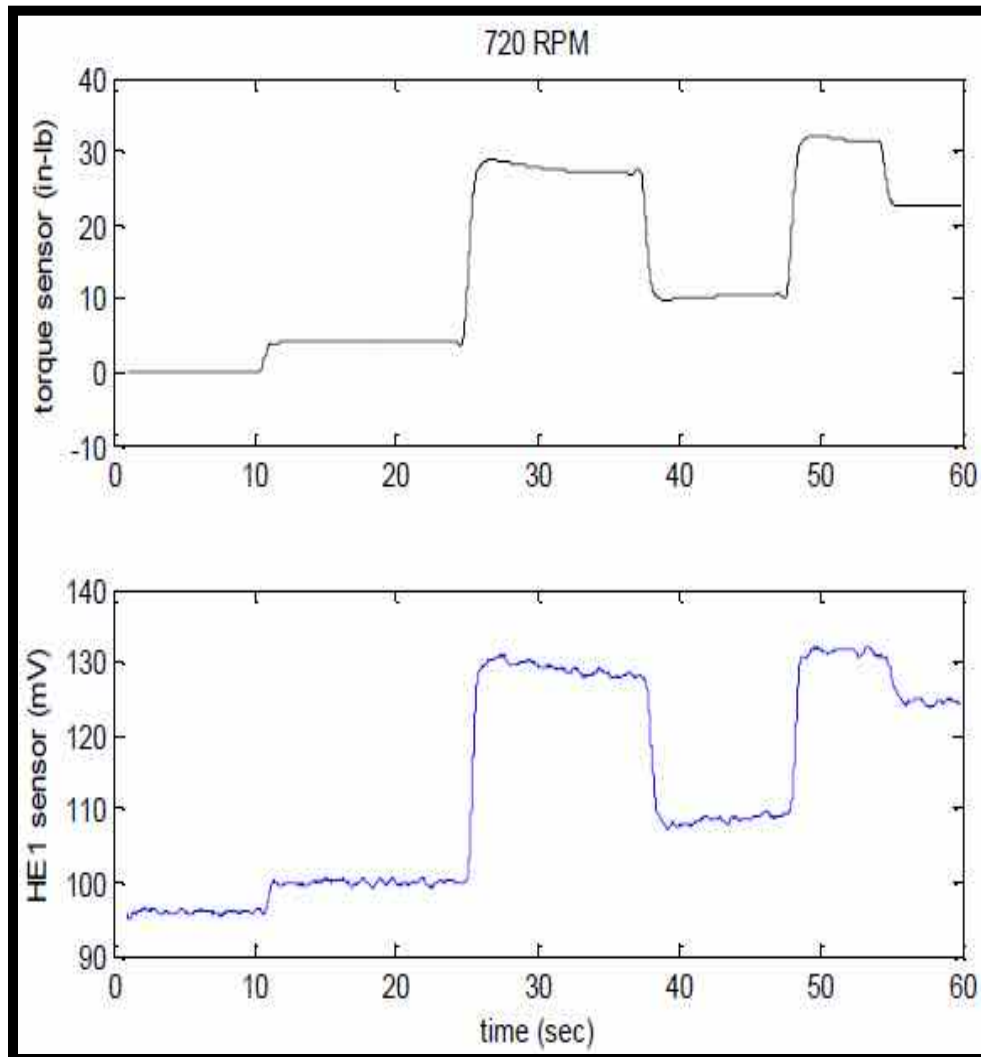
Benchtop Wireless Torque Sensor Setup



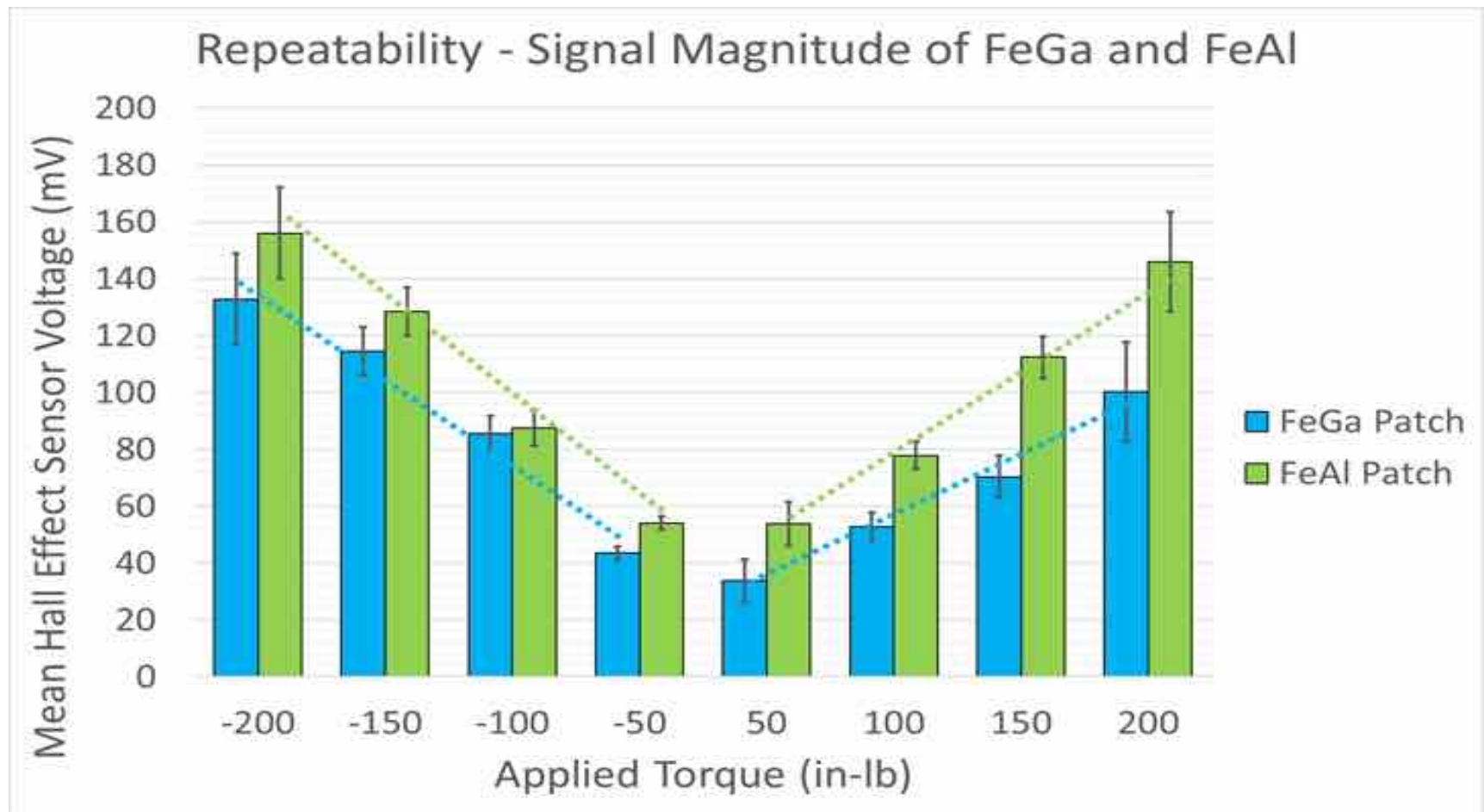
Close up of Galfenol patch on Aluminum shaft and flux piece with attached permanent magnet, coil and Hall effect sensor



Black: COTS torque sensor
Blue: averaged Hall effect sensor



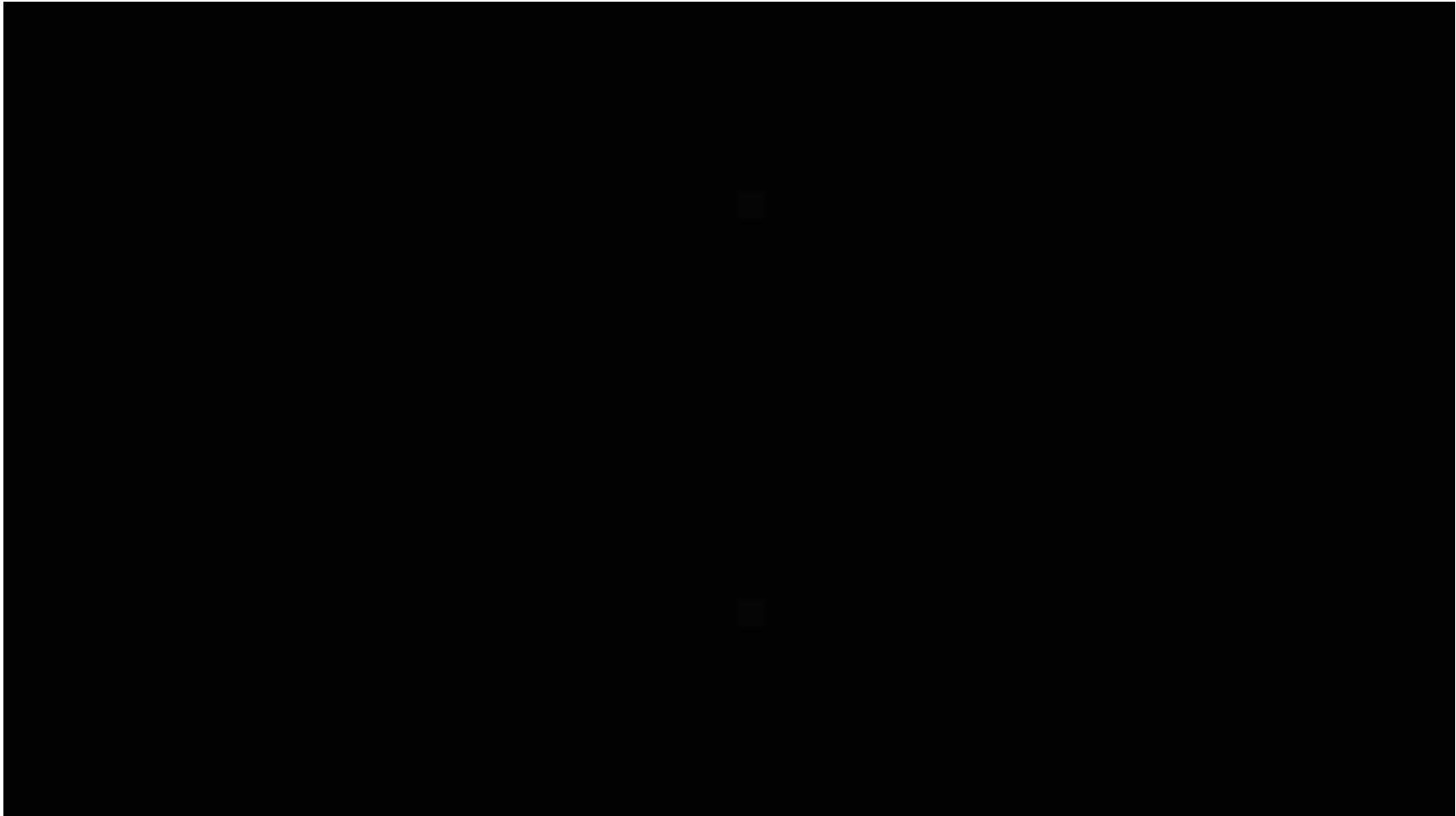
Galfenol and Alfenol patch output for clockwise and counterclockwise torque loading



Spinning shaft at 360 and 1800 rpm

Upper: COTS Torque sensor

Lower: Hall effect sensor output (mean of 4)



Oscilla Power is developing cost-effective magnetostrictive devices to harvest wave energy

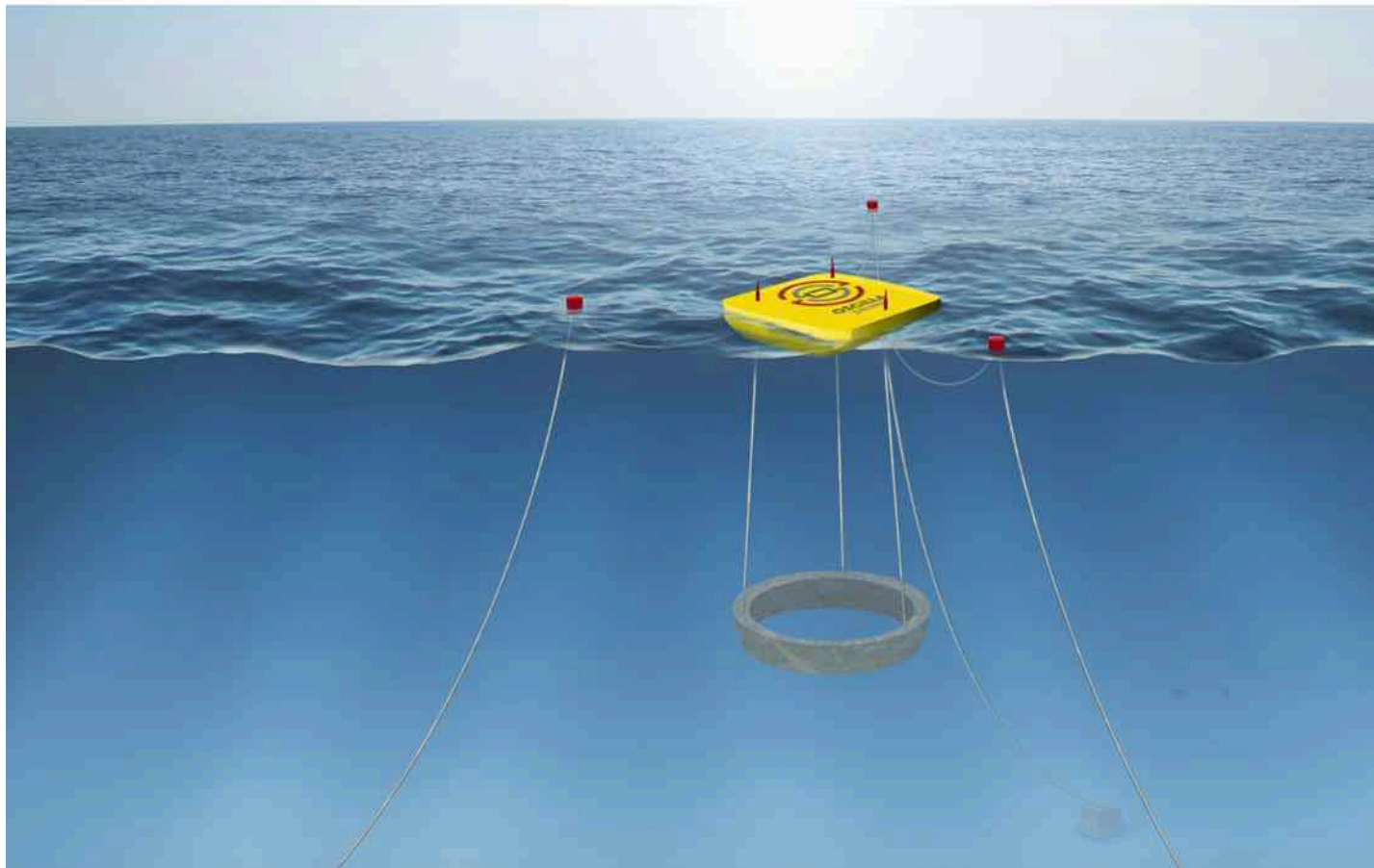


TRITON™ WEC

WAVE ENERGY

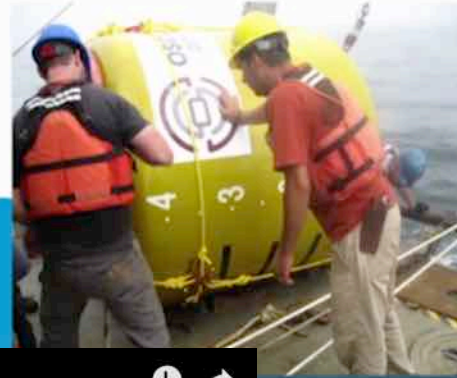
COMPANY

CO



<https://vimeo.com/154632694?swipeboxvideo=1>

Oscilla Power's Magnetostrictive Wave Energy Harvesters



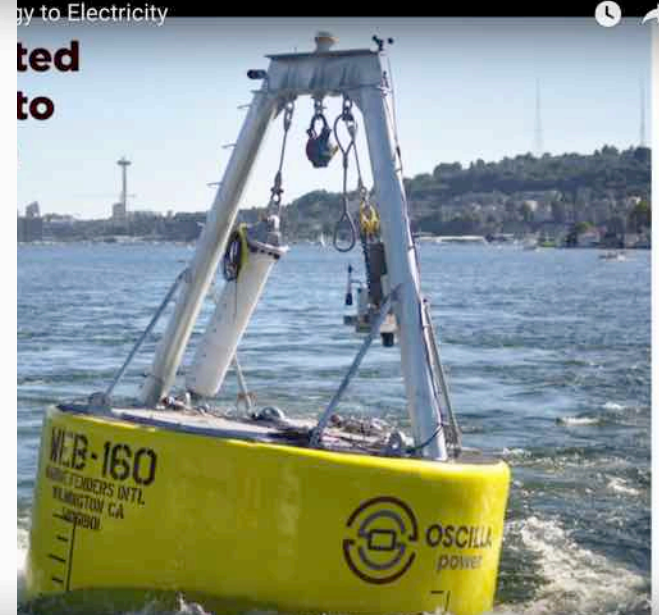
Oscilla Power - Transforming Wave Energy to Electricity



Surface Float Arrival in Seattle



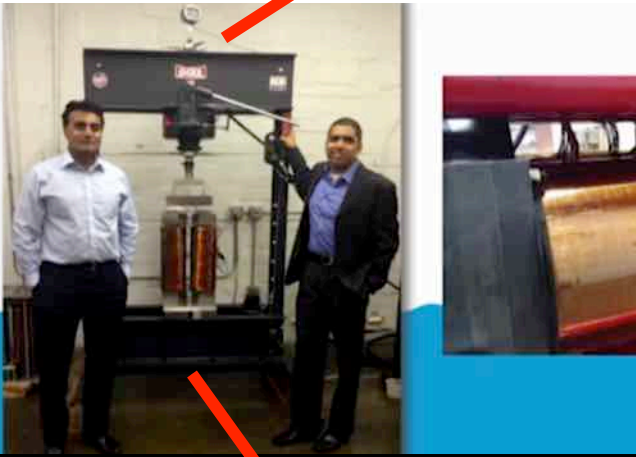
Generator Staging



Oscilla Power - Transforming Wave Energy to Electricity

ted
to

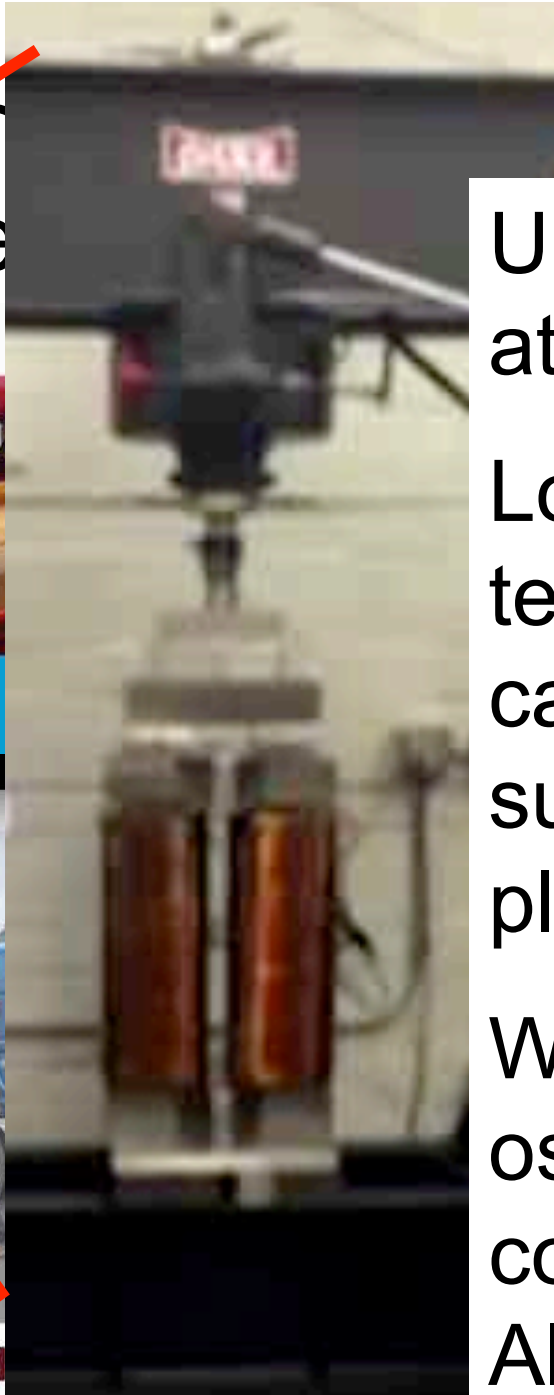
Oscilla Power Energy



Oscilla Power - Transforming Wave Energy to Electricity



Surface Float Arrival in Seattle



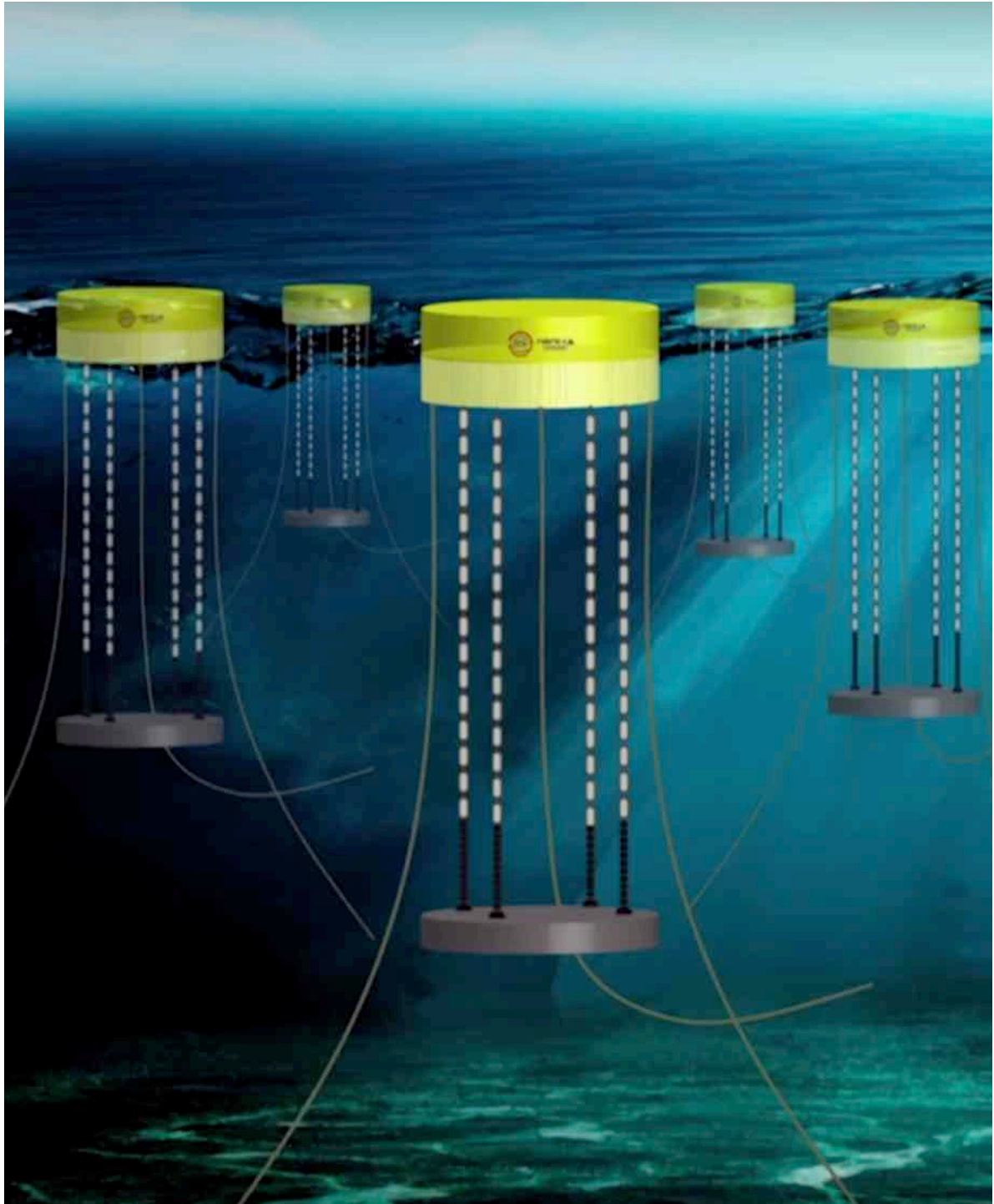
Staging

Frictive Wave

Upper end rigidly attached to float.

Lower end is tethered by cables to a subsurface heave plate.

Waves cause oscillatory axial compression in Alfenol rods





Thank you

With acknowledgement of the efforts of many colleagues and students.

And in particular the support of the NSF/
Sensors and Sensor Technologies Program,
Program manager: Dr. Shih Chi Liu and
ONR MURI, Program Manager Mr. Jan
Lindberg and the IEEE Magnetics Society



Thank you

With acknowledgement of the efforts of many colleagues and students, past and present who have made significant contributions to the work in this presentation. This includes, among many others:

Drs. Rick Kellogg, Pat Downey, Atul Atulasimha, Supratik Datta, Chaitanya Mudivarthi, Ganesh Raghunath Jung Jin Park, Suok Min Na, Jin H. Yoo, and to Michael Marana and Michael Van Order.

At the Univ. Minn: Prof. Bethanie Stadler, Madhukar Reddy

ONR MURI team members: Drs. Tom Lograsso, Rob McQueeney, Marcelo Dapino, Steve Thompson, Dwight Viehland, Manfred Wuttig, Ichiro Takeuchi, Dick James, Uwe Marschner

ETREMA Products, Inc., Eric Summers, Jon Snodgrass

NSWC/CD, Marilyn Wun-Fogel, James Restroff, Art Clark

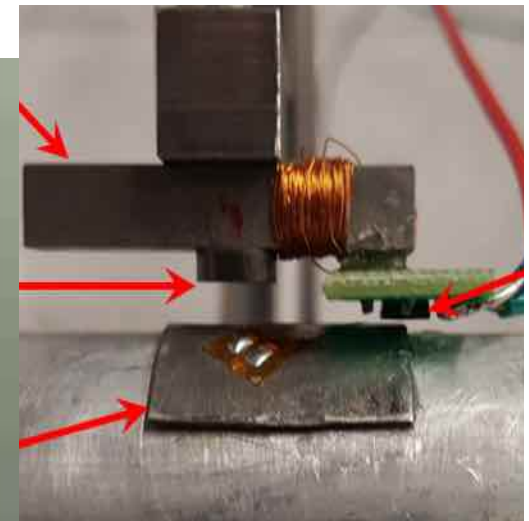
Kanazawa University in Japan, Prof. Toshiyuki Ueno

Oscilla Power: Dr. Balky Nair and Rahul Shendur

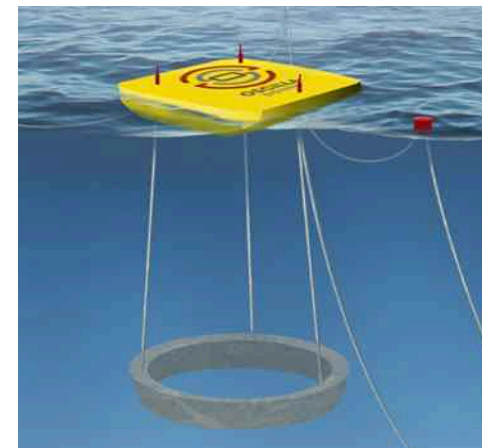
Examples of Structural Magnetostrictive Alloys



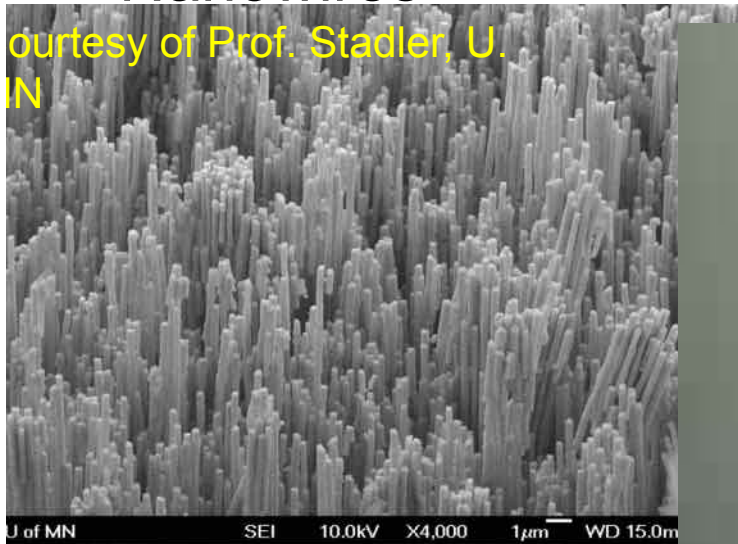
Torque Sensor



Large-scale Wave Energy Harvesting



Nanowires



Rolled Sheet



Micro-scale motion



Courtesy Prof. Ueno, U. Kanazaga

Implanted Bone-Plate Sensor



Courtesy of Profs. Fischer & Marschner
TU Dresden